Gaseous Detectors

Fulvio Tessarotto (I.N.F.N. – Trieste)

Material from F. Sauli, R. Veenhof, L. Ropelewski, S. Dalla Torre, E. Nappi, J. Va'Vra, A. Breskin, …

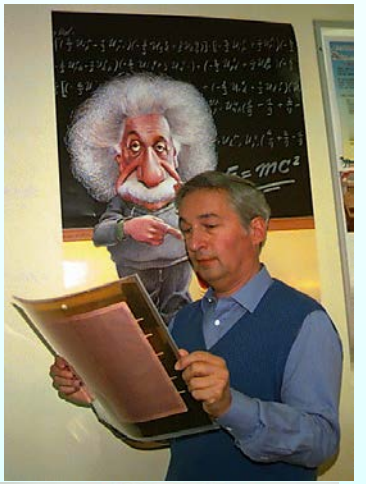

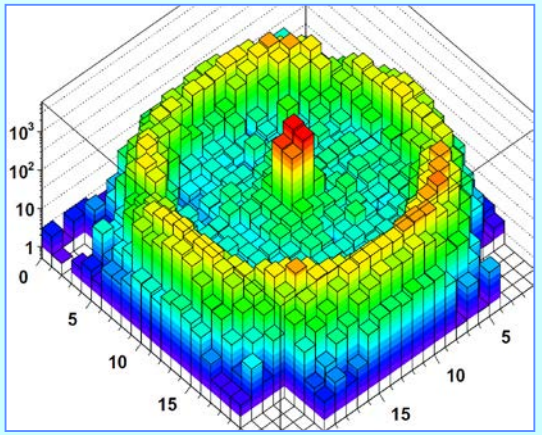

Radioactivity is everywhere

On average a human body has ~30 mg of Potassium 40, corresponding to ~ 4 kBq

$$\beta^- : {}^{40}_{19}K \rightarrow {}^{40}_{20}Ca + e^- + \overline{\nu}_e$$

$$EC : {}^{40}_{19}K + e^- \rightarrow {}^{40}_{18}Ar^* + \nu_e \rightarrow {}^{40}_{18}Ar^* + \nu_e \rightarrow {}^{40}_{18}Ar + \gamma + \nu_e$$

$$\beta^+ : {}^{40}_{19}K \rightarrow {}^{40}_{18}Ca + e^+ + \nu_e$$

My activity is ~ 5000 disintegrations per second

An average banana has 14 Bq

The average annual human exposure to natural background radiation is 2.4 mSv (from 0.4 to 4 mSv/y depending on the location)

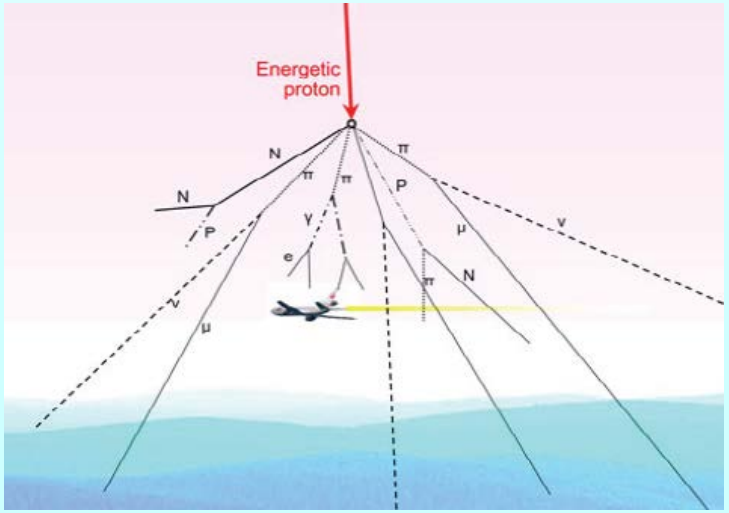

During a flight the background dose rate increases by a factor between 10 and 30

Charged particles:

- ***-heavy (μ, π, p, α, …)***
- ***-light (electrons and positrons)***

Neutral particles:

- ***-photons***
- ***-neutrons***
- ***-neutrinos***

The Particle Data Book

2016 Review of Particle Physics

C. Patrignani et al. (PDG), Chin. Phys. C40, 100001 (2016)

(http://pdg.lbl.gov)

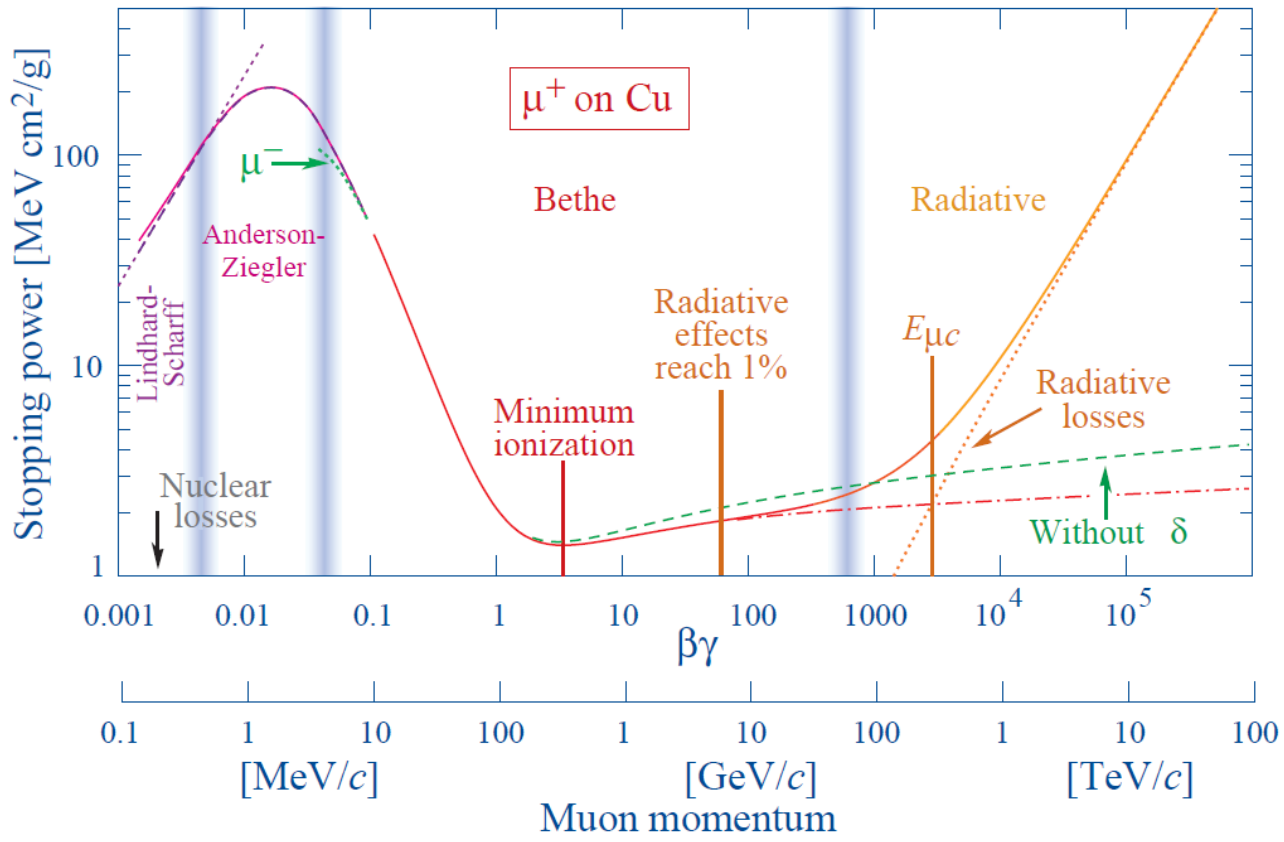

Fig. 32.1: Stopping power ($= \langle -dE/dx \rangle$) for positive muons in copper as a function of $\beta\gamma = p/Mc$ over nine orders of magnitude in momentum (12 orders of magnitude in kinetic energy). Solid curves indicate the total stopping power. Data below the break at $\beta\gamma \approx 0.1$ are taken from ICRU 49 [4], and data at higher energies are from Ref. 5. Vertical bands indicate boundaries between different approximations discussed in the text. The short dotted lines labeled "μ^-" illustrate the "Barkas effect," the dependence of stopping power on projectile charge at very low energies [6]. dE/dx in the radiative region is not simply a function of β.

Glorious traditon: 100 years of gaseous detector developments

1908: FIRST WIRE COUNTER
USED BY RUTHERFORD IN THE STUDY OF NATURAL RADIOACTIVITY

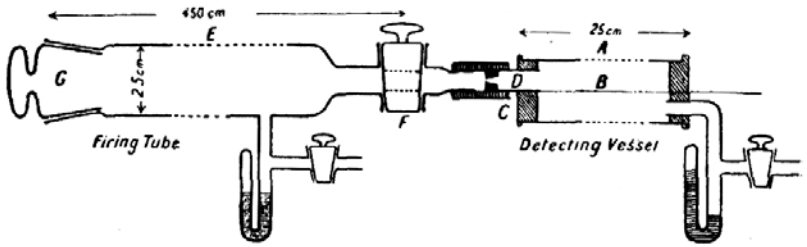

E. Rutherford and H. Geiger ,
Proc. Royal Soc. A81 (1908) 141

Nobel Prize in Chemistry in 1908

1928: GEIGER COUNTER
SINGLE ELECTRON SENSITIVITY

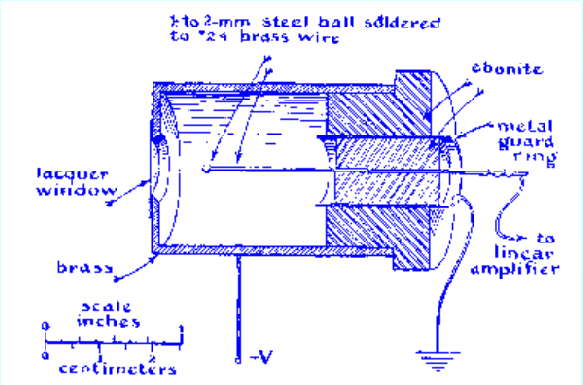

H. Geiger and W. Müller,
Phys. Zeits. 29 (1928) 839

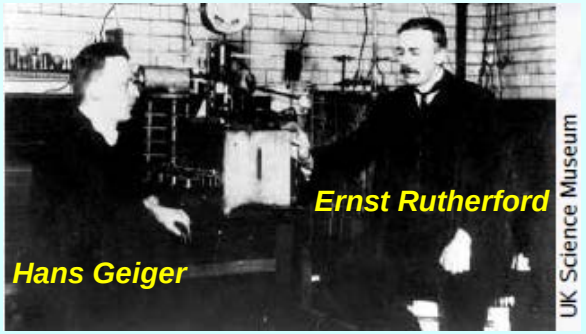

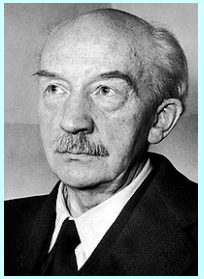

Walther Bothe
Nobel Prize in 1954 for the "coincidence method"

1968: MULTIWIRE PROPORTIONAL CHAMBER

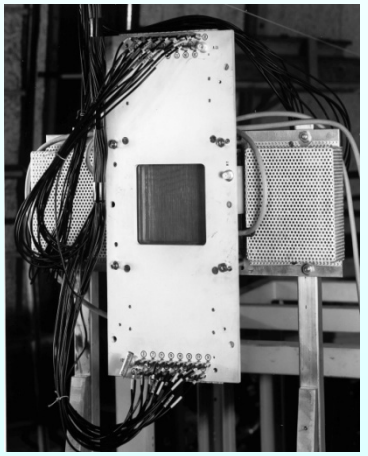

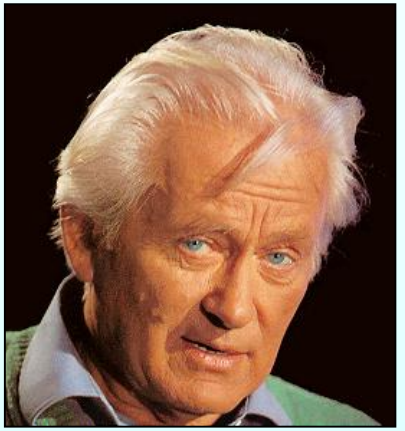

Nobel Prize in 1992

G. Charpak, Proc. Int. Symp. Nuclear Electronics
(Versailles 10-13 Sept 1968)

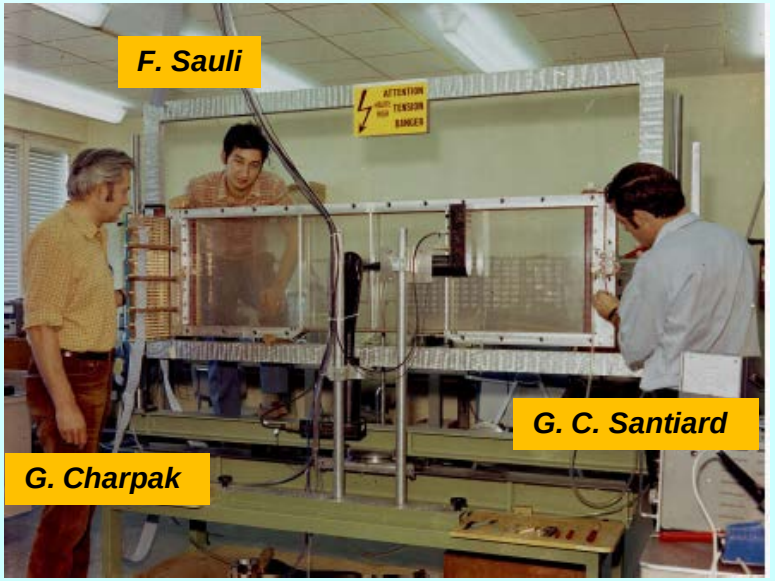

Cloud Chamber, C.T.R. Wilson, 1910

Charges act as condensation nuclei in supersaturated water vapor

Alphas, Philipp 1926

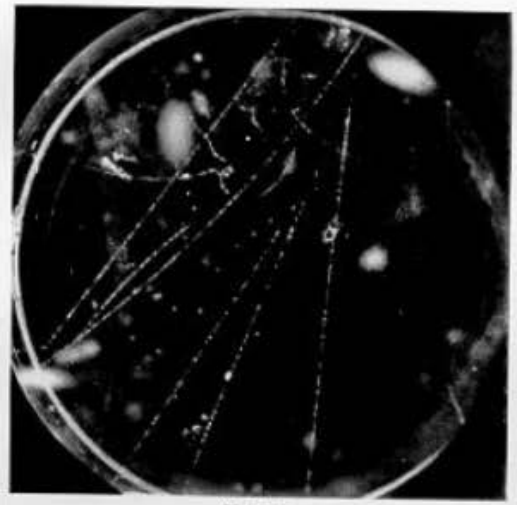

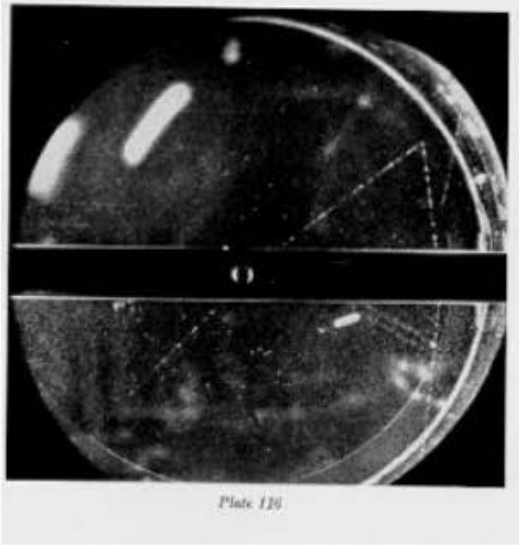

V- particles, Rochester and Wilson, 1940ies

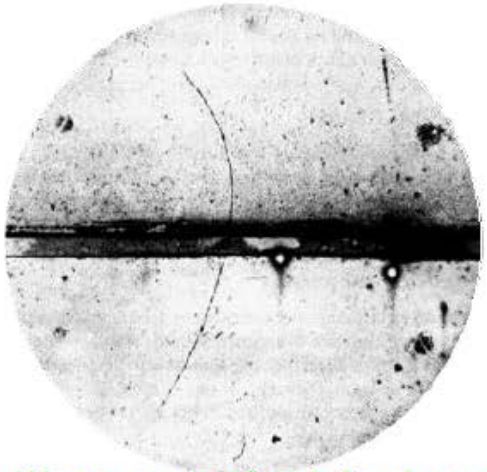

Positron discovery, Carl Andersen 1933

Tip Counter, Geiger 1914

Charges create a discharge of a needle which is at HV with respect to a cylinder.

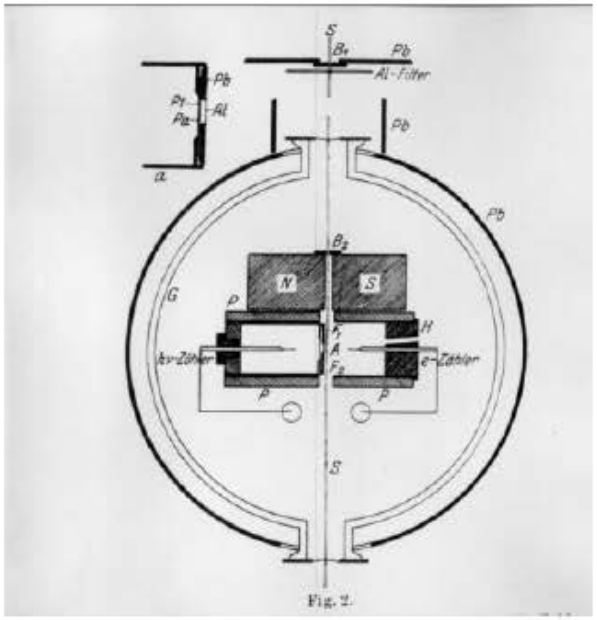

The needle is connected to an electroscope that can detect the produced charge.

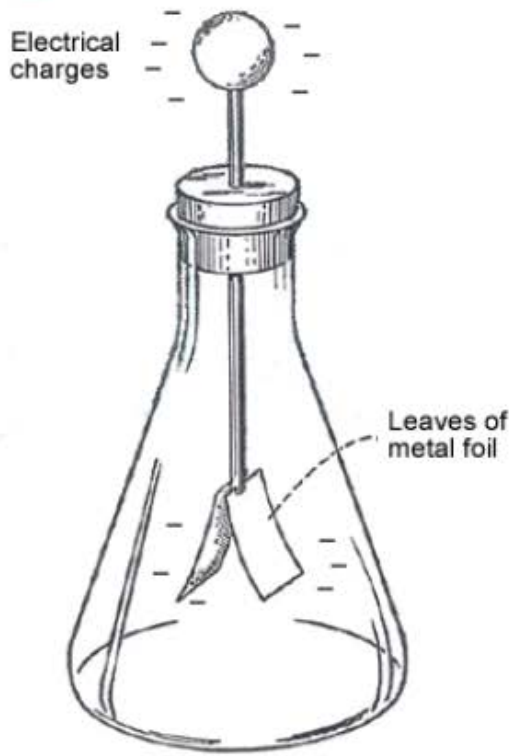

E(a)rnest Rutherford
(1871-1937)

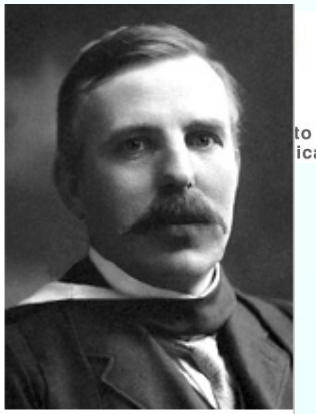

Geiger counter

- Detects radiation by discharge;
- can count α, β and γ particles (at low rates ...);
- no tracking capability.
- 1908: Ernest Rutherford and Hans Geiger
- 1928: Hans Geiger and Walther Müller

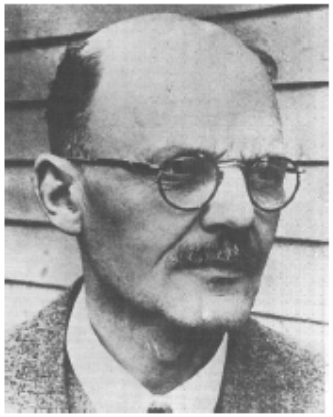

Hans Geiger
(1882-1945)

Walt(h)er Müller
(1905-1979)

A Geiger-Muller counter built in 1939 and used in the 1947-1950 for cosmic ray studies in balloons and on board B29 aircraft by Robert Millikan et al.

Made of copper, 30 cm long

Electric Registration of Geiger Müller Tube Signals

Charges create a discharge in a cylinder with a thin wire set to HV. The charge is measured with a electronics circuit consisting of tubes → electronic signal.

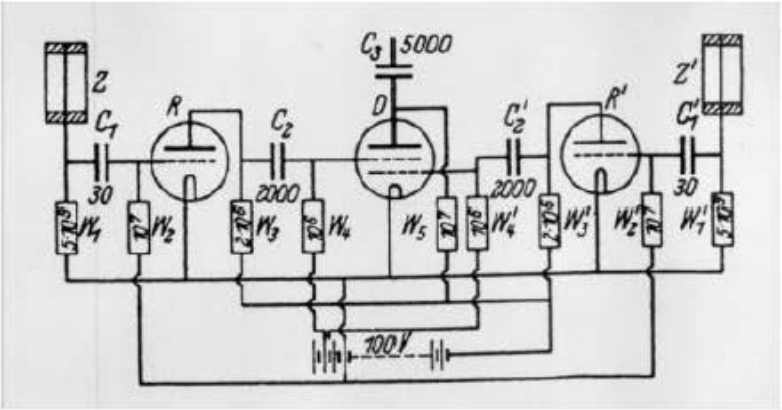

W. Bothe, 1928

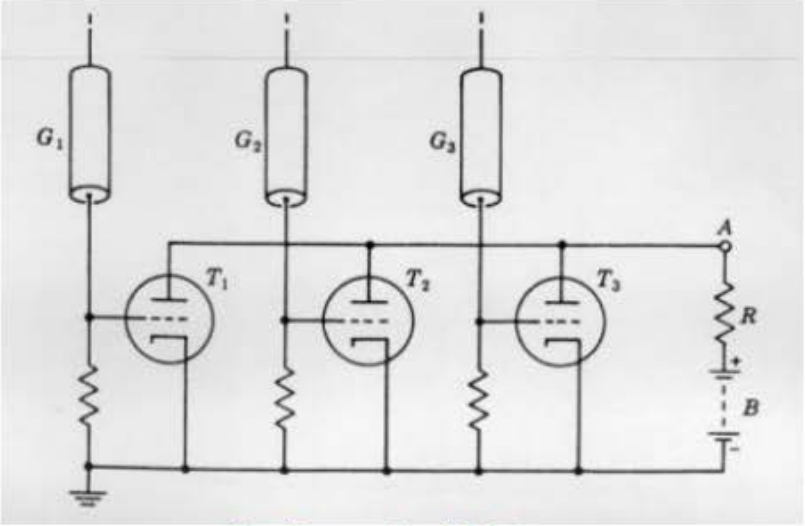

B. Rossi, 1932

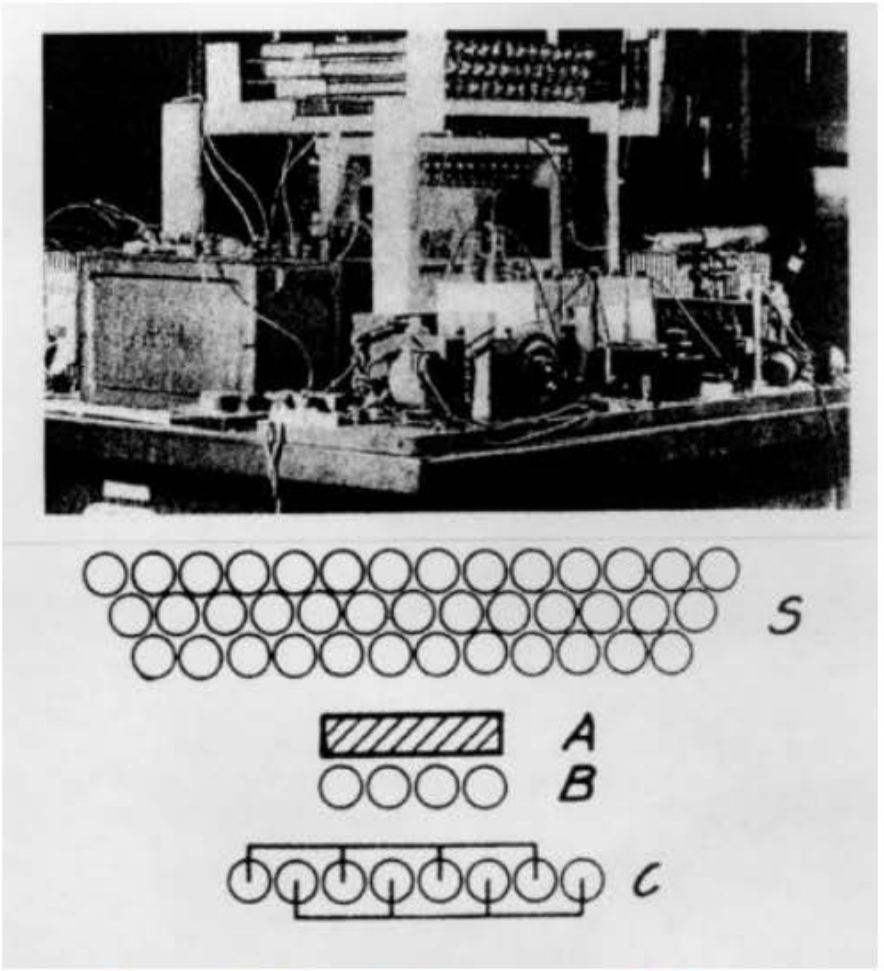

Cosmic Ray Telescope 1930ies

Nuclear Emulsion, M. Blau, 1930ies

Charges initiate a chemical reaction that blackens the emulsion (film)

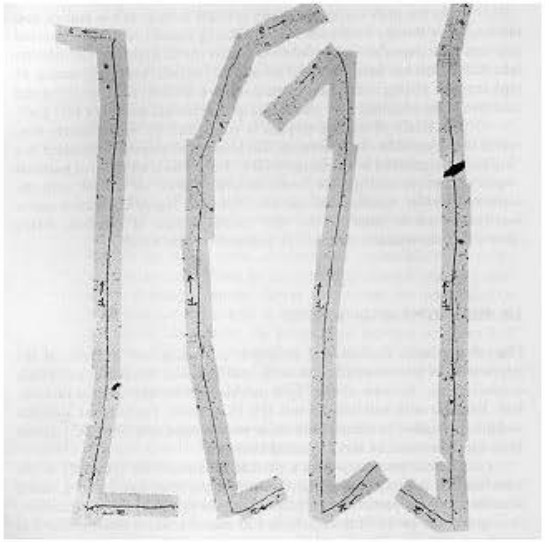

C. Powell, Discovery of muon and pion, 1947

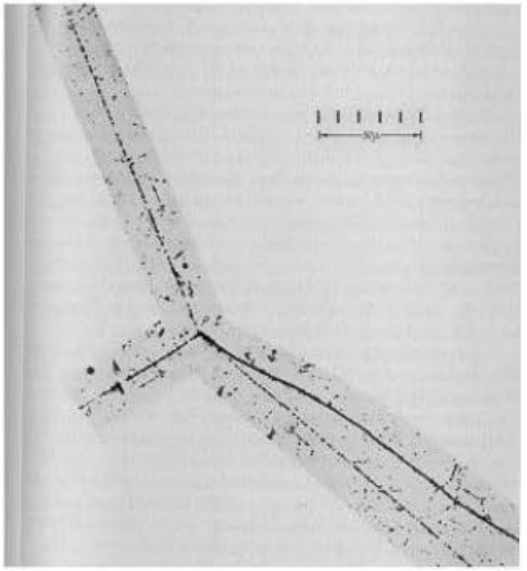

Kaon Decay into 3 pions, 1949

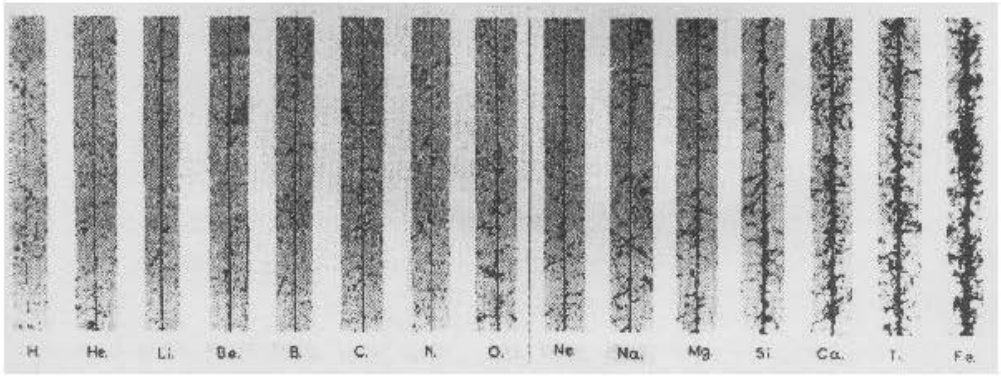

Cosmic Ray Composition

Bubble Chamber, D. Glaser 1952

Charges create bubbles in superheated liquid, e.g. propane or Hydrogen (Alvarez)

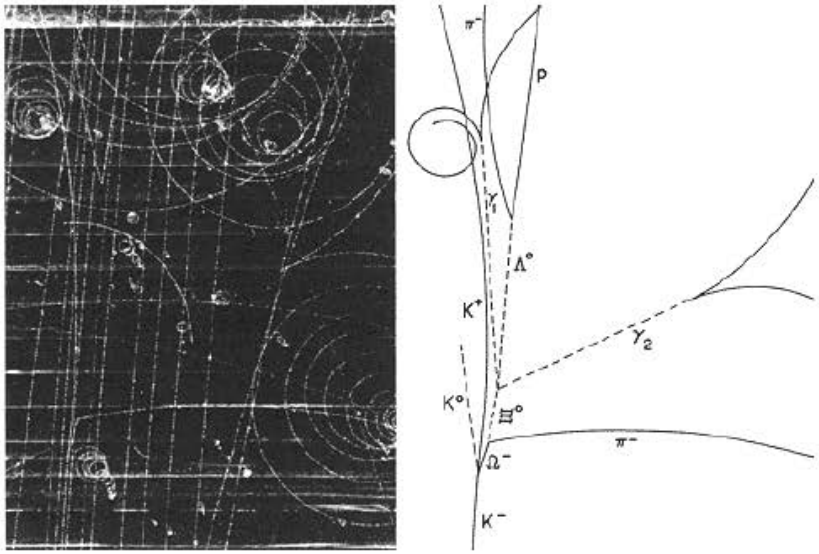

Discovery of the Ω^- in 1964

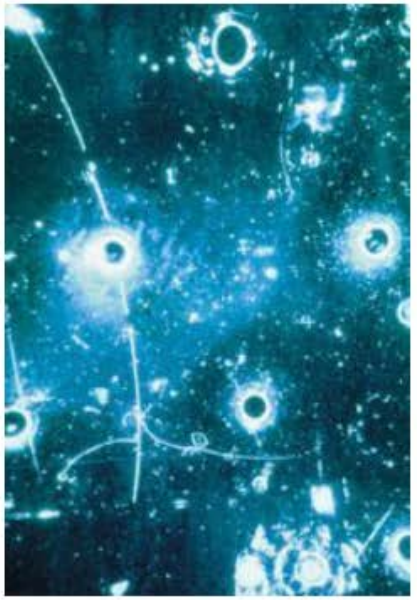

Neutral Currents 1973

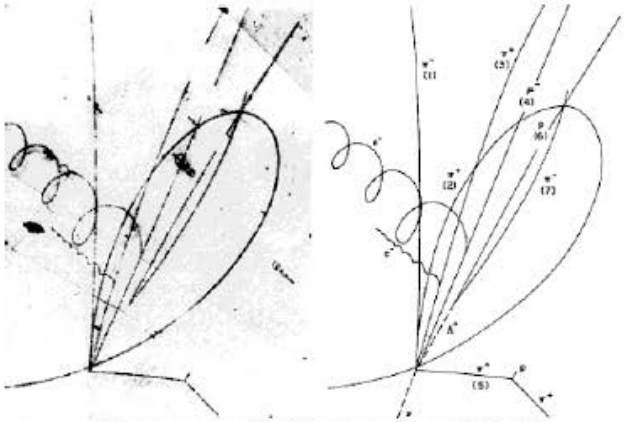

Charmed Baryon, 1975

Spark Chamber, 1960ies

Charges create 'conductive channel' which initiates a spark in case HV is applied.

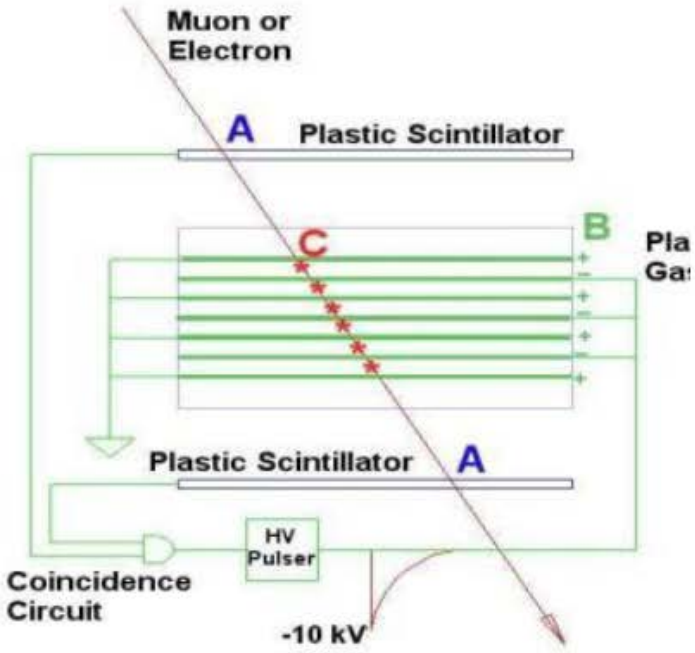

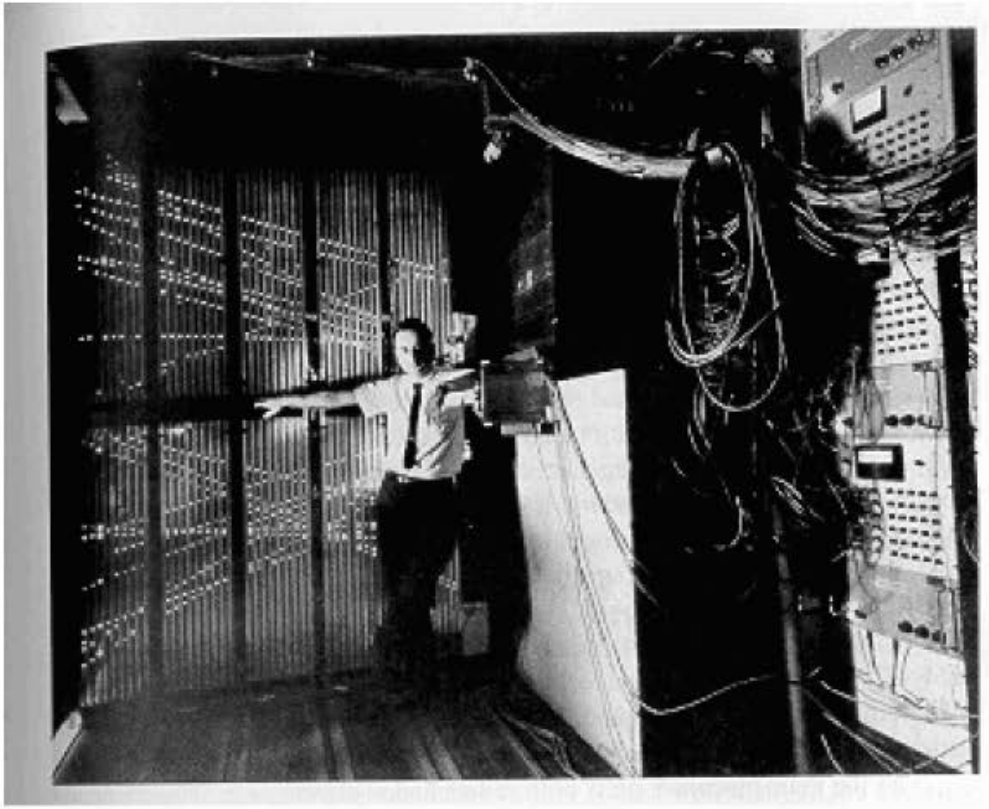

Discovery of the Muon Neutrino 1960ies

MWPC

- First gaseous tracking device
- 1968: Georges Charpak

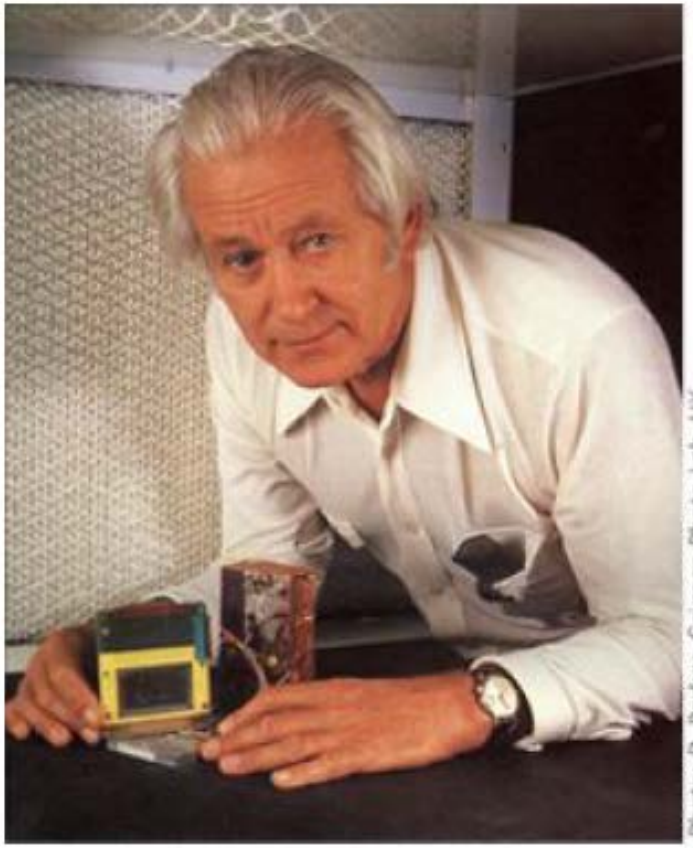

Photo: D. Parker, Science Photo Lab, UK

Georges Charpak
(1924-2010)

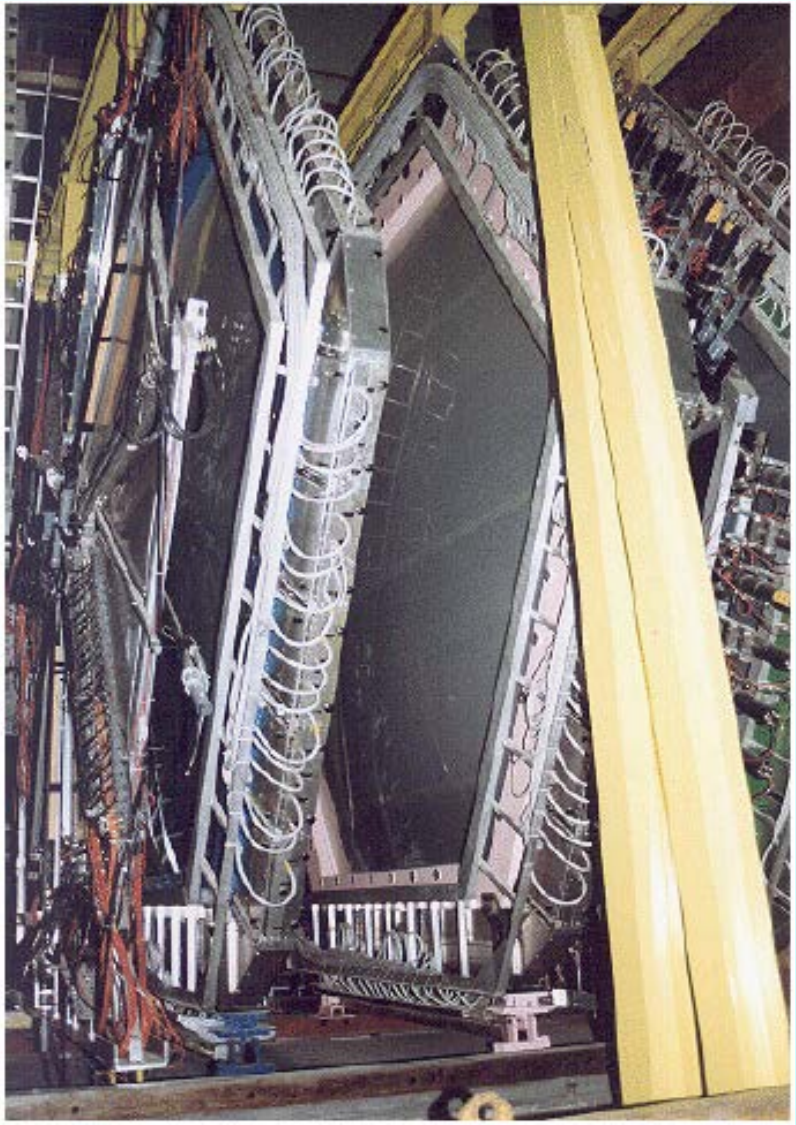

One of the NA60 muon chambers

Drift Chambers, TPCs, …

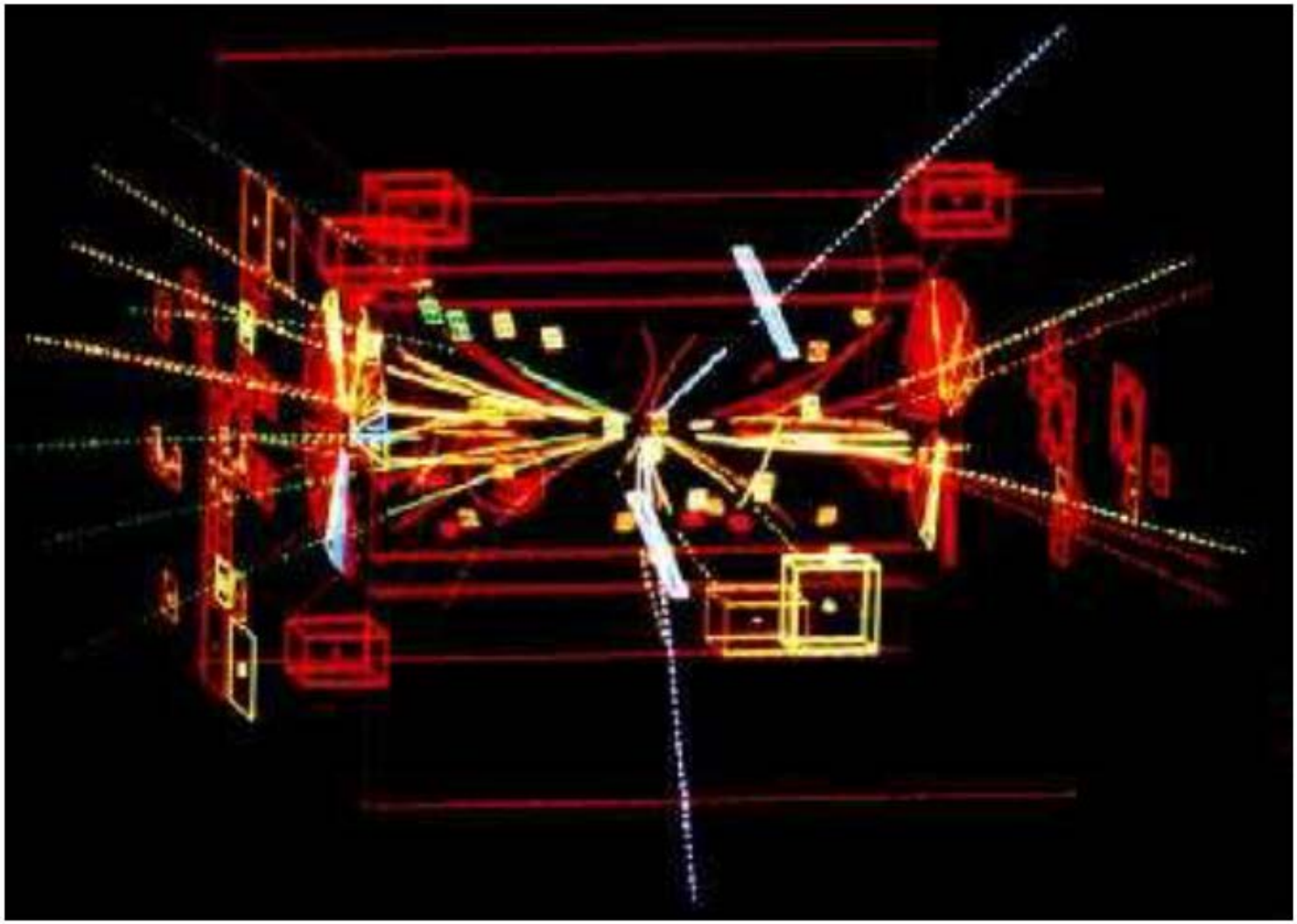

Z-Event at UA1 / CERN

How do gaseous detectors work?

- a charged particle passing through the gas ionises some of the gas molecules;
- the electric field in the gas volume transports the ionisation electrons and provokes multiplication;
- the movement of electrons and ions leads to induced currents in electrodes;
- the signals are processed and recorded.

Gas choice

- Which gas would be suitable ?
  - easily ionisable;
  - not attaching: doesn't swallow electrons;
  - no polymerisation: electrodes do not get coated with plastic;
  - neither flammable, nor explosive, nor toxic;
  - discharges do not produce aggressive chemicals;
  - affordable.

- Common choice: noble gas with an admixture of molecular gas called quencher – reasons will become apparent.

- Today, we concentrate on Ar pure and mixed with CO_2 but there are many alternatives, in particular with Ne and Xe.

Gas choice

Argon

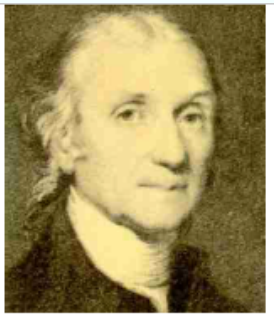

Henry Cavendish
(1731-1810)

JohnWilliam Strutt,
3rd Baron Rayleigh of
Terling Place
(1842-1919)

Sir William Ramsey
(1852-1916)

- Ocurrence:
  - abundant in the atmosphere !
- Other qualities:
  - chemically exceedingly inert, hence not toxic
  - cheap: 0.001 €/l (CERN stores)

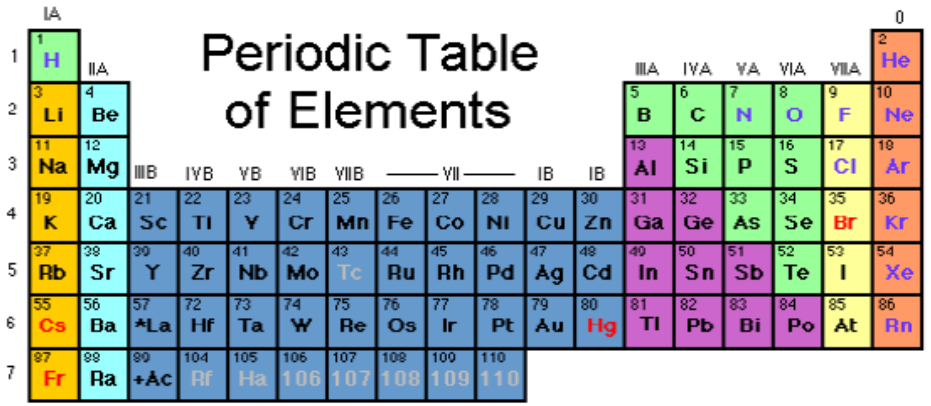

Gas	Percent volume
nitrogen	78.080000
oxygen	20.950000
argon	0.930000
water	up to 4 %
carbon dioxide	0.036000
neon	0.001800
helium	0.000500
methane	0.000170
hydrogen	0.000050
nitrous oxide	0.000030
ozone	0.000004

Polyatomic gases

- Commonly used:
  - CH_4, C_2H_6, C_3H_8, iC_4H_{10}, ...
  - DME,
  - CF_4, $C_2F_4H_2$, SF_6 ...
- Qualities:
  - inelastic scattering;
  - photon absorption.
- Problems:
  - dissociation;
  - attachment;
  - polymerisation (ageing);
  - environmental issues;
  - flammable ...

CO_2

- Non-flammable, not too toxic ...
- easily available;
- no ageing (polymerisation);
- positive electron affinity, but clusters do attach.

Simulation example (from R. Veenhof)

At the 100 µm scale

- Example:
  - CSC-like structure,
  - Ar 80 % CO_2 20 %,
  - 10 GeV µ.
- The electron is shown every 100 collisions, but has been tracked rigorously.
- Ions not shown.

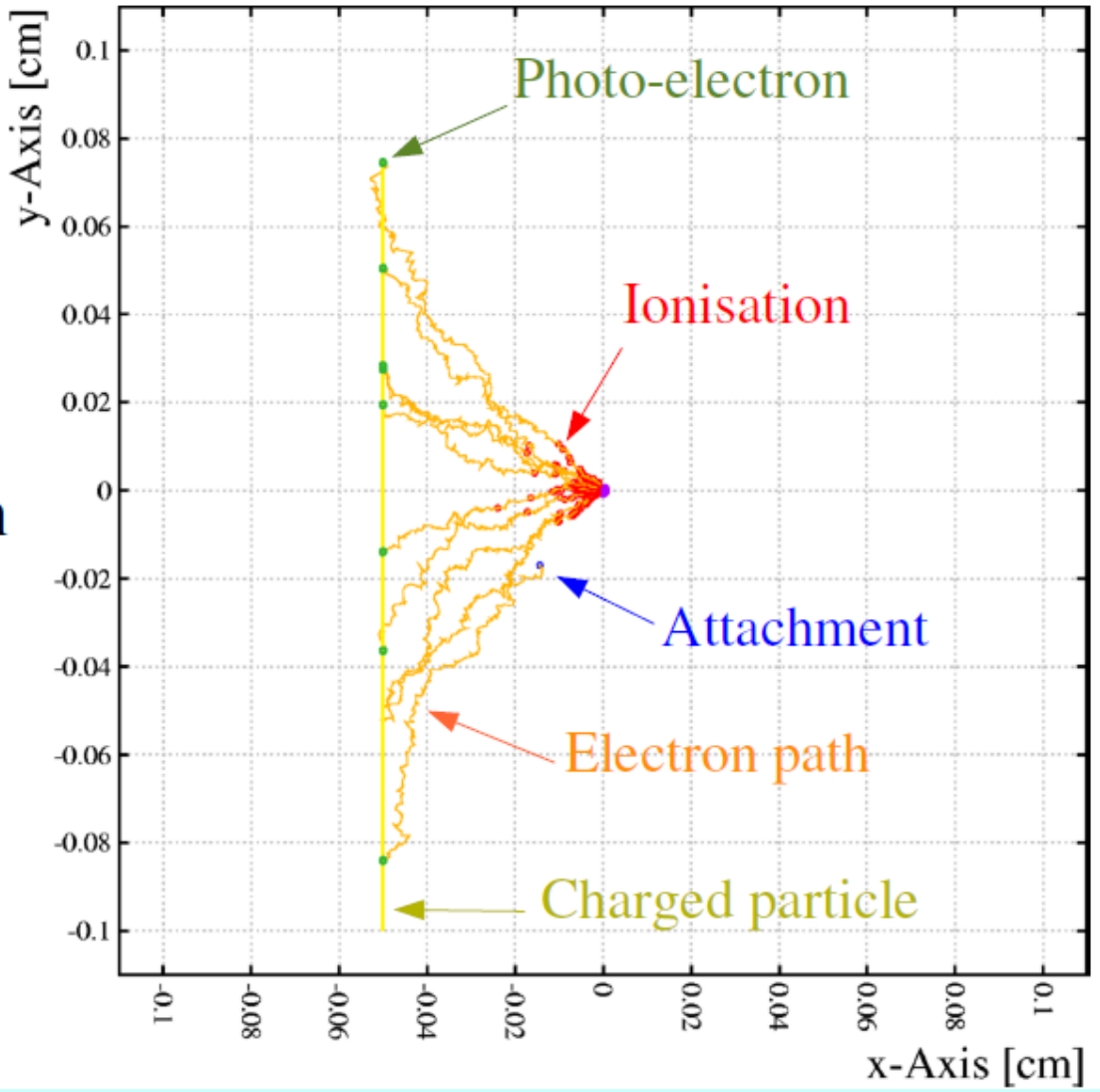

Ionization

[Four Curies: Pierre, Marie, Irène and Pierre's father, around 1904 at the BIPM]

1896: Ionisation by radiation

- Early in the study of radioactivity, ionisation by radiation was recognised:

" Becquerel discovered in 1896 the special radiating properties of uranium and its compounds. Uranium emits very weak rays which leave an impression on photographic plates. These rays pass through black paper and metals; they make air electrically conductive. "
[Pierre Curie, Nobel Lecture, June 6th 1905]

"A sphere of charged uranium, which discharges spontaneously in the air under the influence of its own radiation, retains its charge in an absolute vacuum. The exchanges of electrical charges that take place between charged bodies under the influence of the new rays, are the result of a special conductivity imparted to the surrounding gases, a conductivity that persists for several moments after the radiation has ceased to act."
[Antoine Henri Becquerel, Nobel Lecture, December 11th 1903]

Ionization

Hans Bethe
(1906-2005)

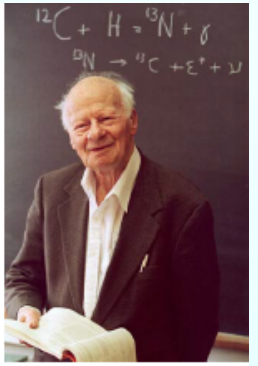

Ionisation losses: Bethe formula

- If we make the assumptions:
  - projectile mass $M \gg m$, the e$^-$ mass,
  - only Coulomb energy transfer to free e$^-$, not to the nuclei;
  - *effective* ionisation energy $I <$ energy transfer $<$ kinematics.

- The ionisation losses are given by (Hans Bethe formula):

$$\frac{\mathrm{d}E}{\mathrm{d}x} \propto -\frac{Z^2}{m\beta^2}\frac{z}{A}\left[\log\left(\frac{2m\beta^2\gamma^2 T_{\max}}{I}\right) - \beta^2 - \text{corrections}\right]$$

  - β, γ: velocity of projectile;
  - Z^2: projectile charge squared (i.e. independent of sign);
  - no dependence of projectile mass;
  - z and A of target (linear: number of e$^-$ encountered);
  - $T_{\max}$: highest energy that can be transferred to the target.

Ionization

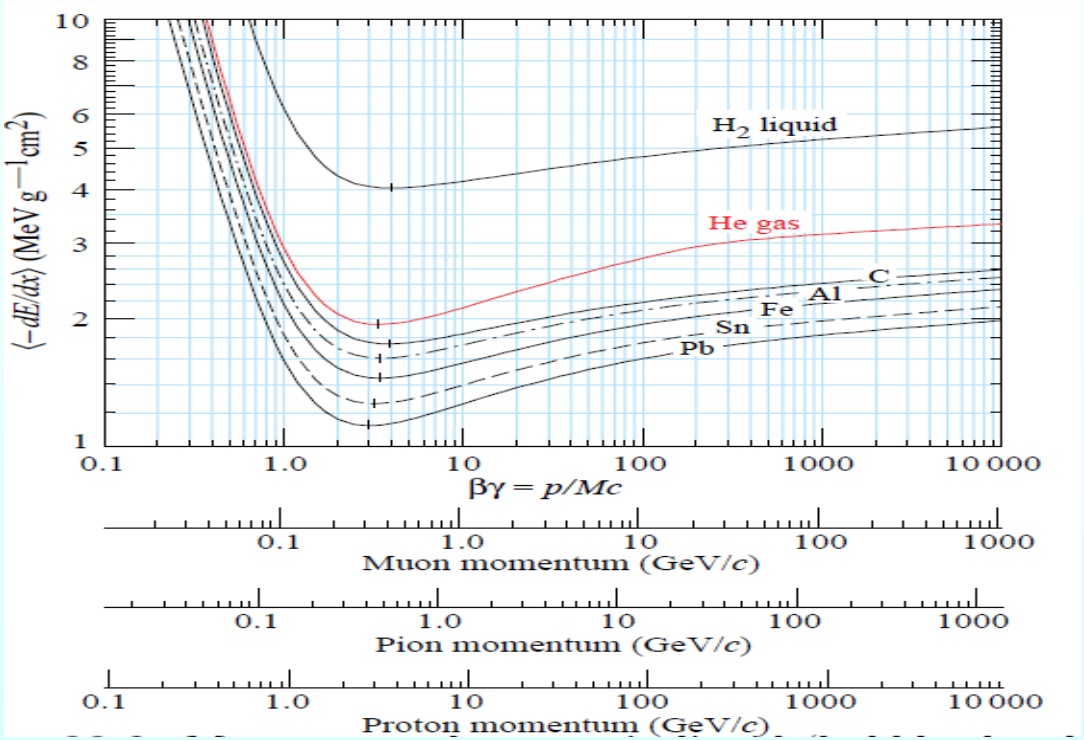

Gas	Density, mg cm^{-3}	E_x eV	E_I eV	W_I eV	$dE/dx\|_{\min}$ keV cm^{-1}	N_P cm^{-1}	N_T cm^{-1}
He	0.179	19.8	24.6	41.3	0.32	3.5	8
Ne	0.839	16.7	21.6	37	1.45	13	40
Ar	1.66	11.6	15.7	26	2.53	25	97
Xe	5.495	8.4	12.1	22	6.87	41	312
CH_4	0.667	8.8	12.6	30	1.61	28	54
C_2H_6	1.26	8.2	11.5	26	2.91	48	112
iC_4H_{10}	2.49	6.5	10.6	26	5.67	90	220
CO_2	1.84	7.0	13.8	34	3.35	35	100
CF_4	3.78	10.0	16.0	54	6.38	63	120

Bethe formula and particle identification

- The formula holds in the high projectile mass limit – the projectile mass does not appear.
  - only the projectile velocity β and charge Z^2 are present;
  - at equal charge (± 1): particle identification below the $\gamma \approx 3$ "minimum ionising" dip;
  - differentiation by energy loss for particles of higher charge.

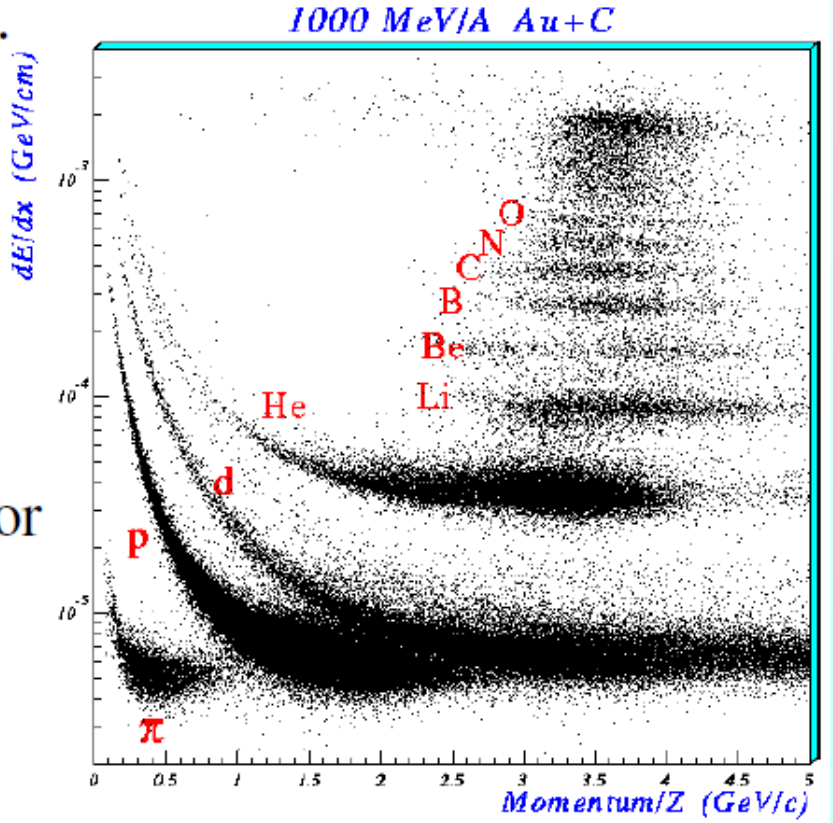

[Diagram: EOS collaboration]

Ionization

- gas-based detectors: ~50 e^--ion^+ pairs/cm;
- lH_2 bubble chamber: ~100 bubbles/cm;
- semi-conductor (Si): ~10^6 e^-/h pairs/cm

Virtual photon exchange

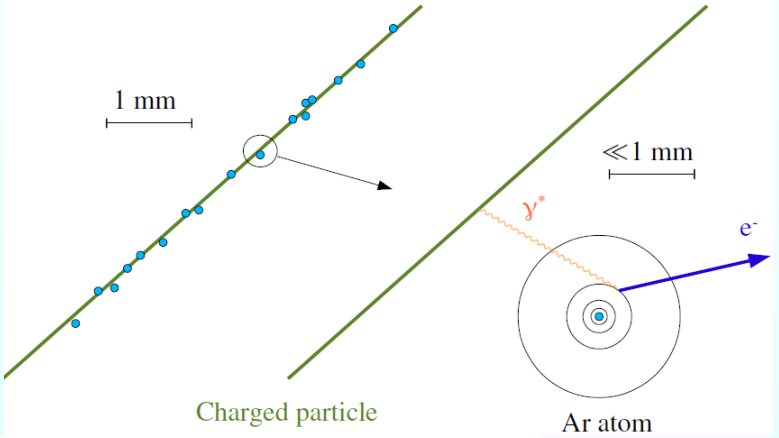

6. ATOMIC AND NUCLEAR PROPERTIES OF MATERIALS

Table 6.1 Abridged from pdg.lbl.gov/AtomicNuclearProperties by D. E. Groom (2007). See web pages for more detail about entries in this table including chemical formulae, and for several hundred other entries. Quantities in parentheses are for NTP (20° C and 1 atm), and square brackets indicate quantities evaluated at STP. Boiling points are at 1 atm. Refractive indices n are evaluated at the sodium D line blend (589.2 nm); values $\gg 1$ in brackets are for $(n-1)\times 10^6$ (gases).

Material	Z	A	$\langle Z/A\rangle$	Nucl.coll. length λ_T {g cm^{-2}}	Nucl.inter. length λ_I {g cm^{-2}}	Rad.len. X_0 {g cm^{-2}}	$dE/dx\|_{\rm min}$ { MeV g^{-1}cm^2}	Density {g cm^{-3}} ({gℓ^{-1}})	Melting point (K)	Boiling point (K)	Refract. index (@ Na D)
H_2	1	1.00794(7)	0.99212	42.8	52.0	63.04	(4.103)	0.071(0.084)	13.81	20.28	1.11[132.]
D_2	1	2.01410177803(8)	0.49650	51.3	71.8	125.97	(2.053)	0.169(0.168)	18.7	23.65	1.11[138.]
He	2	4.002602(2)	0.49967	51.8	71.0	94.32	(1.937)	0.125(0.166)		4.220	1.02[35.0]
N_2	7	14.0067(2)	0.49976	61.1	89.7	37.99	(1.825)	0.807(1.165)	63.15	77.29	1.20[298.]
O_2	8	15.9994(3)	0.50002	61.3	90.2	34.24	(1.801)	1.141(1.332)	54.36	90.20	1.22[271.]
F_2	9	18.9984032(5)	0.47372	65.0	97.4	32.93	(1.676)	1.507(1.580)	53.53	85.03	[195.]
Ne	10	20.1797(6)	0.49555	65.7	99.0	28.93	(1.724)	1.204(0.839)	24.56	27.07	1.09[67.1]
Ar	18	39.948(1)	0.45059	75.7	119.7	19.55	(1.519)	1.396(1.662)	83.81	87.26	1.23[281.]
Xe	54	131.293(6)	0.41129	100.8	172.1	8.48	(1.255)	2.953(5.483)	161.4	165.1	1.39[701.]

- A minimum-ionising particle loses (only !)

$$1.519\,\mathrm{MeV\,cm^2/g}\times 1.662\times 10^{-3}\,\mathrm{g/cm^3} = 2.5\,\mathrm{keV/cm}$$

Ionization

from e.g. `http://www.webelements.com`

Shell	Orbital	Binding energy
K	1s	3205.9 eV
L I	2s	326.3 eV
L II	2p 1/2	250.6 eV
L III	2p 3/2	248.4 eV
M I	3s	29.3 eV
M II	3p 1/2	15.9 eV
M III	3p 3/2	15.76 eV

- One might expect $2.5\,\mathrm{keV/cm} \div 15.8\,\mathrm{eV/e^-} \approx 160\,\mathrm{e^-/cm}$

- Heed, a photo-absorption & ionisation model, finds for a minimum ionising μ±:
  - Peak: $n_e = 41/\mathrm{cm}$
  - "Mean": $n_e = 72/\mathrm{cm}$
- Degrad, an e⁻ transport program, finds for an e⁻ at the same βγ:
  - Peak: $n_e = 50/\mathrm{cm}$
  - "Mean": $n_e = 62/\mathrm{cm}$
- Mean is ill-defined due to rare but large deposits.

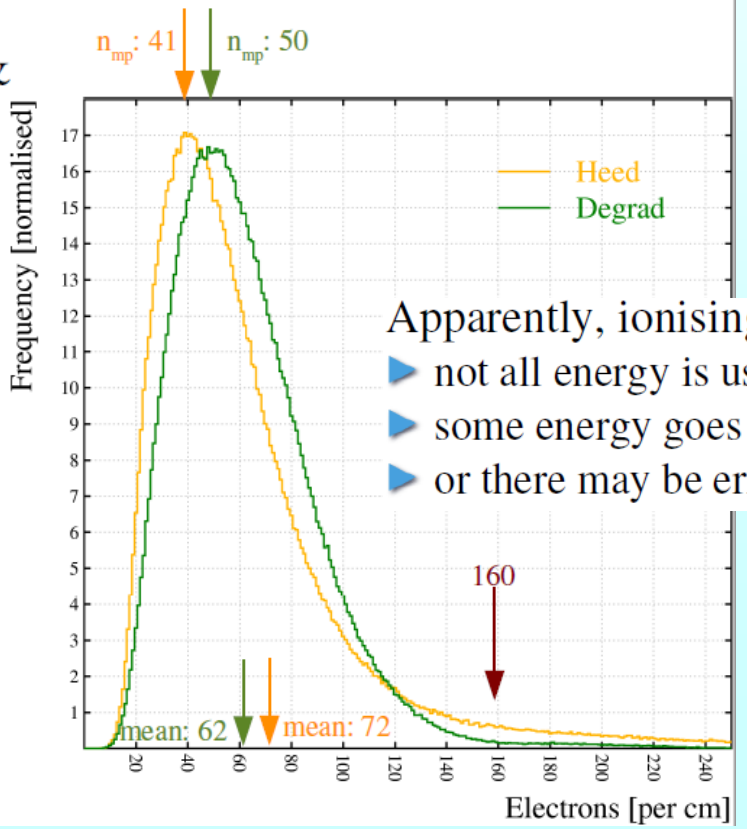

Apparently, ionising takes more than the binding energy:
- not all energy is used (→ Fano factor),
- some energy goes into excitations (→ Work function),
- or there may be errors in the d*E*/d*x* tables ?

Ionization

Electrons are not evenly spaced, not even exponentially:

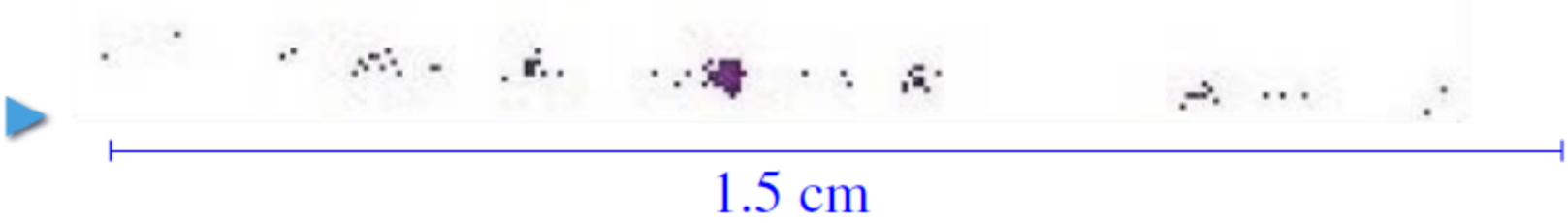

- 25-30 clusters/cm

δ-electrons

- Deposits are not always "lumps":

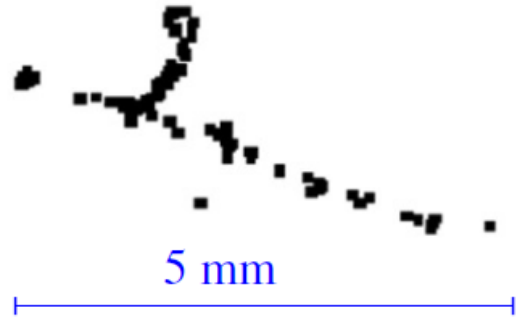

Number of primary ionising interactions per cm in Ar,

- by $\mu^{\pm}$ at minimum ionising energy,
- at 300 K and 1 atm,

according to

Degrad:	23.1 / cm
Heed:	24.1 / cm
Rieke-Prepejchal:	24.3 / cm
CERN 77-9:	29.4 / cm

De-excitation

Ralph de Laer Kronig
(1904-1995)

Dirk Coster
(1889-1950)

Lise Meitner
(1878-1968)

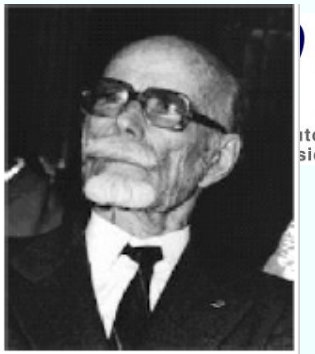

Pierre Victor Auger
(1899-1993)

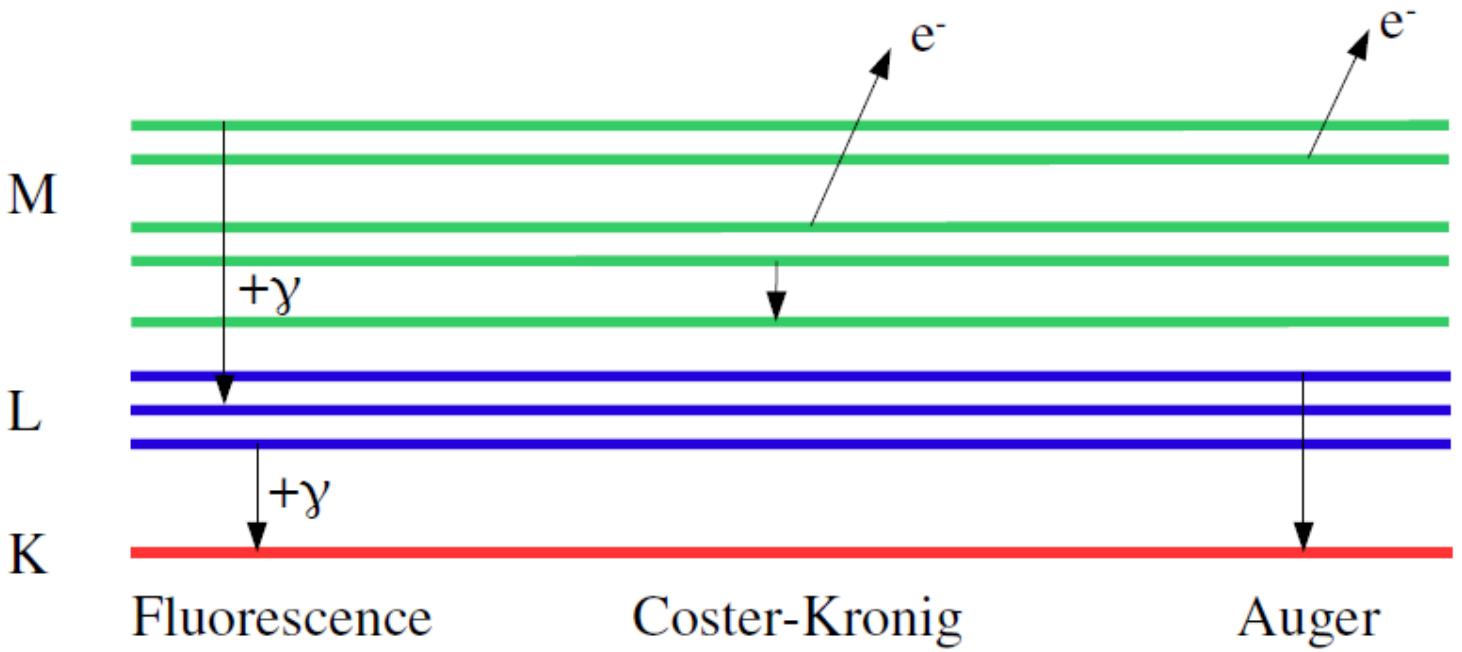

References:

D. Coster and R. de L. Kronig, Physica **2** (1935) 13-24.

Lise Meitner, *Über die β-Strahl-Spektra und ihren Zusammenhang mit der γ-Strahlung*, Z. Phys. **11** (1922) 35-54.

L. Meitner, *Das β-Strahlenspektrum von UX_1 und seine Deutung*, Z. Phys. **17** (1923) 54-66.

P. Auger, Comptes rendus hebdomadaires des séances de l'Académie des sciences, 1923/07 (T177)-1923/12, 169-171.

P. Auger, J. Phys. Radium **6** (1925) 205.

De-exitation

K Yields

- Light atoms de-excite by Auger e$^-$ emission, heavy atoms via fluorescence.
- Precision of the fluorescence yields:
  - Ar: ~5 %
  - Xe: ~1 %

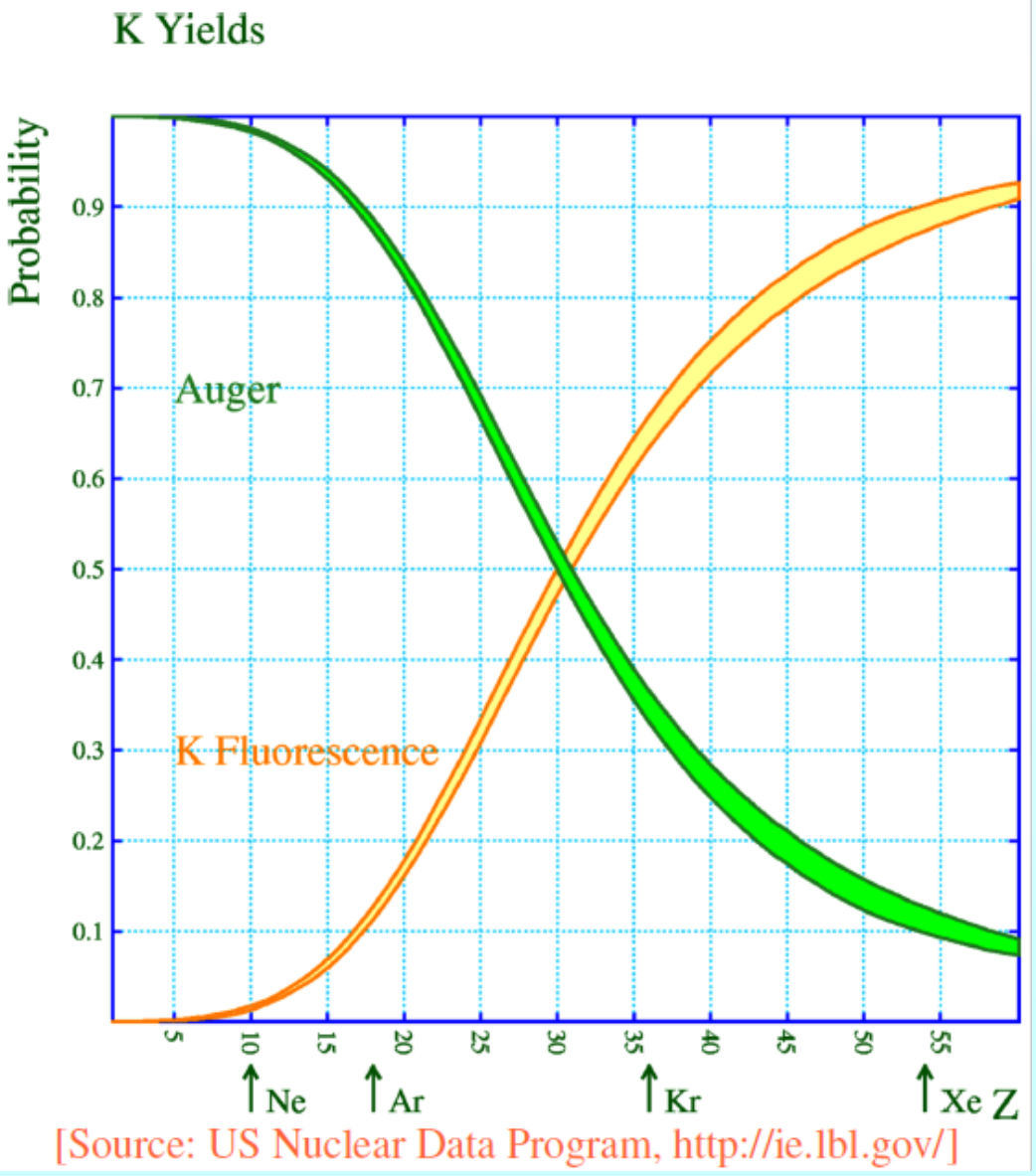

[Source: US Nuclear Data Program, http://ie.lbl.gov/]

Photo-absorption in Ar

- Argon has 3 shells, hence 3 groups of lines:

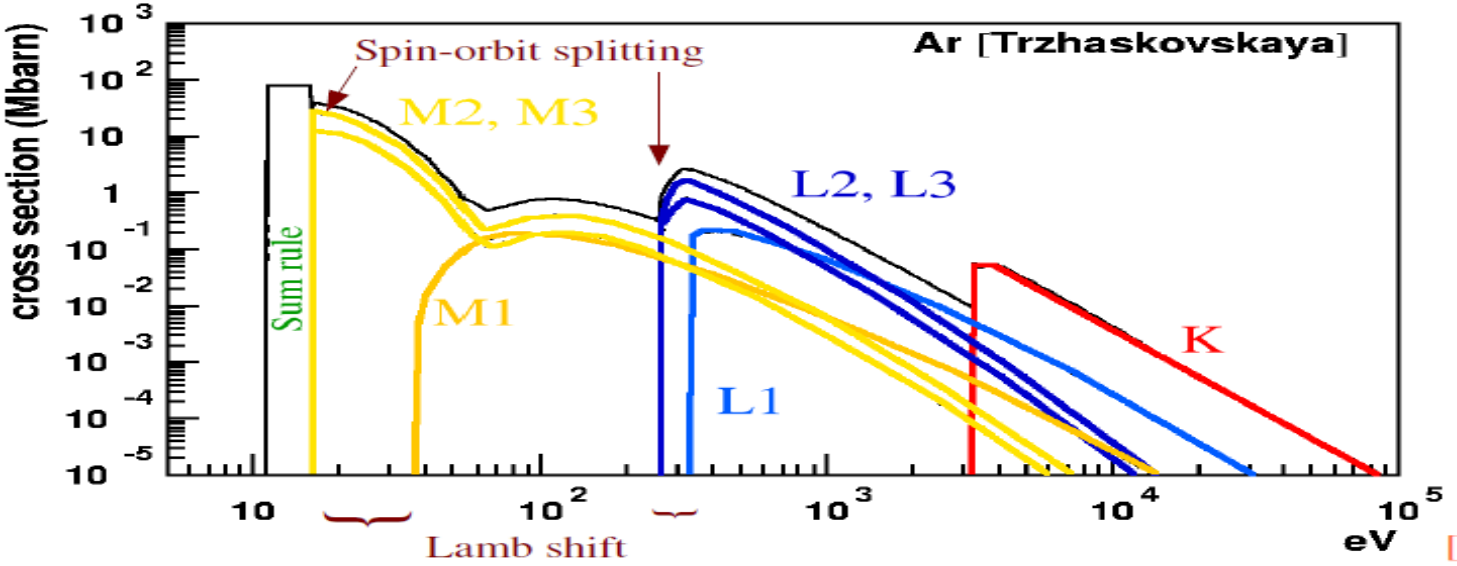

K = 1s

L1 = 2s
L2 = 2p 1/2
L3 = 2p 3/2

M1 = 3s
M2 = 3p 1/2
M3 = 3p 3/2

[Plot from Igor Smirnov]

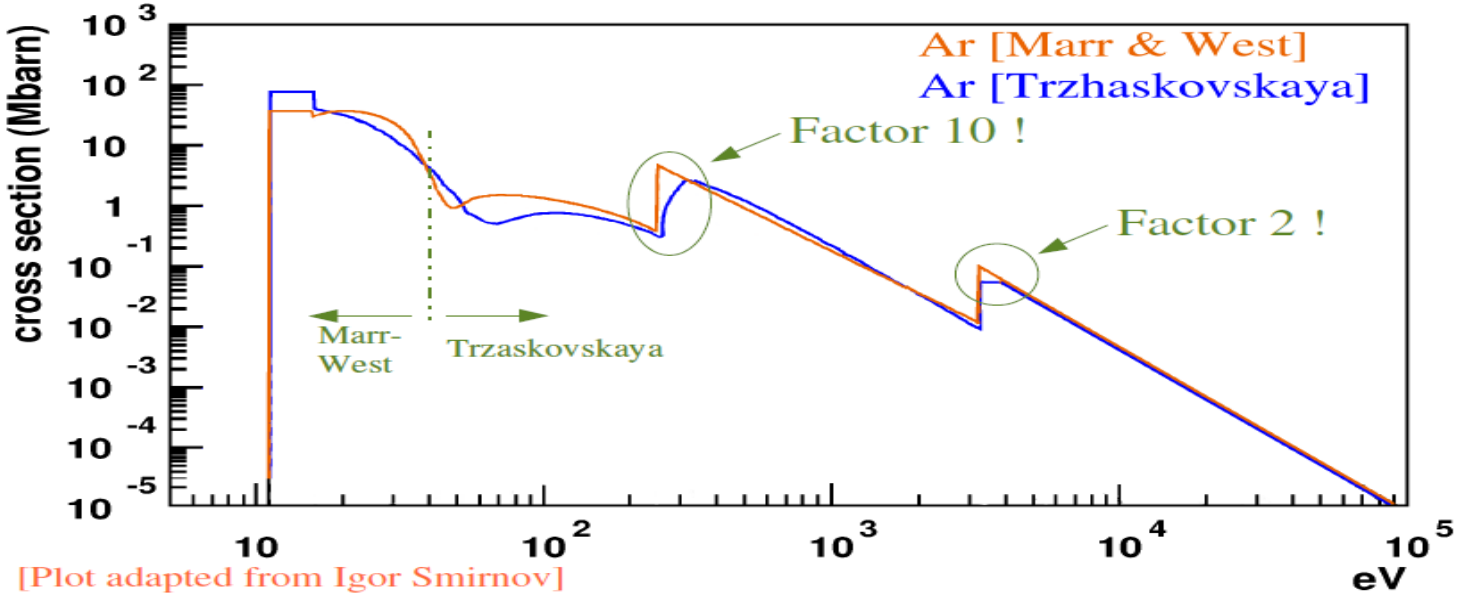

[Plot adapted from Igor Smirnov]

Ionization summary

- Primary ionisation: (~25/cm in Ar)
  - photo-ionisation:
    - emission of a photo-electron (PAI, energy can be low or high);

  - de-excitation of ion^{+*}:
    - emission of Auger electron;
    - emission of fluorescence photon.

- Secondary ionisation:
  - Auger- and photo-electrons above IP ("δ-electron") dissipate their energy by making a string of low-energy electrons;
  - fluorescence photons escape or ionise.

- Yield: most probably 40-50 electrons + ions per cm of Ar, and they are not evenly spread.

- Ionisation electrons are typically produced at sub-μm distances from the track, but they can be at several mm.

Mean distance between Ar atoms

Amedeo Avogadro
(1776-1856)

Atoms per unit volume

- Number of Ar atoms in a cm³: [273.15 K, 100 kPa]
  - Avogadro's number: $6.022\ 10^{23}$ atoms/mole ÷
  - atomic weight of Ar: 39.948 g/mole ×
  - density of Ar: $1.761\ 10^{-3}$ g/cm³ ≈
  - Loschmidt constant n_0: $2.652\ 10^{19}$ atoms/cm³

- Distance between neighbouring Ar atoms:

$$\frac{4}{3}\pi r^3 \times n_0 = 1: \quad \text{distance} = 2r \approx 4\,\text{nm}$$

Josef Loschmidt
(1821-1895)

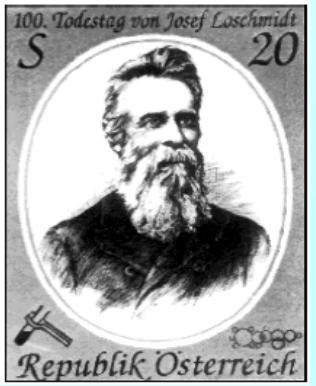

Electron Cross-section

Remember the unit:
1 Mb = 10^{-18} cm^2
100 Mb = 10^{-16} cm^2

Cross section of argon

- Cross section in a hard-sphere model:
  - Radius: ~70 pm
  - Surface: $\sigma = \pi(70\ 10^{-10}\,\mathrm{cm})^2 \approx 1.5\ 10^{-16}\,\mathrm{cm}^2 = 150\,\mathrm{Mb}$

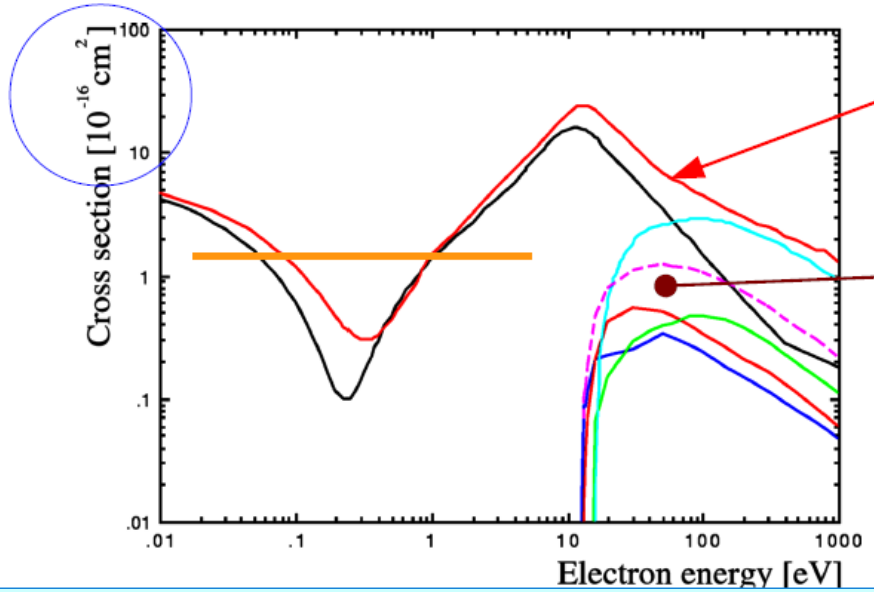

Elastic cross section (total)

Excitations, ionisation, attachment

[Data: webelements.com
Plot: simplified Magboltz]

Electron mean free path in Ar

- We know already that:
  - Cross section of 1 atom: $\sigma \approx 1.5\ 10^{-16}$ cm^2
  - Atoms per volume: $n_0 \approx 2.7\ 10^{19}$ atoms/cm^3

- Mean free path for an electron ?
  - An electron hits all atoms of which the centre is less than a cross section σ radius from its path;
  - over a distance L, the electron hits $n_0\ \sigma\ L$ atoms;
  - mean free path = distance over which it hits 1 atom;

$$\lambda_e = 1/(\sigma\ n_0) \approx 2.5\ \mu m$$

  - much larger than
    - 4 nm distance between atoms, and
    - 140-600 pm typical gas molecule diameters.

Electron drift velocity

- Imagine that an electron stops every time it collides with a gas molecule and then continues along E.

- To cover a distance λ_e, it will need a time t:

$$\frac{1}{2}\frac{qE}{m_e}t^2=\lambda_e, \quad i.e. \quad t=\sqrt{\frac{2\lambda_e m_e}{qE}}, \quad i.e. \quad \bar{v}=\frac{\lambda_e}{t}=\sqrt{\frac{\lambda_e qE}{2m_e}}$$

- For example:

$$\bar{v} \approx 13\,\mathrm{cm}/\mu\mathrm{s} \quad \text{for} \quad E = 1\,\mathrm{kV/cm}$$

The measured values are much smaller

Electron drift velocity

Adding CO_2

- CO_2 makes the gas faster, dramatically.
- Calculated by Magboltz for Ar/CO_2 at 3 bar.

(Note where the arrow is !)

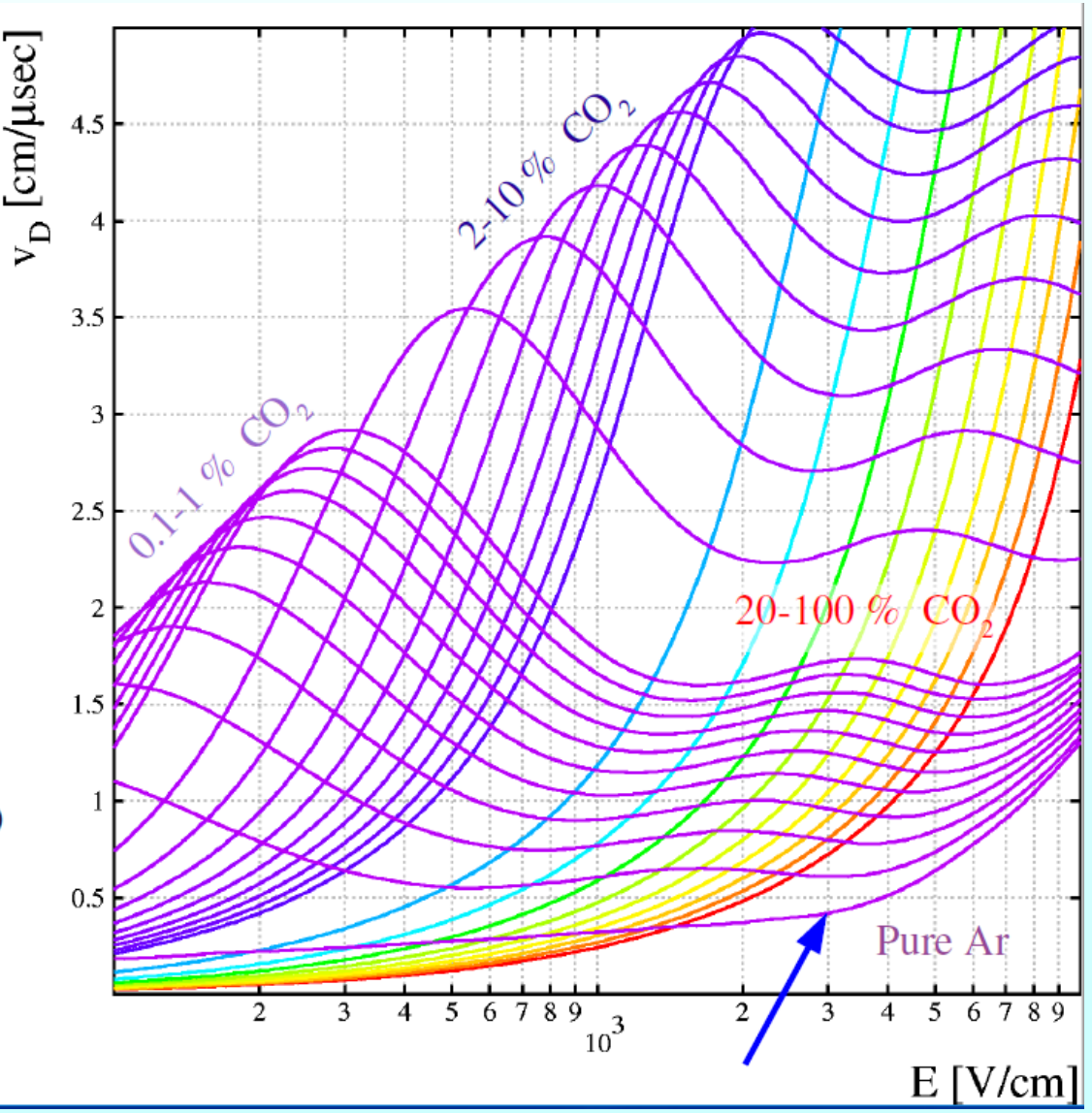

Inelastic cross-section

CO_2 – vibration modes

- CO_2 is linear:
  - O – C – O
- Vibration modes are numbered V(*ijk*)
  - *i*: symmetric,
  - *j*: bending,
  - *k*: anti-symmetric.

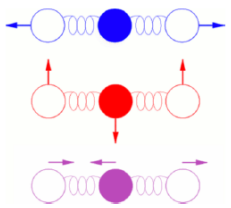

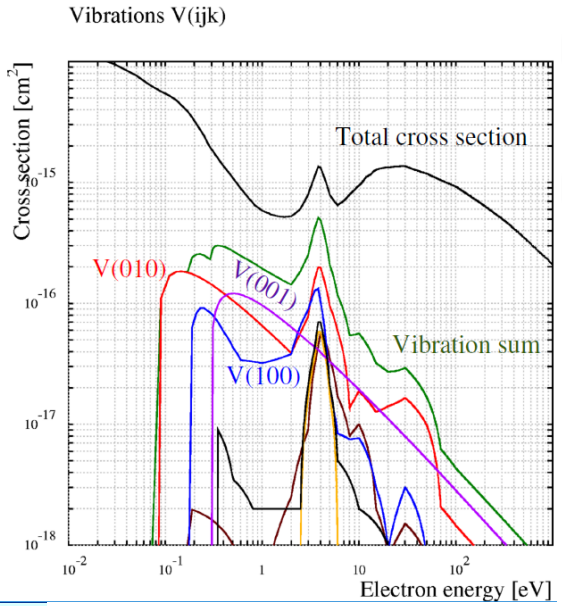

CO_2 – rotational modes

- Major cross section at an energy of ~1 eV.
- Implemented as pairs of inelastic and super-elastic terms.

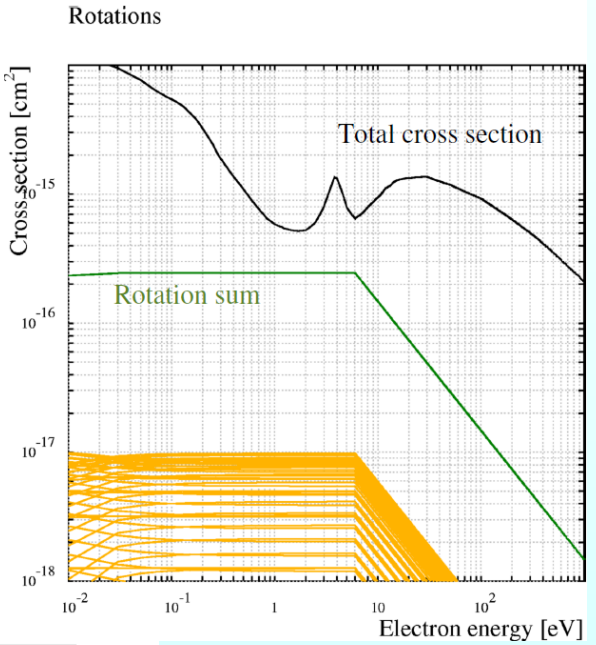

CO_2 – polyads

- Fermi polyads:
  - Closely spaced vibrational & rotational levels which couple by overlap.
  - Magboltz separates polyads 3-9 and sums the higher ones.
- Cause energy loss.

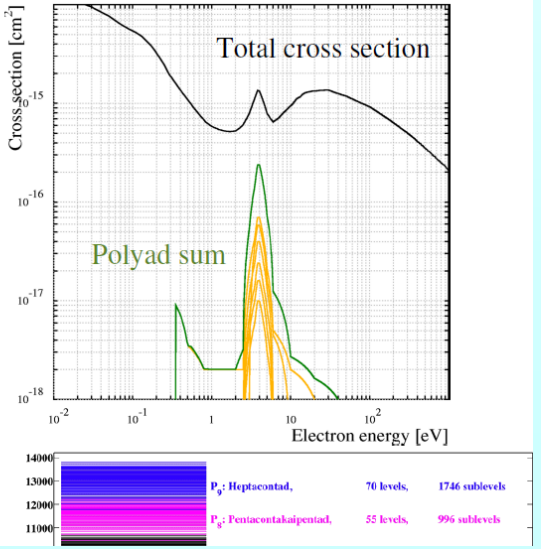

Electron transport simulation

Electrons in Ar/CO_2 at E=1 kV/cm

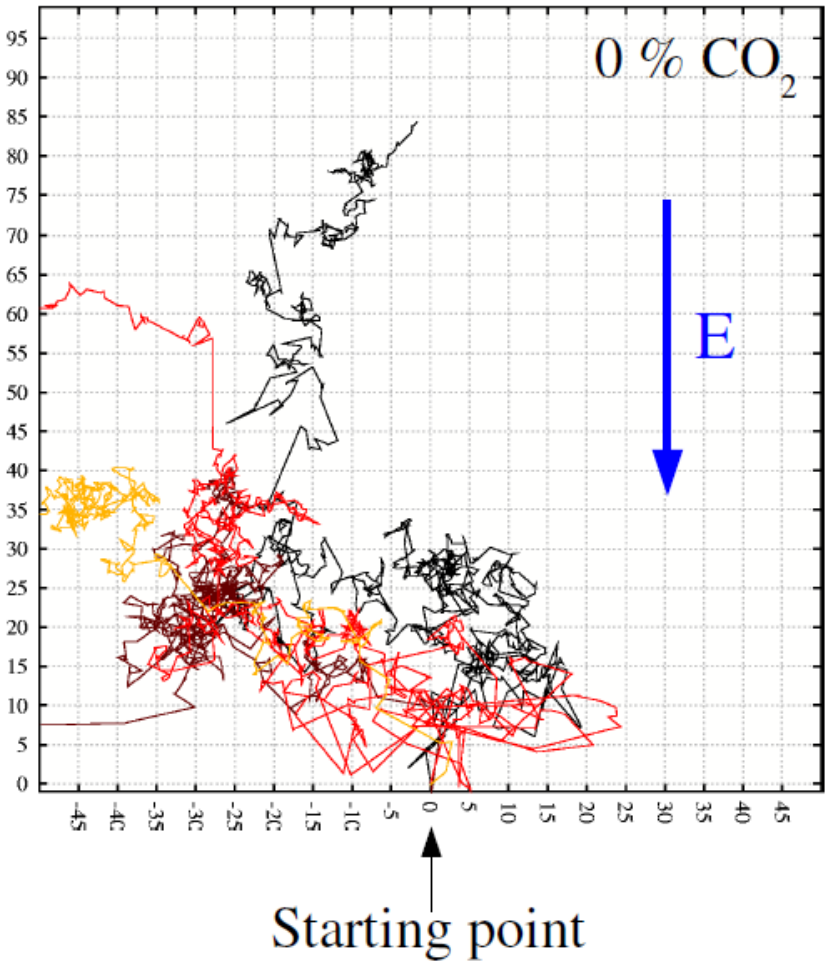

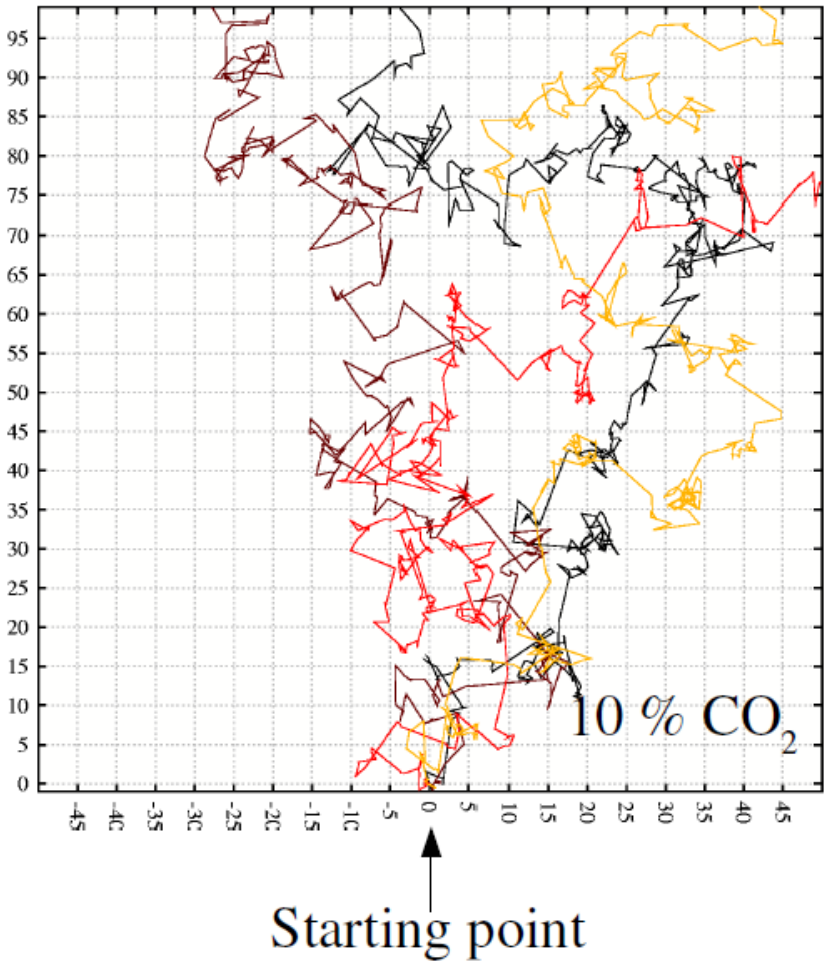

Electron transport simulation

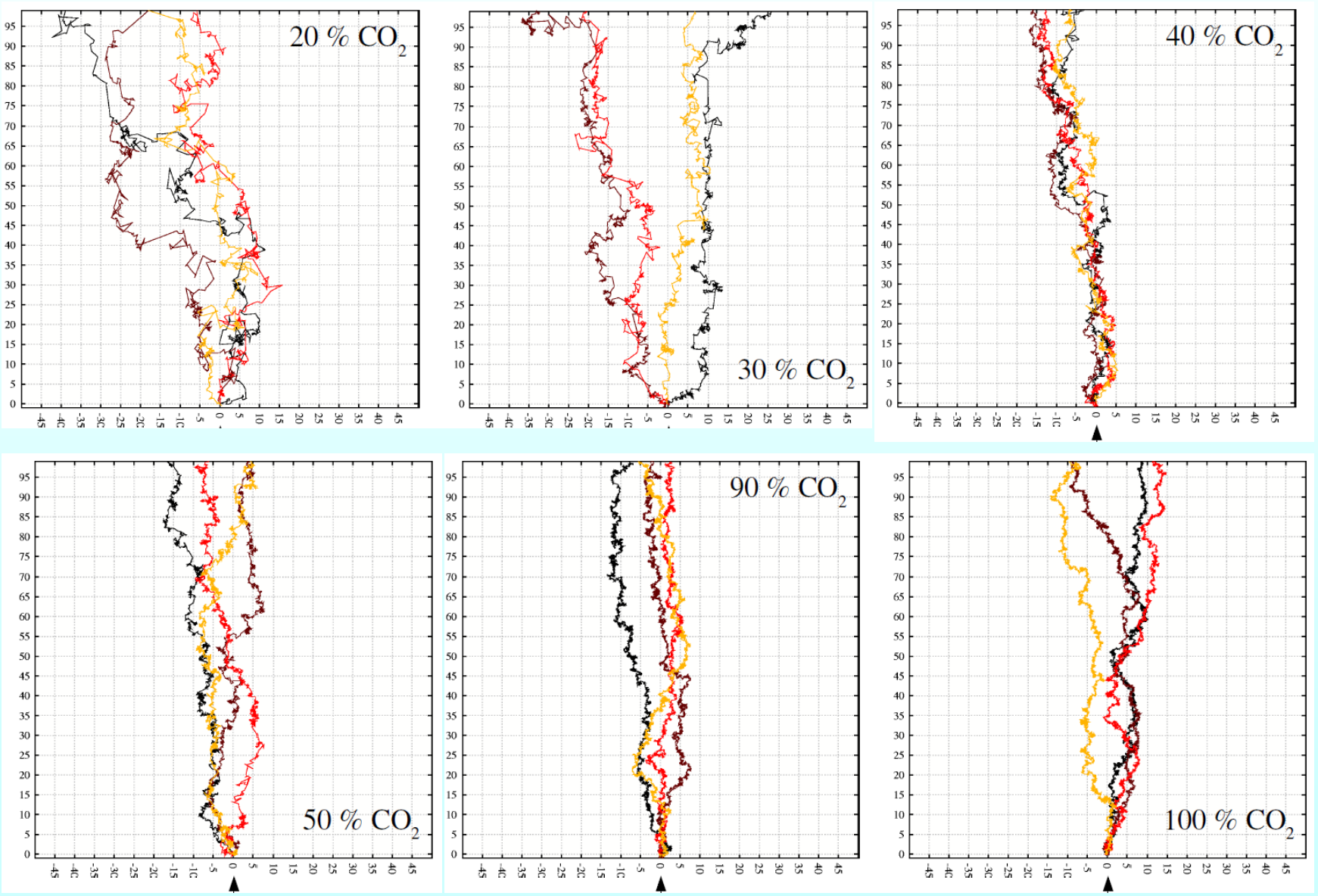

Electron Cross-section

Energy dependence of e^- scattering

- Elastic scattering:
  - dominant contribution for much of the energy range that concerns us;
  - only term < 15.7 eV (ionisation threshold).
- Non-trivial structure:
  - Ramsauer dip.

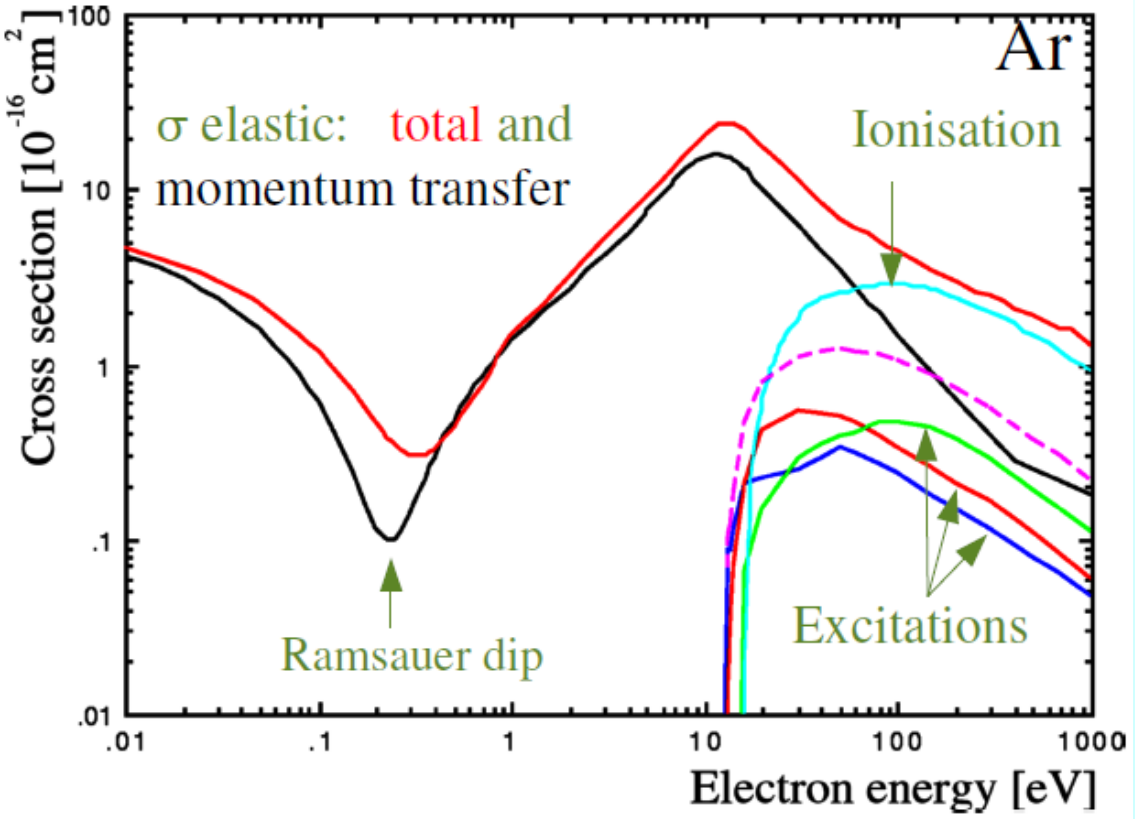

Townsend coefficient

- Energy after a distance λ_e:
  - $\epsilon = E\lambda_e, \quad \lambda_e \approx 2.5\,\mu\,\mathrm{m}$
- ionisation energy of argon:
  - $IP \sim 15.7$ eV
- ionisation would occur at:
  - $E > 60$ kV/cm,
  - indeed a typical field for multiplication, avalanches start much earlier, though.

- α: Townsend coefficient, # new e^- per unit length.

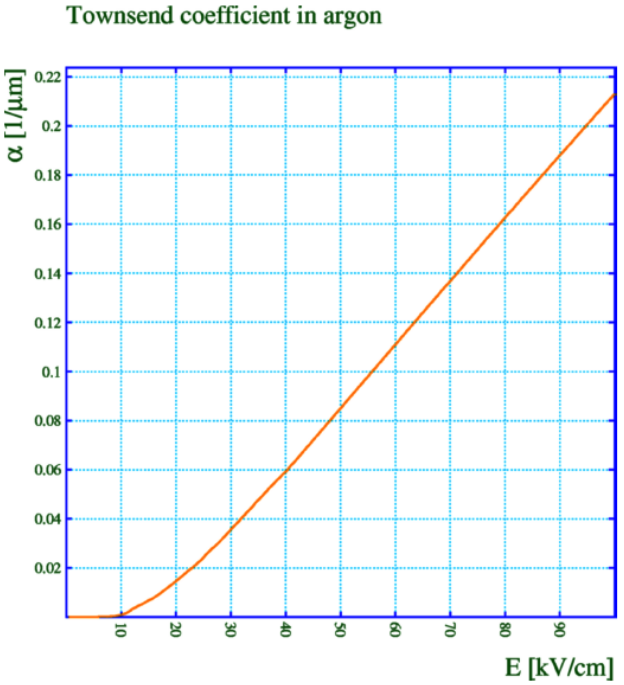

- Townsend coefficient α: probability per unit length that an electron creates an additional electron.

- Avalanches grow proportionally to their size:

$$\mathrm{d}\,n(x) = n(x)\,\alpha(x)\;\mathrm{d}\,x$$

$$n(x) = n(0)\,e^{\int_0^x \alpha(y)\,\mathrm{d}\,y}$$

Gaseous detectors regimes

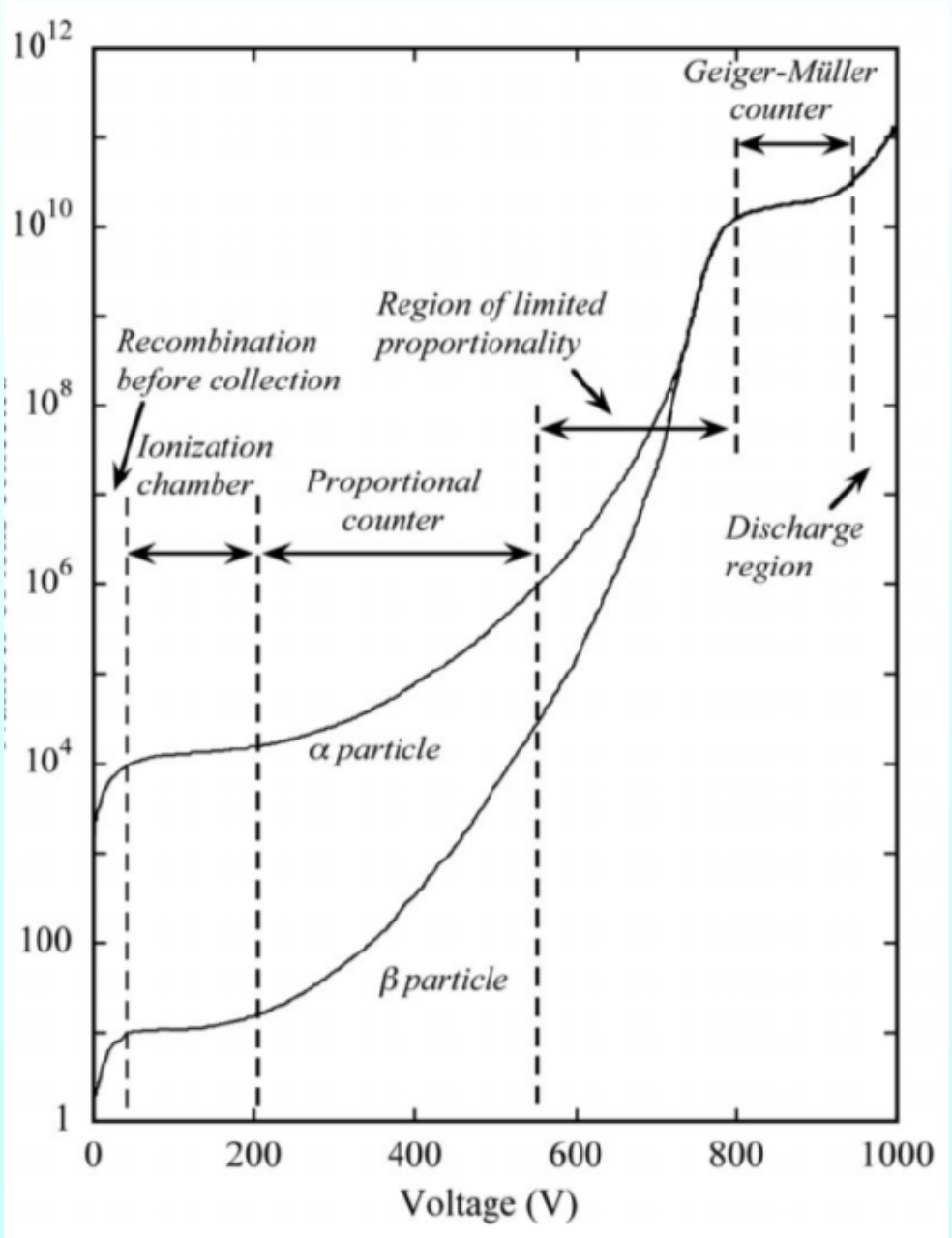

Induction signals

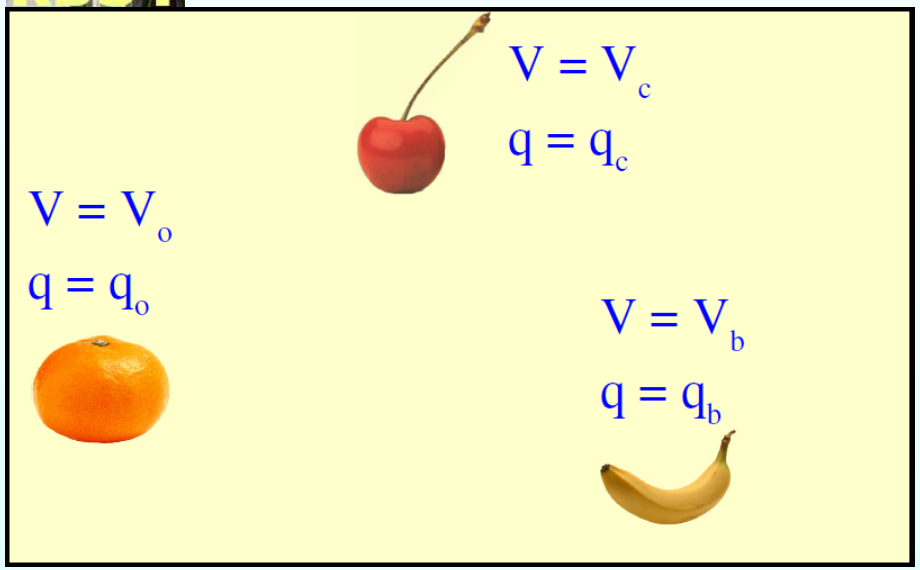

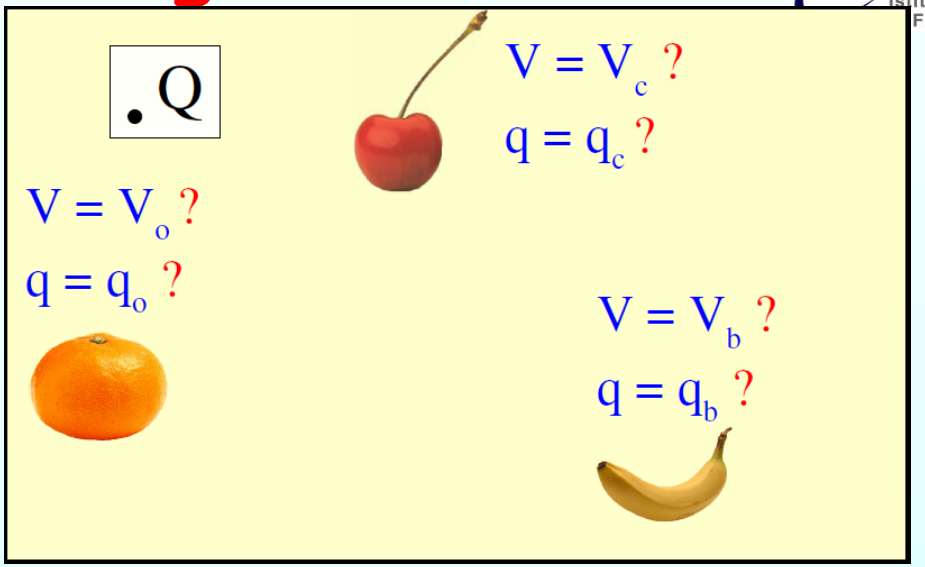

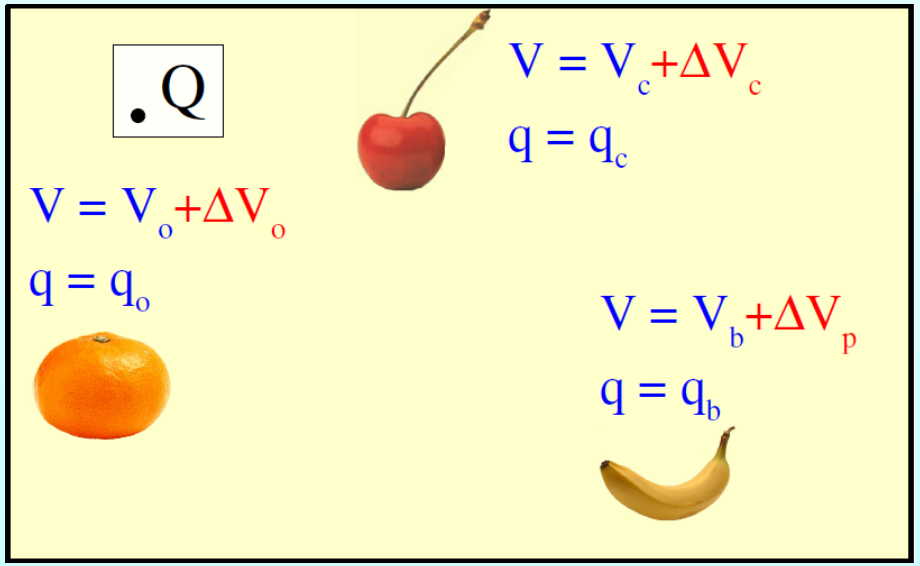

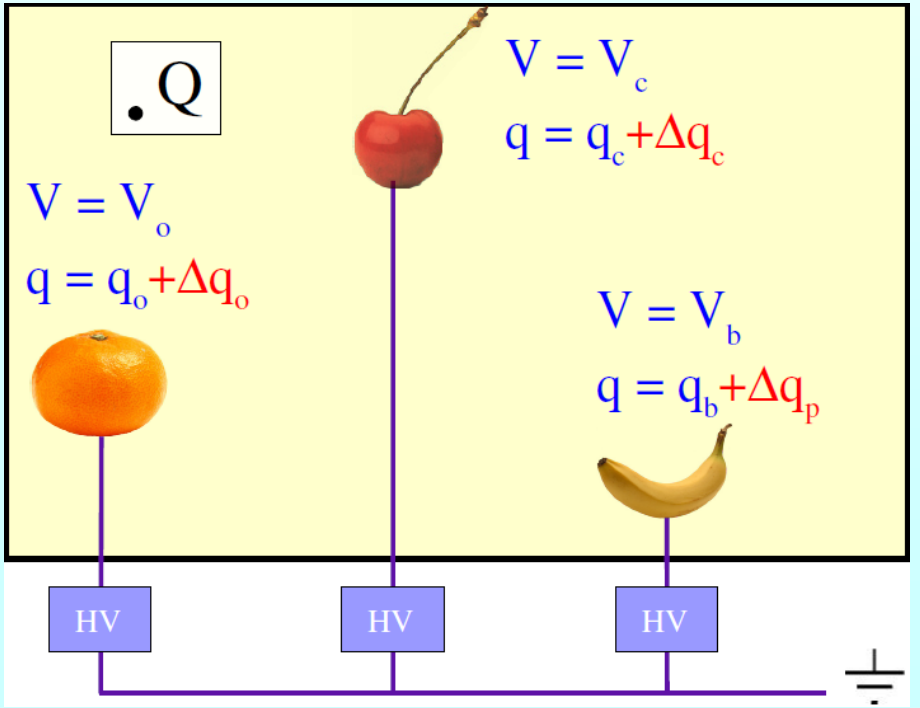

Induction signals

No charge creation:

$\Delta q_o + \Delta q_c + \Delta q_p = 0$

Properties of the current induced in an electrode:

- proportional to the charge Q;
- proportional to the velocity of the charge $\vec{v}_d$;
- dependent on the geometry.

$$I = -Q\,\vec{v}_d \cdot \vec{E}_W$$

The geometry is contained in $\vec{E}_W$, necessarily a vector, the *weighting field*:

- each electrode has its own weighting field;

Weighting field – examples

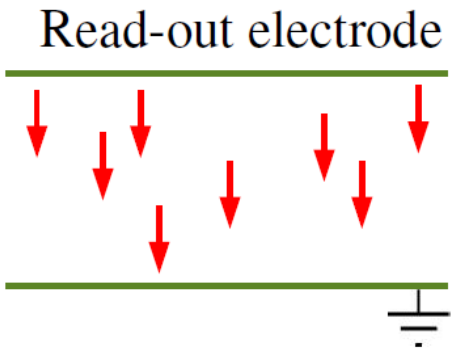

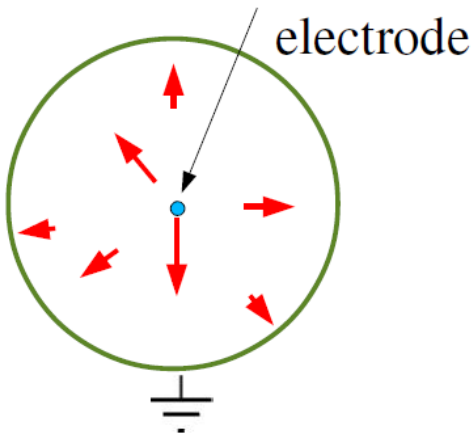

$$I_{tot}(t) = \sum_i I_i(t) = 0$$

the sum of all currents is zero at all times.

Induction signals

Observe that the following are equivalent in terms of *total* charge induced – the time dependence will differ:

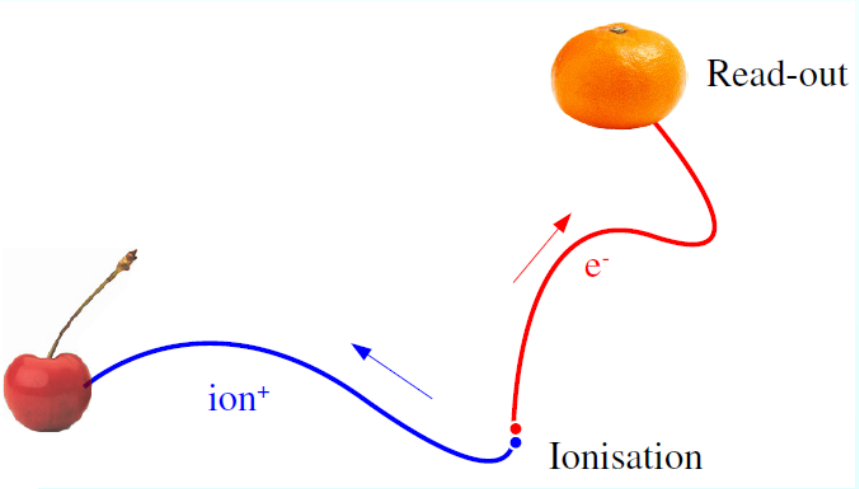

Parallel plate chamber with:

- d = 1 mm — gap
- α = 100/cm — field & gas chosen accordingly
- $\lambda = 1/\alpha$ = 100 μm — mean free path of ionisation
- $G = \exp(\alpha\, d)$ = 22000 — average gain

The avalanche reaches half its final size at a distance $\lambda \log(2)$ = 70 μm from the cathode.
The weighting potential there is 1 – 70/1000 = 0.930.

Of each electron-ion pair created there, the

- electron induces 7 % and the
- ion 93 % of the total charge.

Induced charges

A point charge q at a distance z_0 above a grounded metal plate 'induces' a surface charge.

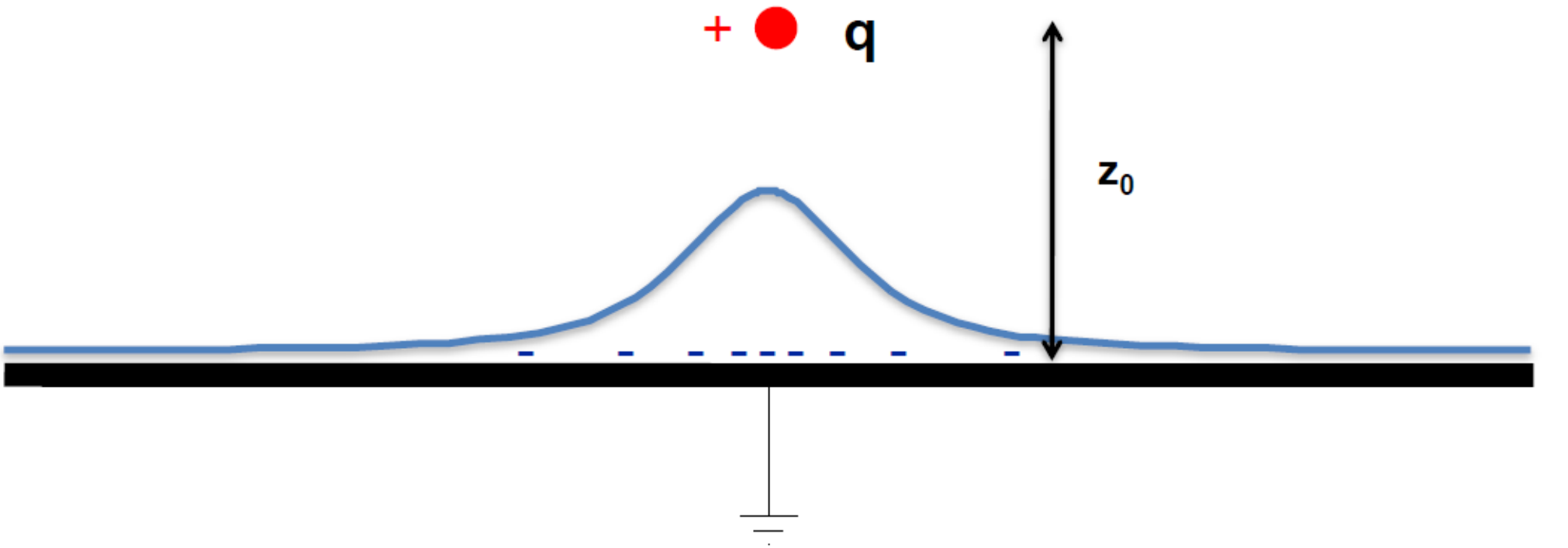

Induced charges

The total charge induced by a point charge q on an infinitely large grounded metal plate is equal to –q, independent of the distance of the charge from the plate.

The surface charge distribution is however depending on the distance z_0 of the charge q.

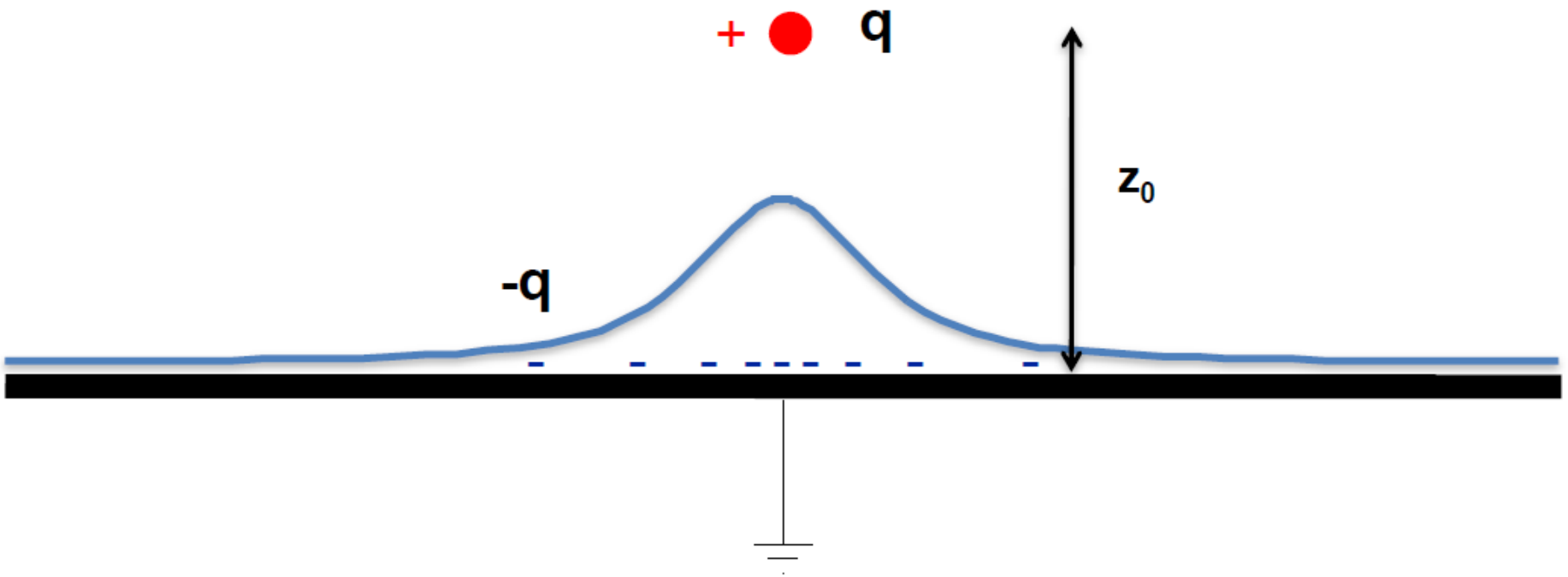

Induced charges

Moving the point charge closer to the metal plate, the surface charge distribution becomes more peaked, the total induced charge is however always equal to –q.

$$\sigma(x,y) = -\frac{qz_0}{2\pi(x^2+y^2+z_0^2)^{\frac{3}{2}}}$$

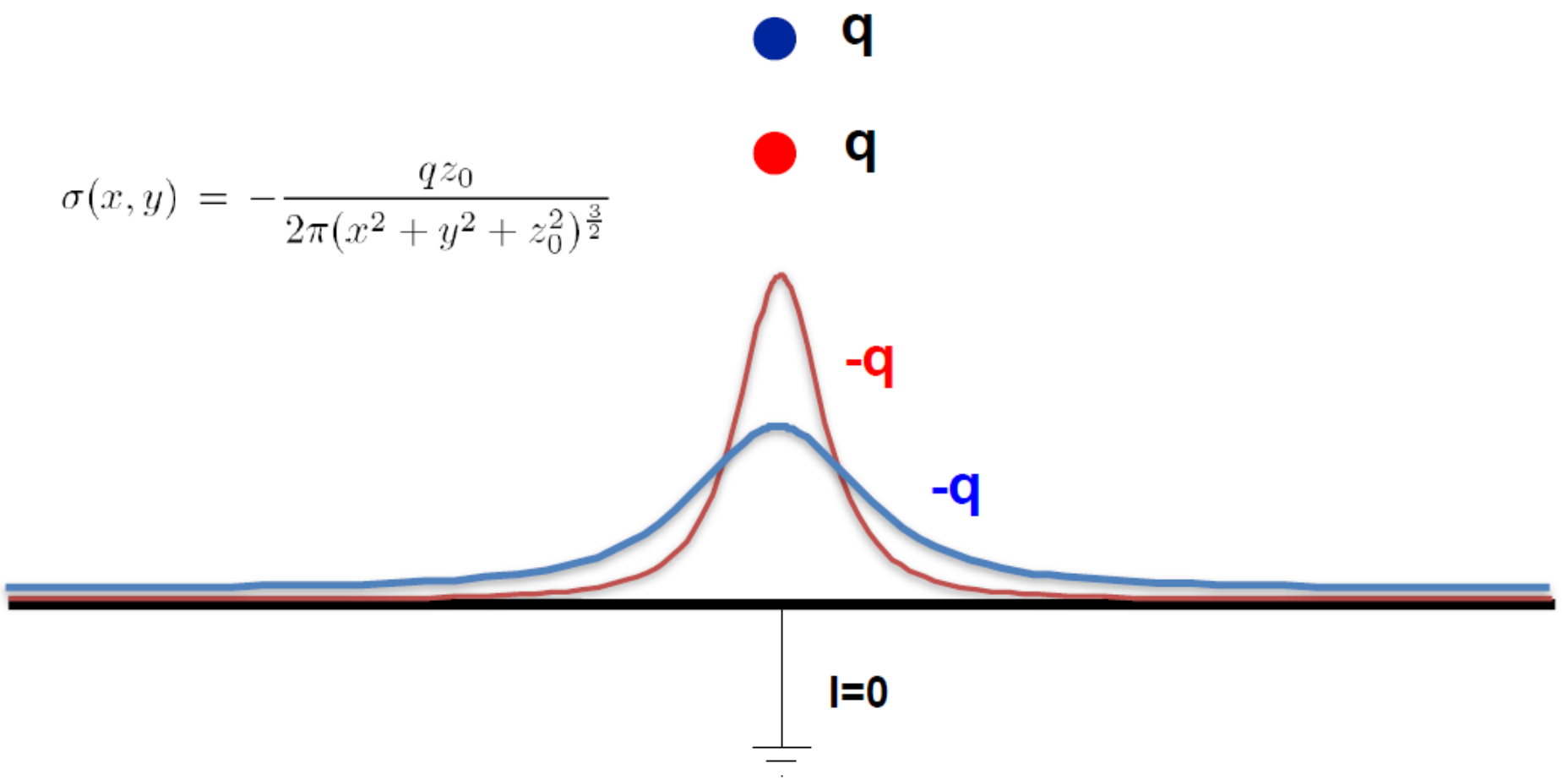

Induced charges

If we segment the grounded metal plate and if we ground the individual strips, the surface charge density doesn't change with respect to the continuous metal plate.

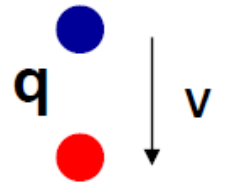

The charge induced on the individual strips is now depending on the position z_0 of the charge.

If the charge is moving there are currents flowing between the strips and ground.

→ The movement of the charge induces a current.

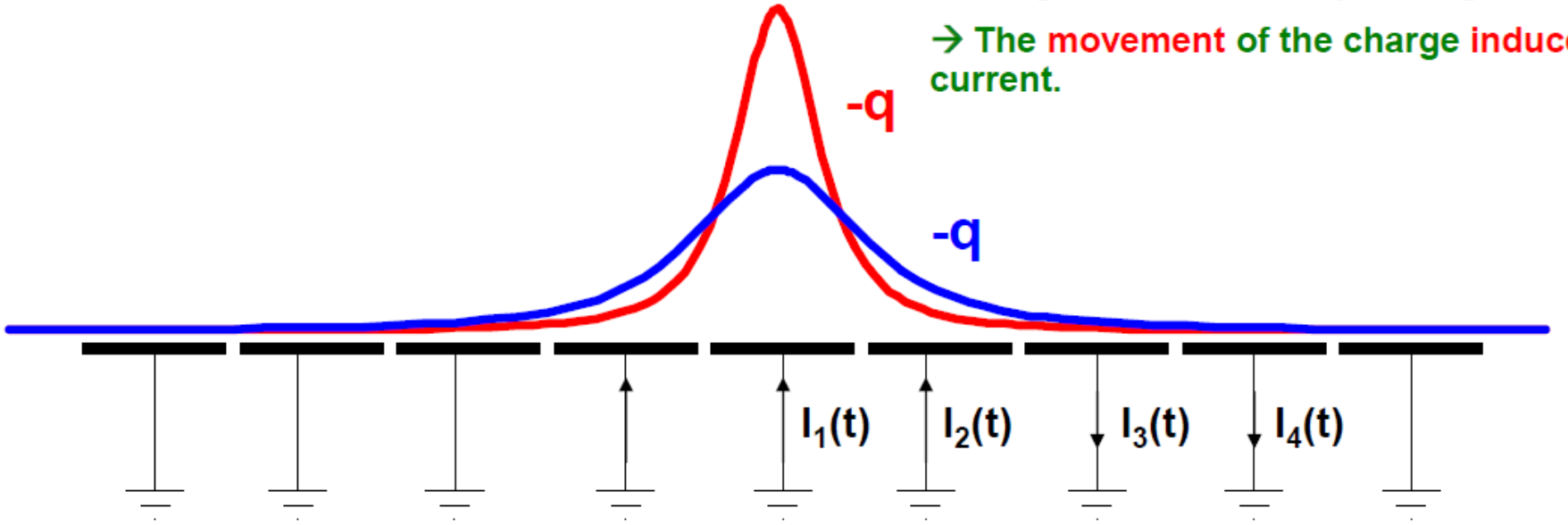

$$Q_1(z_0) = \int_{-\infty}^{\infty}\int_{-w/2}^{w/2} \sigma(x,y)dxdy = -\frac{2q}{\pi}\arctan\left(\frac{w}{2z_0}\right) \qquad z_0(t) = z_0 - vt$$

$$I_1^{ind}(t) = -\frac{d}{dt}Q_1[z_0(t)] = -\frac{\partial Q_1[z_0(t)]}{\partial z_0}\frac{dz_0(t)}{dt} = \frac{4qw}{\pi[4z_0(t)^2 + w^2]}v$$

The signal is not from "collected" charges

Imagine an avalanche in a drift tube, caused by a single electron.
Let's assume that the gas gain is 10^4.
We read out the wire signal with an ideal integrator

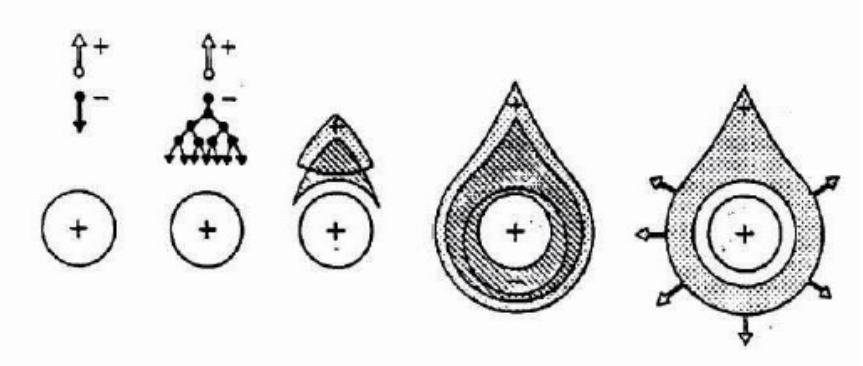

The 10^4 electrons arrive at the wire within <1ns, so the integrator should instantly see the full charge of -10^4 e_0 electrons ?

No ! The ions close to the wire induce the opposite charge on the wire, so in the very beginning there is zero charge on the integrator and only once the Ions have moved away from the wire the integrator measures the full -10^4 e_0

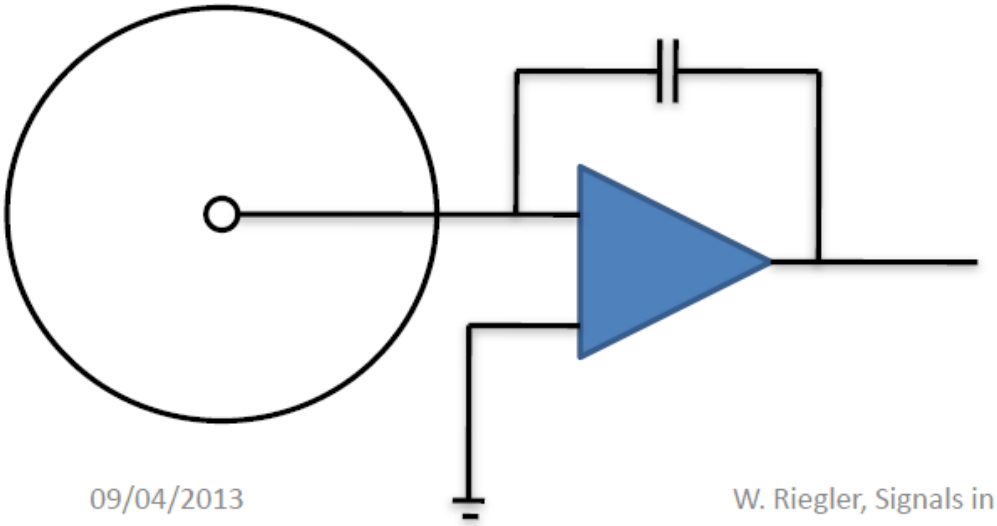

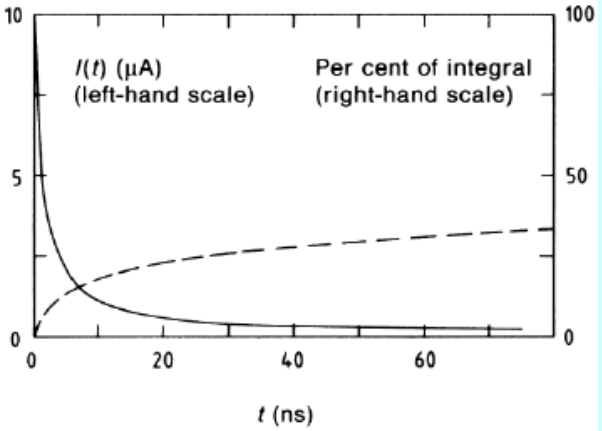

MWPCs

Extraordinary success and ubiquitous use of MWPCs: in many discoveries they played an essential role

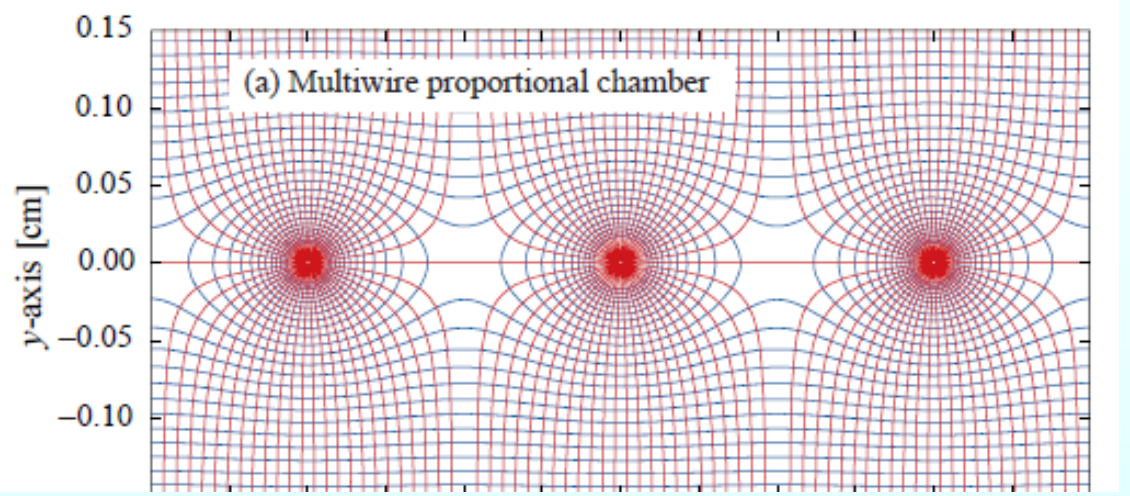

I think every experimental physicist working with gaseous detector should try to build and operate a small MWPC in his lab

if you search for the word "catastrophic" in the 2016 Review of Particle Physics, you will find it only ones, for the effects of electrostatic forces on MWPC wires non countered by a sufficiently large mechanical tension:

Because of electrostatic forces, anode wires are in equilibrium only for a perfect geometry. Small deviations result in forces displacing the wires alternatively below and above the symmetry plane, sometimes with catastrophic results. These displacement forces are countered by the mechanical tension of the wire, up to a maximum unsupported stable length, L_M [58], above which the wire deforms:

$$L_M = \frac{s}{CV_0}\sqrt{4\pi\epsilon_0 T_M}$$

Table 33.7: Maximum tension T_M and stable unsupported length L_M for tungsten wires with spacing s, operated at $V_0 = 5$ kV. No safety factor is included.

Wire diameter (μm)	T_M (newton)	s (mm)	L_M (cm)
10	0.16	1	25
20	0.65	2	85

Even the best wires (Au coated, Rhenium/Tungsten) with a diameter of 5 µm cannot hold the tension needed to operate a 10 cm long MWPC.

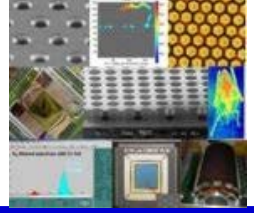

GASEOUS DETECTORS

was the only approach to achieve good space resolution before introducing the Si trackers

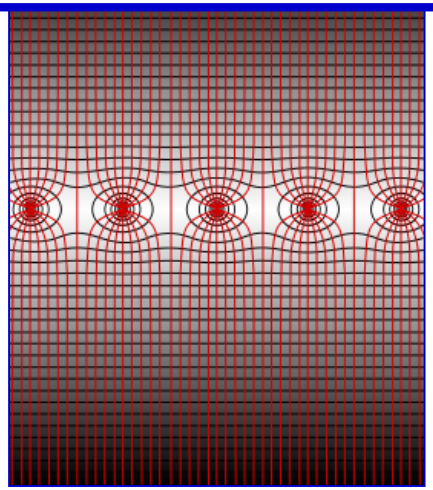

Still today the only way to equip large volumes at a reasonable cost, with good space resolution and limited material budget

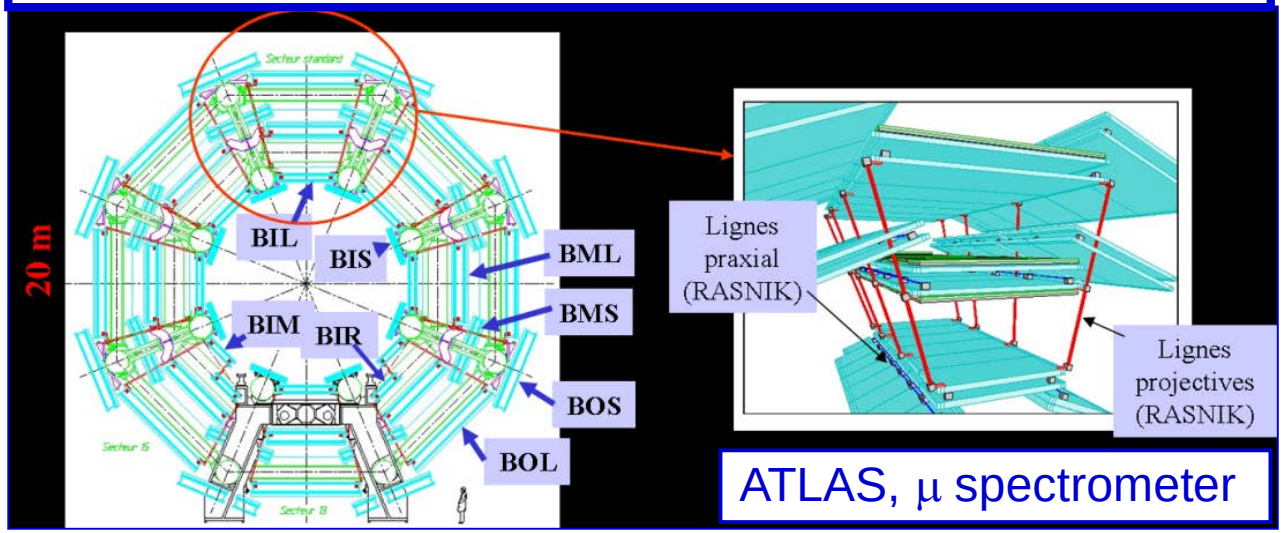

ATLAS, μ spectrometer

Time resolution record in extended counters

RPC: $\sigma_t \leq 1$ ns

trigger in ALICE, ATLAS, CMS

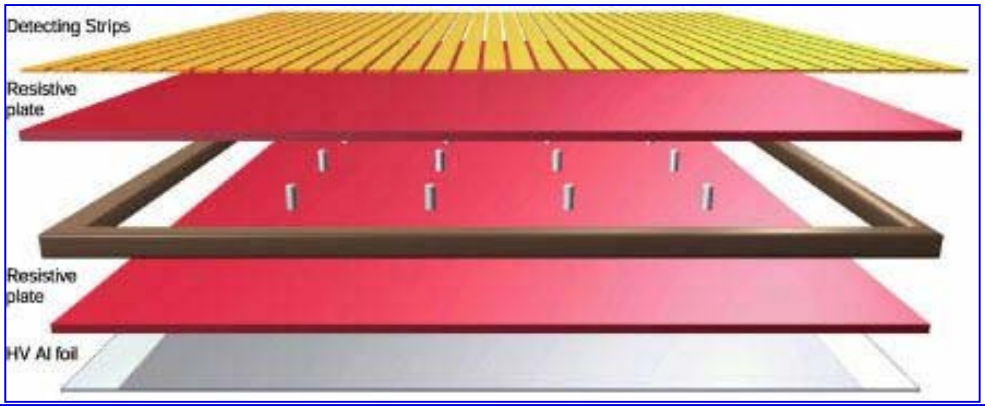

After MWPCs

Advantages of gas detectors:

- low radiation length
- large areas at low price
- flexible geometry
- space and energy resolution

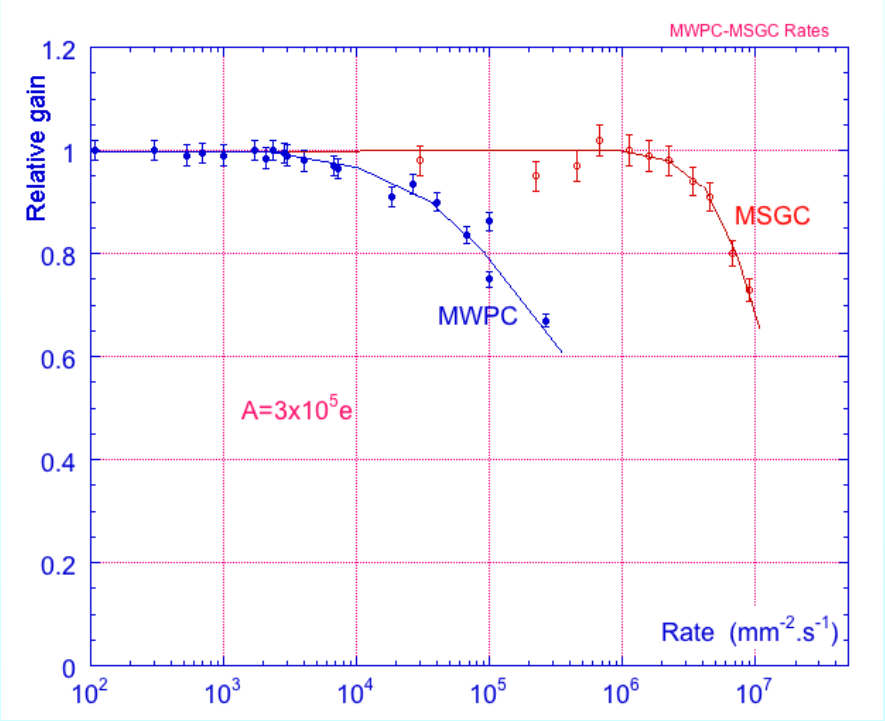

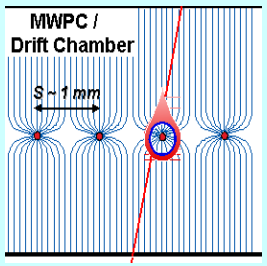

Amplifying cell size reduction by factor of 10

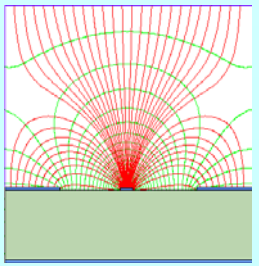

EXAMPLES OF ORGANIC POLYMERS AND SILICON COMPOUNDS DEPOSITS IN MWPC

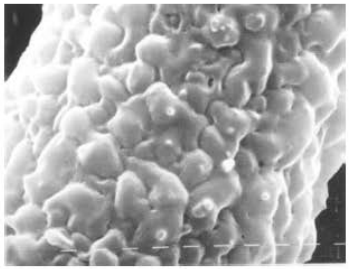

R. Kotthaus, Nucl. Instr. and Meth. A252(1986) 531

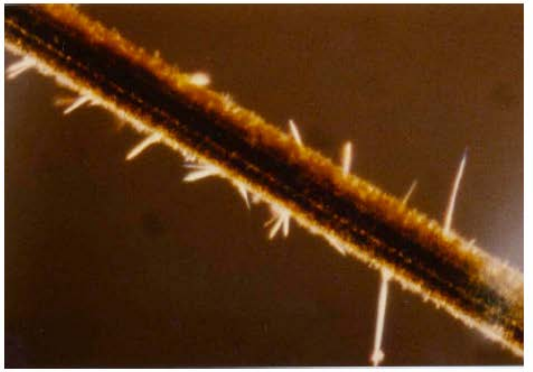

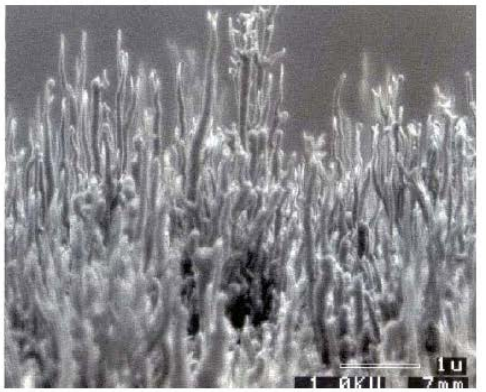

M. Binkley et al, Nucl. Instr. and Meth.A515(2003)53

J. Kadyk, Nucl. Instr. and Meth. A300(1991)436

The MWPC limits in:

- **rate capability** (space charge ➔ E distortion)
- **space resolution** (cell size limitation)
- **time resolution** (signal from ion drift)
- **aging**

have been overcome by a change in technology since the anode is no more self supporting: strip on insulating substrate, …

MicroStrip Gas Chamber

MWPC

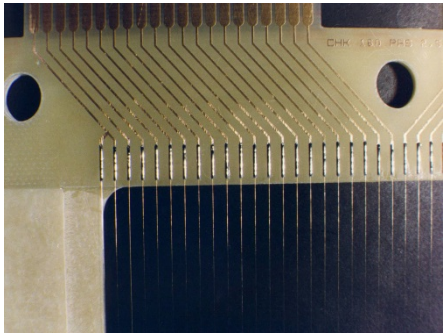

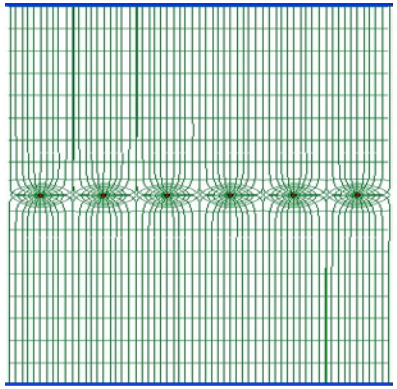

Typical distance between wires limited to 1 mm

MSGC

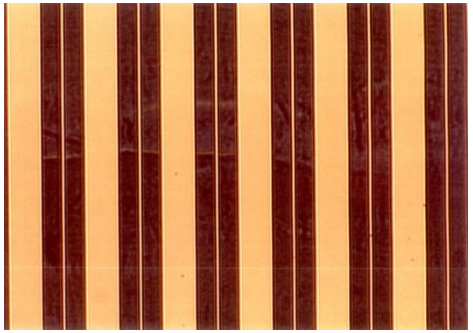

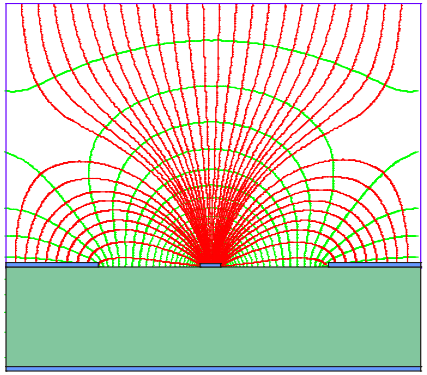

Typical distance between anodes 200 μm thanks to semiconductor etching technology

Semiconductor industry technology:

Photolithography
Etching
Coating
Doping

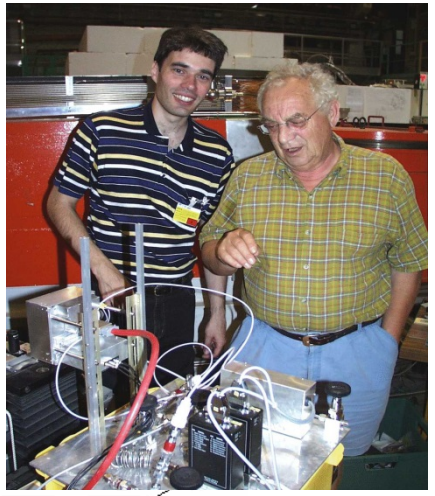

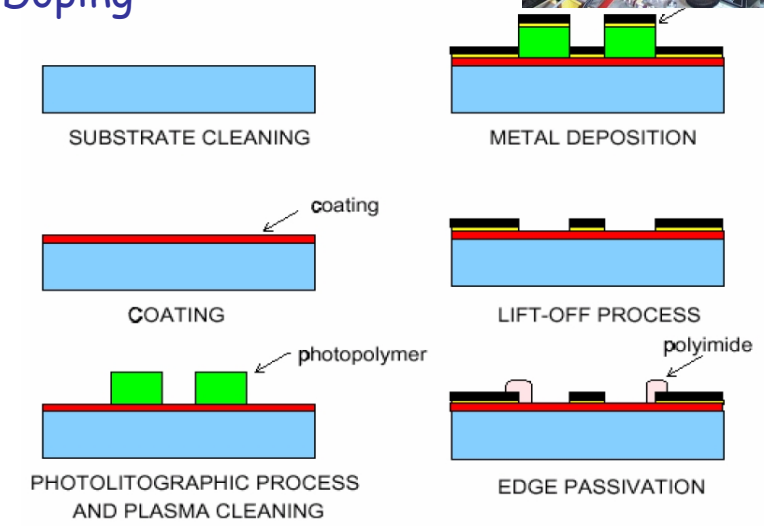

A. Oed, Nucl. Instr. and Meth. A263 (1988) 351.

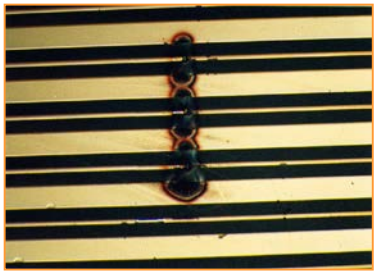

In the early days:
high E-values at the edge between insulator and strips → damages
Charge accumulation at the insulator → gain evolution vs time

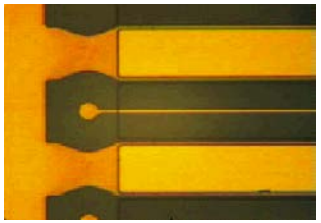

Later (~ 1999-2000): Passivation of the cathode edges → MSGC operational

MSGC – MicroStrip Gas Chamber

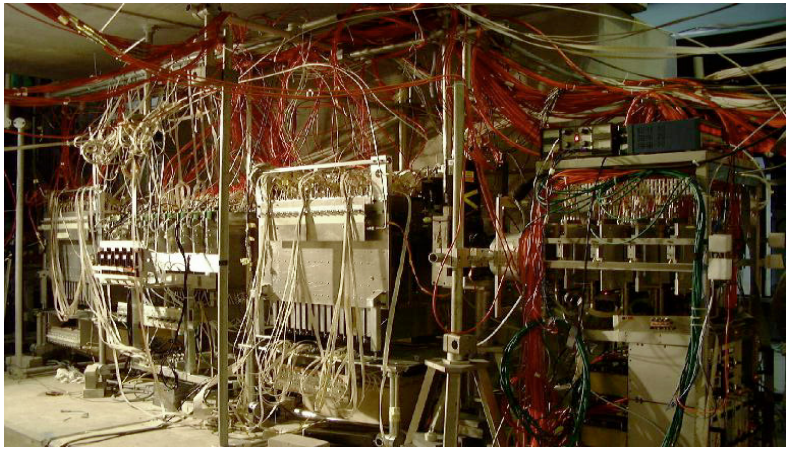

Telescope of 32 MSGCs tested at PSI in Nov99 (CMS Milestone)

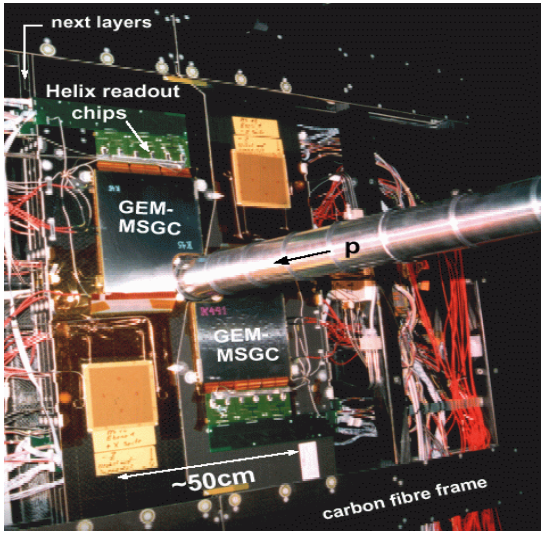

HERA-B Inner Tracker
MSGC-GEM detectors
R_{min} ~ 6 cm
$\Rightarrow 10^6$ particles/cm^2•sec
300 μm pitch
184 chambers: max 25x25 cm^2
~ 10 m^2; 140.000 channels

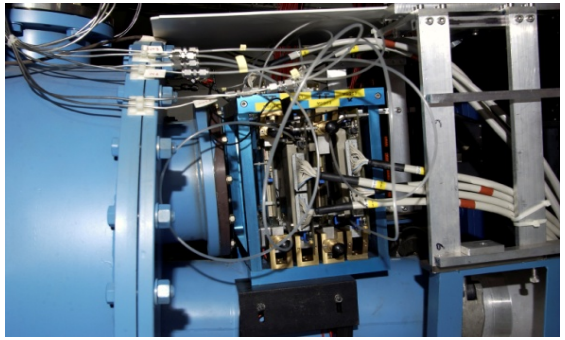

DIRAC
4 planes MSGC-GEM
Planes 10x10 cm^2

The D20 diffractometer MSGC is working since Sept 2000
1D localisation
48 MSGC plates (8 cm x 15 cm)
Substrate: Schott S8900
Angular coverage : 160° x 5,8°
Position resolution : 2.57 mm (0,1°)
5 cm gap; 1.2 bar CF4 + 2.8 bars 3He
Efficiency 60% @ 0.8 Å

ILL Grenoble (partnership with India)

Limitations of Gas Detectors

Classical ageing

Avalanche region → plasma formation

(complicated plasma chemistry)

- Dissociation of detector gas and pollutants
- Highly active radicals formation
- Polymerization (organic quenchers)
- Insulating deposits on anodes and cathodes

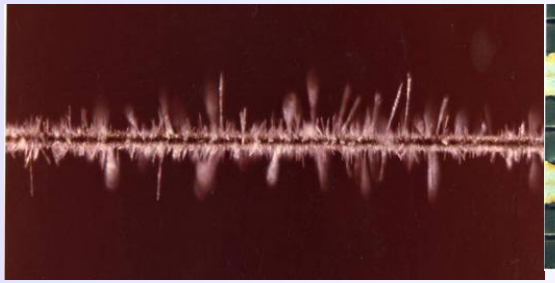

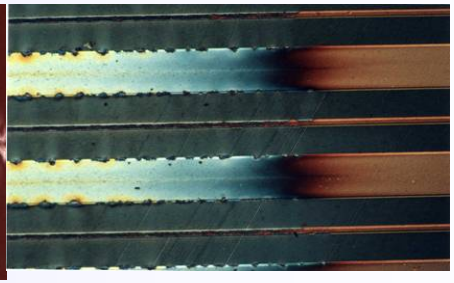

Anode: increase of the wire diameter, reduced and variable field, variable gain and energy resolution.

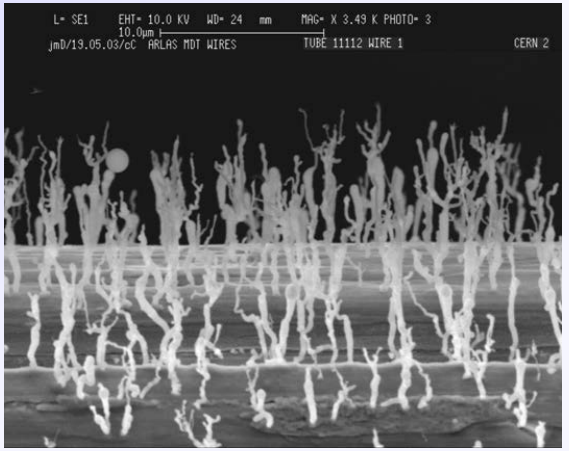

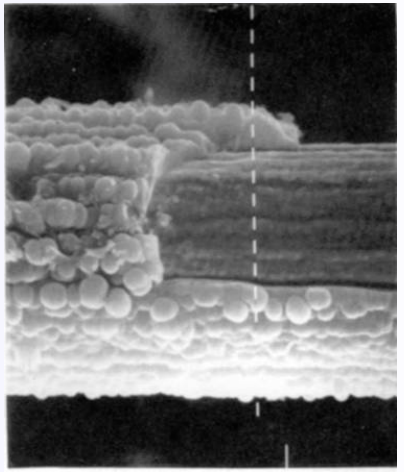

Cathode: formation of strong dipoles, field emmision and microdischarges (Malter effect).

Limitations of Gas Detectors

Solutions: carefull material selection for the detector construction and gas system, detector type (GEM is resitant to classical ageing), working point, non-polymerizing gases, additives supressing polymerization (alkohols, methylal), additives increasing surface conductivity (H_2O vapour), clening additives (CF_4).

Creation of database of "radiation-hard" materials & detectors depending on application, commercially available materials

Source	Product	Outgas	Effect in G.D.	Note
CERN/GDD	**STYCAST 1266 (A+B)**	NO	NO	Long curing time
HERA-B/OTR	**STYCAST 1266 (A+Catalyst 9)**	NO	NO	In Use
CERN/GDD	**HEXCEL EPO 93L**	NO	NO	Out of production
HERA-B/ITR	**ECCOBOND 285**	NO	NO	In Use
CERN/GDD ATLAS/TRT	**ARALDITE AW103 (Hardener HY 991)**	NO	NO	In Use
ATLAS/TRT	**TRABOND 2115**	NO	NO	In Use

Low Outgassing room-T epoxies

Source	Product	Outgas	Effect in G.D.	Result
CERN/GDD ATLAS/TRT	**ARALDITE AW 106 (Hardener HV 935 U)**	YES		**BAD**
CERN/GDD	**DURALCO 4525**	YES	YES	**BAD**
CERN/GDD	**DURALCO 4461**	YES	YES	**BAD**
CERN/GDD	**HEXCEL A40**	YES	-	**BAD**
CERN/GDD	**TECHNICOLL 8862 + (Hardener 8263)**	YES	-	**BAD**
CERN/GDD	**NORLAND NEA 155**	YES	-	**BAD**
CERN/GDD	**EPOTEK E905**	YES	-	**BAD**
CERN/GDD	**NORLAND NEA 123 (UV)**	YES	-	**BAD**

Outgassing room-T epoxies

Gas Detectors in LHC Experiments

ALICE: TPC (tracker), TRD (transition rad.), TOF (MRPC), HMPID (RICH-pad chamber), Muon tracking (pad chamber), Muon trigger (RPC)

ATLAS: TRD (straw tubes), MDT (muon drift tubes), Muon trigger (RPC, thin gap chambers)

CMS: Muon detector (drift tubes, CSC), RPC (muon trigger)

LHCb: Tracker (straw tubes), Muon detector (MWPC, GEM)

TOTEM: Tracker & trigger (CSC , GEM)

Several different detectors have been developed

MICRO-GAP CHAMBER

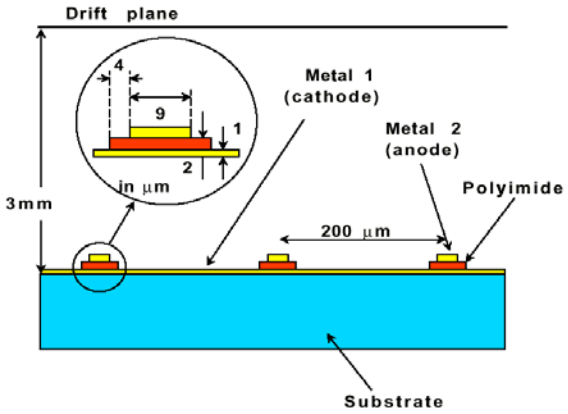

MICRO-GROOVE CHAMBER

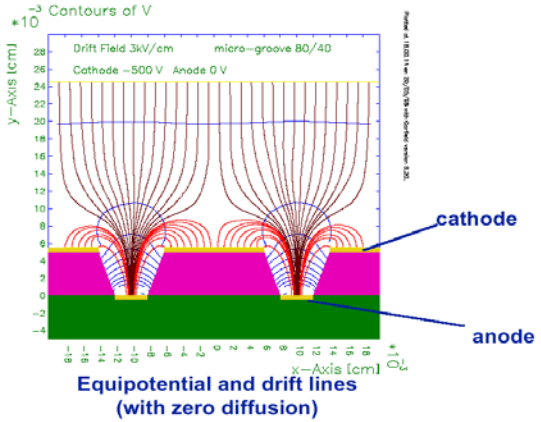

MICRO-PIN ARRAY

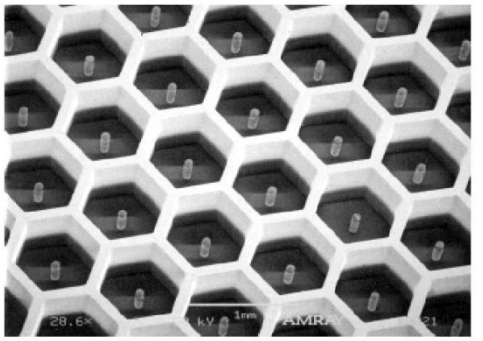

MICRO-WIRE CHAMBER

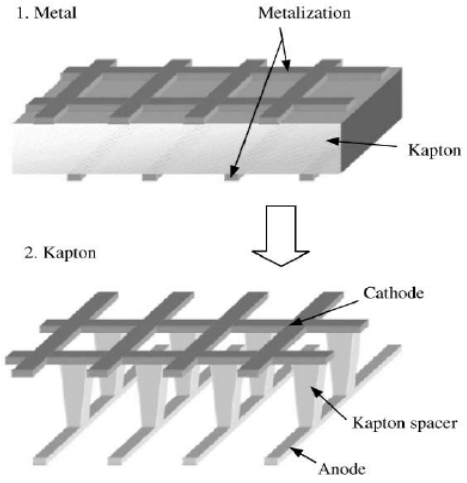

COMPTEUR A TROUS

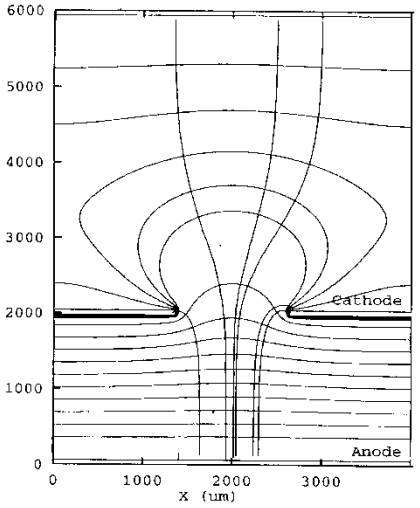

MICRO-PIXEL CHAMBER

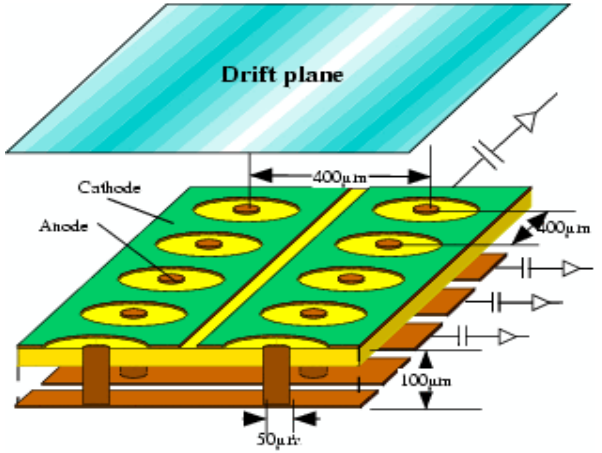

Two very solid, fully established technologies:

MICRO MEsh GAseous Structure (MICROMEGAS)
Thin gap Parallel Plate Chamber: micromesh stretched over readout electrode.

Y. Giomataris et al., Nucl. Instr. and Meth. A376(1996)29

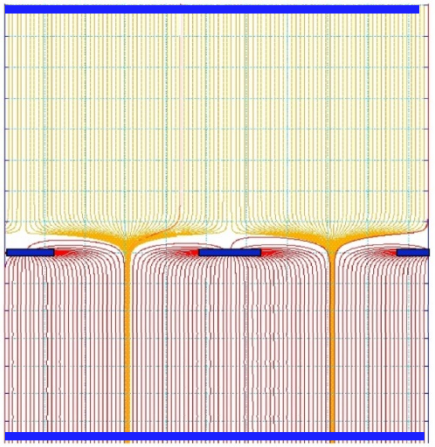

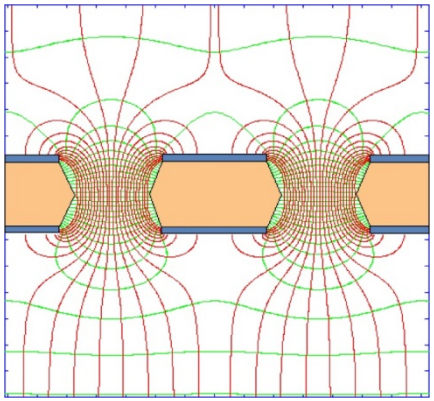

GAS ELECTRON MULTIPLIER (GEM)
Thin, metal-coated polymer foil with high density of holes, each hole acting as an individual proportional counter.

F. Sauli, Nucl. Instrum. Methods A386(1997)531

HIGHER LUMINOSITIES, HIGHER PRECISION EXPERIMENTS

1. ***MPGDs allow for***
   - ***High rates (granularity & occupancy, signal formation time)***
   - ***Fine space resolution***
2. ***Technological maturity and accurate engineering FUNDAMENTAL for successful MPGDs***

Two very solid, fully established technologies:

First Large Scale Use of GEMs and MICROMEGAs

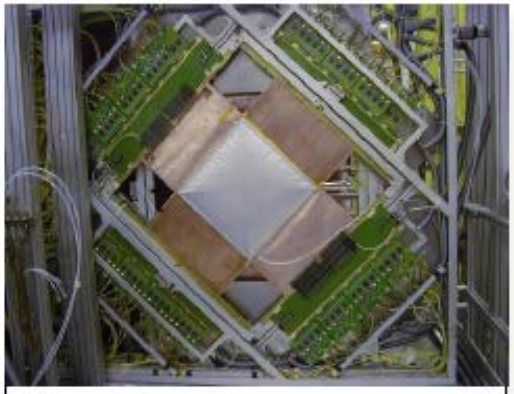

Micromegas: σ_x~90μm

Tracking in the COMPASS Experiment

GEM: σ_x~70μm

B. Ketzer

slide by W. Riegler, CERN Academic Training, April 2008

Operational 12 years ago

GEM

Thin metal-coated polymer foil pierced by a high density of holes (50-100/mm^2)
Typical geometry: 5 μm Cu on 50 μm Kapton, 70 μm holes at 140 μm pitch

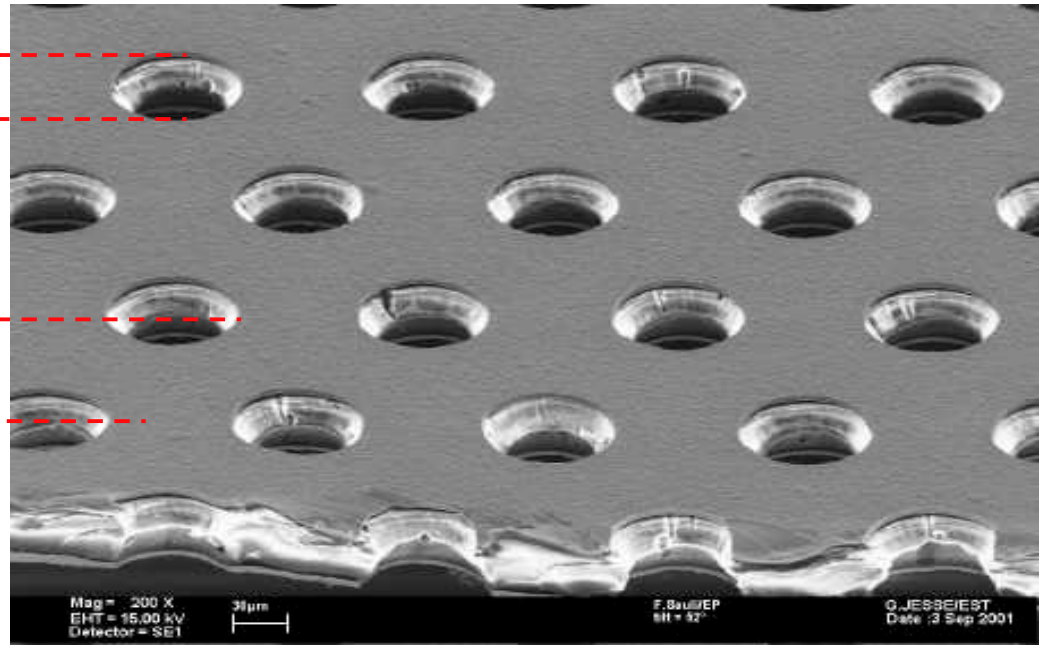

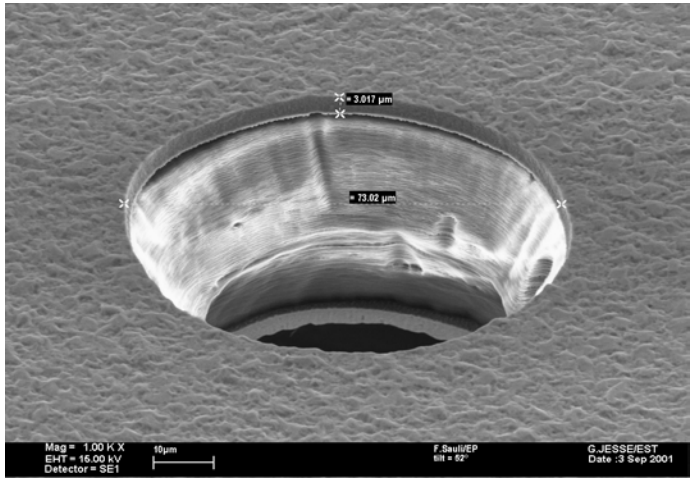

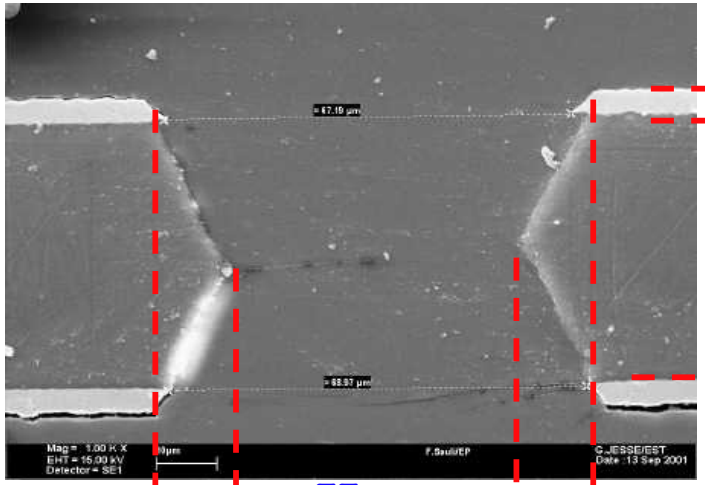

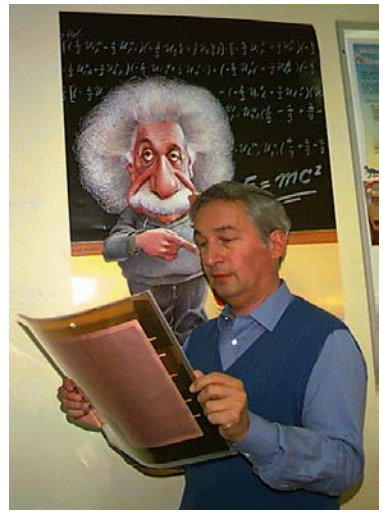

Ions

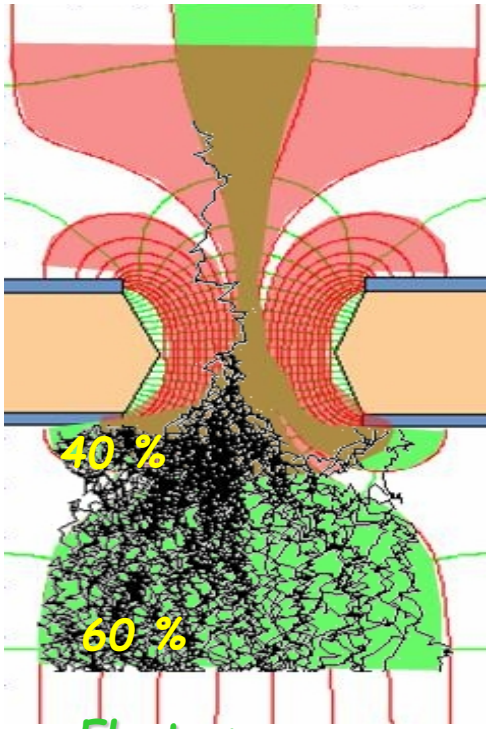

Electrons

GEM Manufacturing

GEM foils are produced at CERN using proprietary process.

Rui De Oliveira
CERN-EST-DEM

50 μm Kapton
5 μm Cu both sides

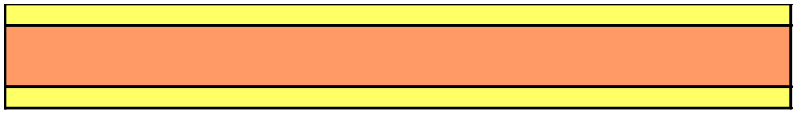

Photoresist coating, masking and exposure to UV light

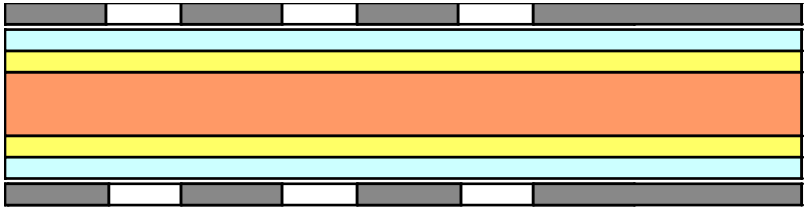

Metal etching

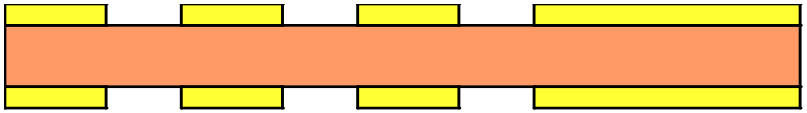

Kapton etching

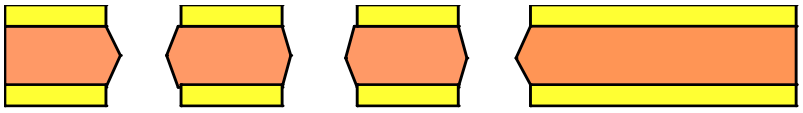

Second masking

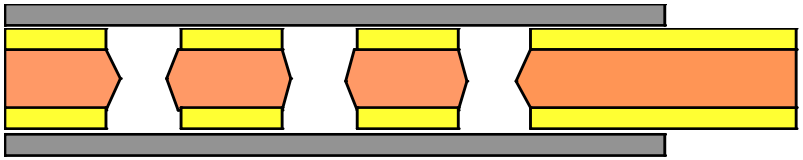

Metal etching and cleaning

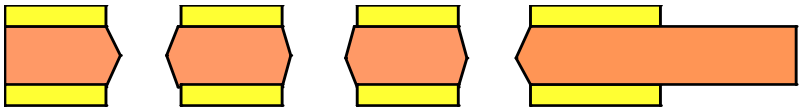

J. Benlloch et al, IEEE NS-45(1998)234

GEM – Gas Electron Multiplier

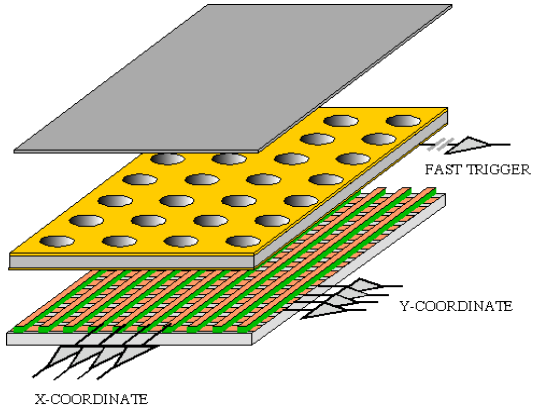

Full decoupling of the charge amplification structure from the charge collection and readout structure.
Both structures can be optimized independently !

A. Bressan et al, Nucl. Instr. and Meth. A425(1999)254

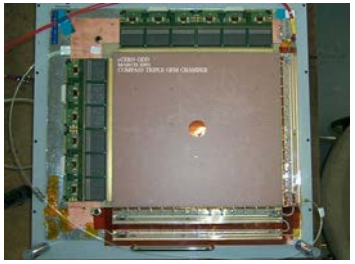

Compass

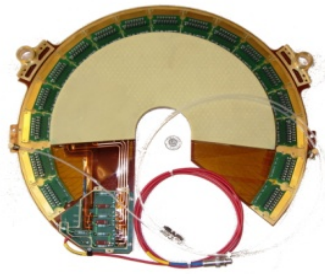

Totem

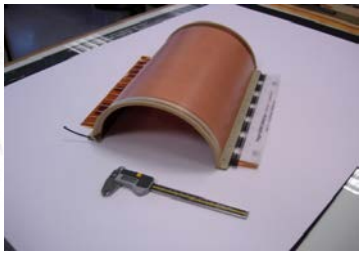

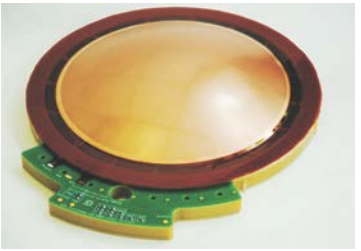

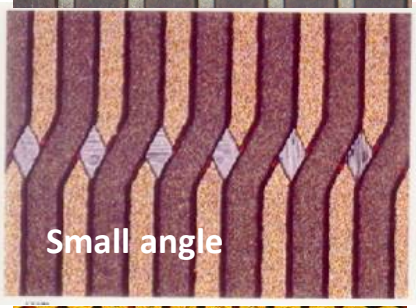

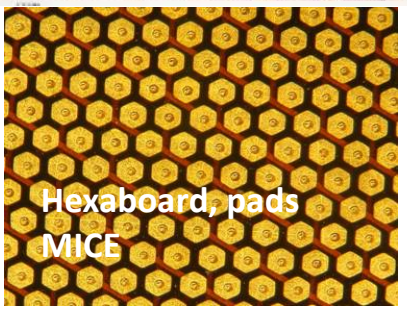

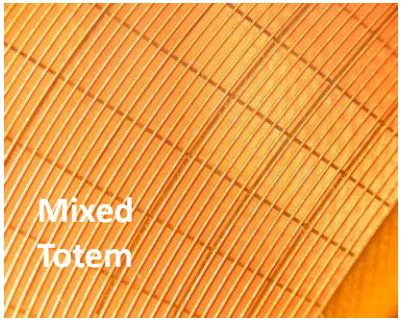

Most of the detectors use three GEM foils in cascade for amplification to reduce discharge probability by reducing field strength.

Multi-GEM Detectors are operated in discharge free mode

Discharge Probability on Exposure to 5 MeV Alphas

Multiple structures provide equal gain at lower voltage.

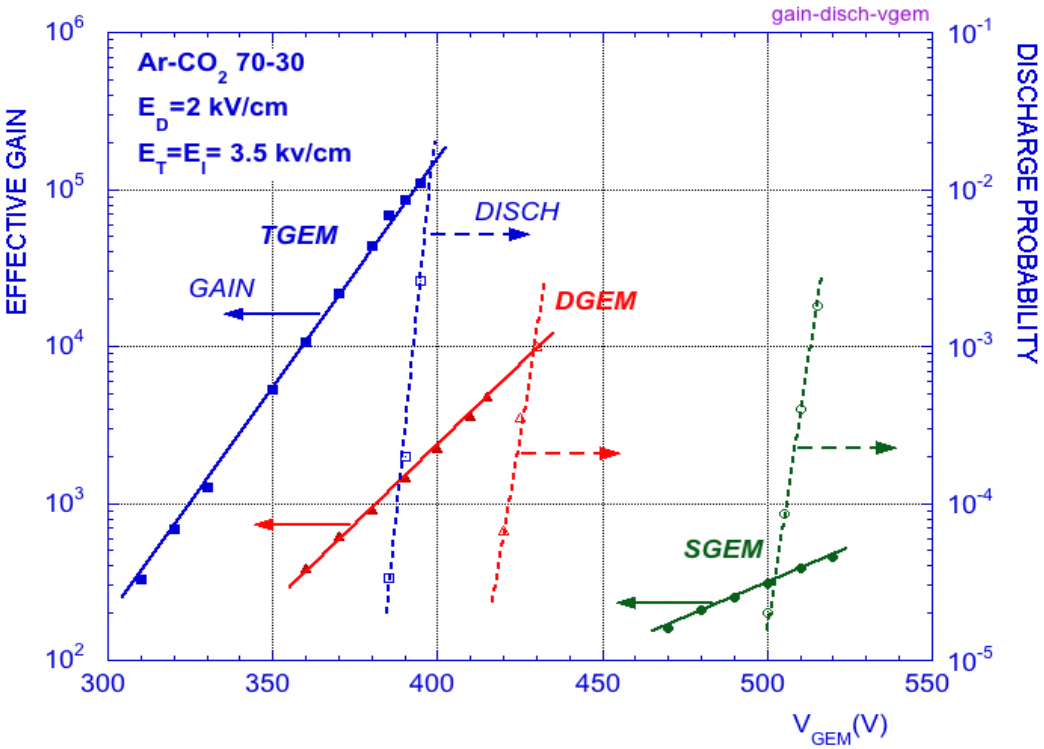

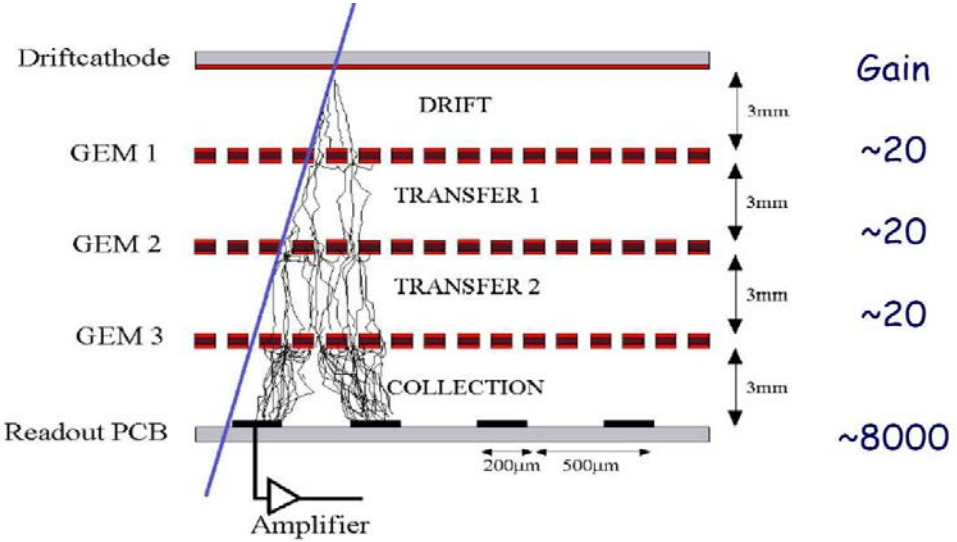

S. Bachmann et al Nucl. Instr. and Meth. A479(2002)294

GEM performance

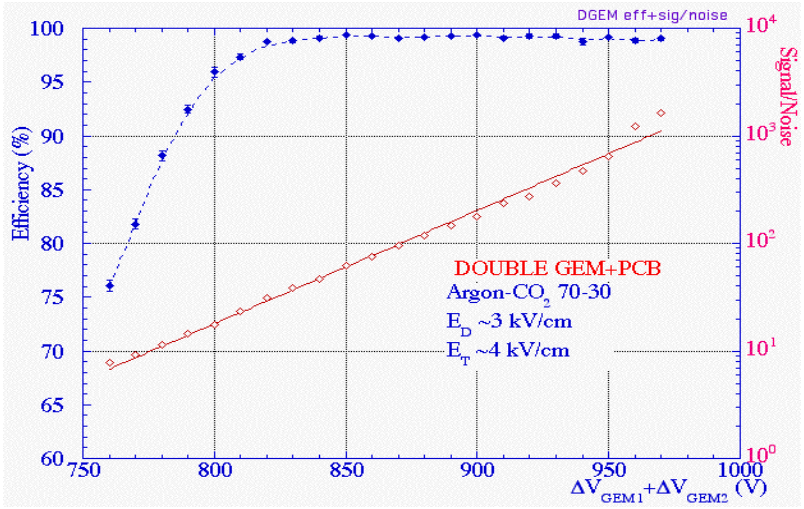

Efficiency for charged particles with 3 mm gap

A. Bressan et al, Nucl. Instr. And Meth. A425(1999)262

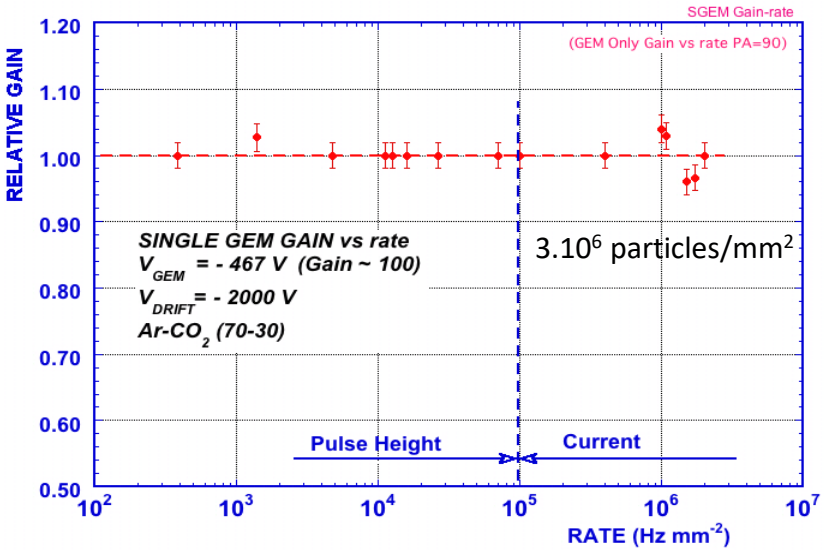

Rate capability > 10^6 Hz mm^{-2}

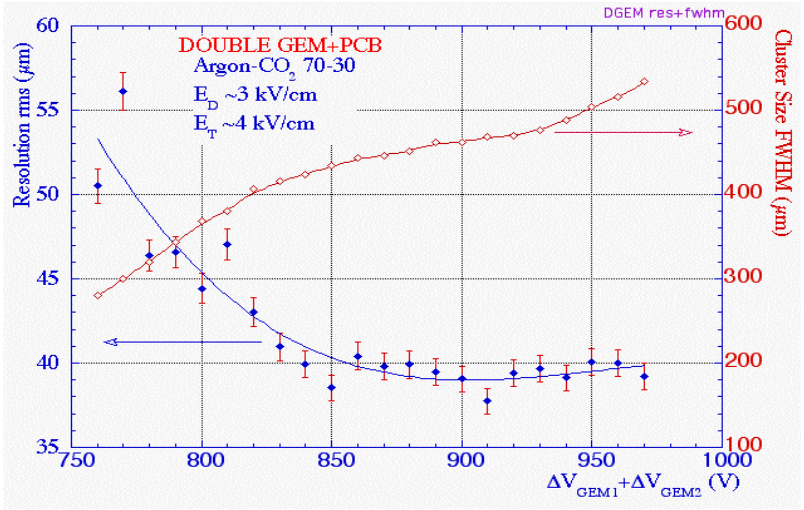

Space resolution ~ 40 μm rms

Cluster size ~ 500 μm FWHM

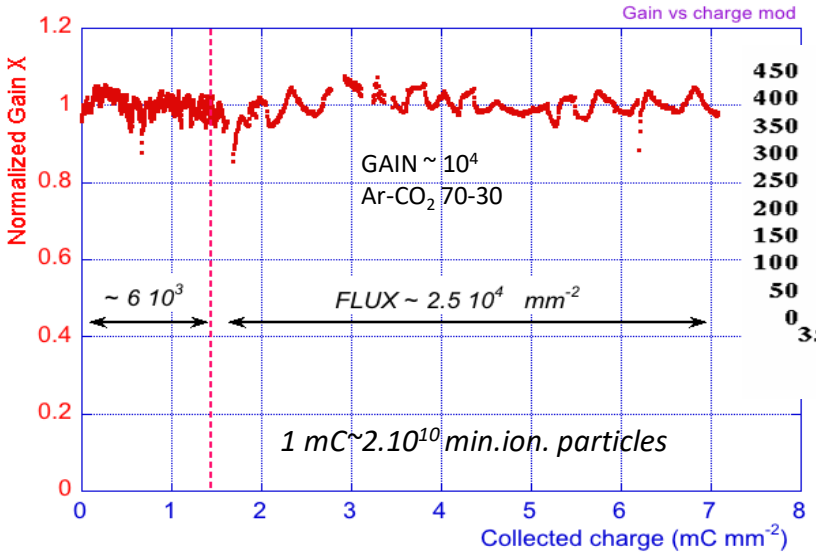

J. Benlloch et al, IEEE NS-45(1998)234

Time resolution

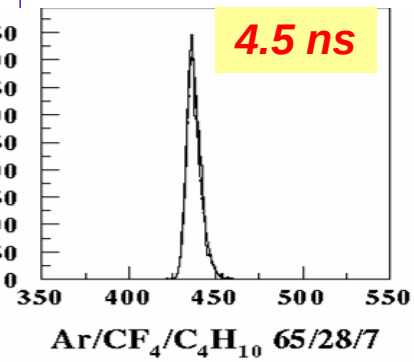

GAIN DEPENDENCE FROM HOLE DIAMETER

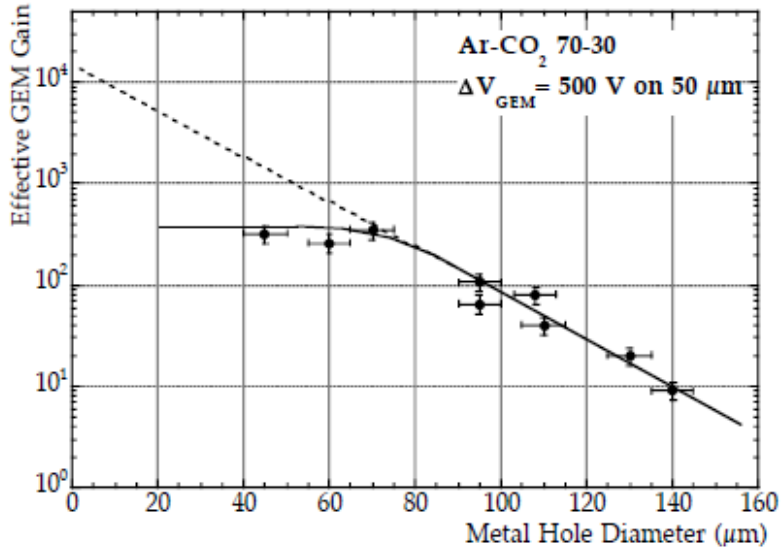

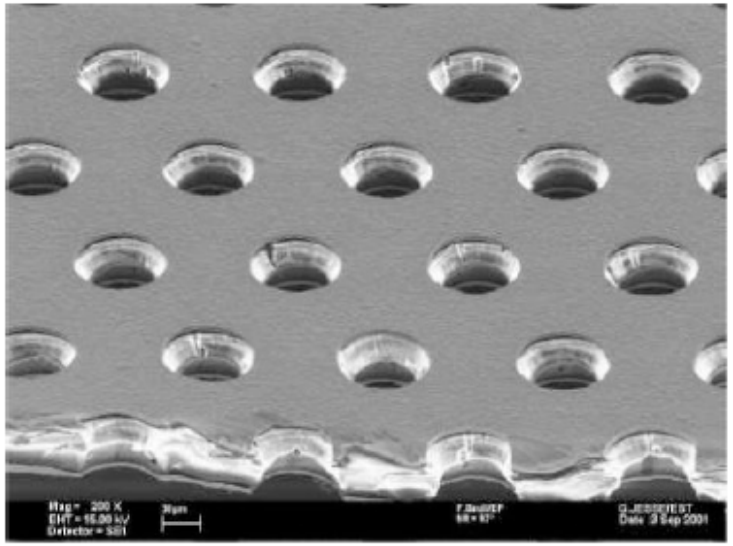

GAIN STABILITY UNDER IRRADIATION (CHARGING)

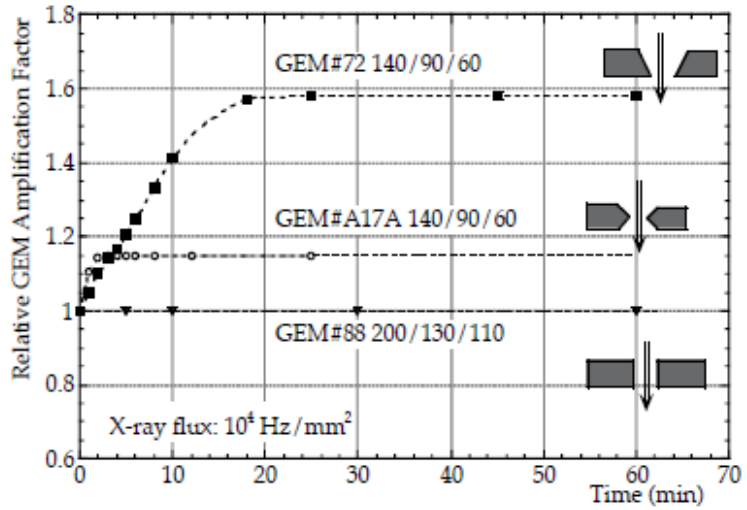

J. Benlloch et al, Nucl. Instr. And Meth. A419(1998)410

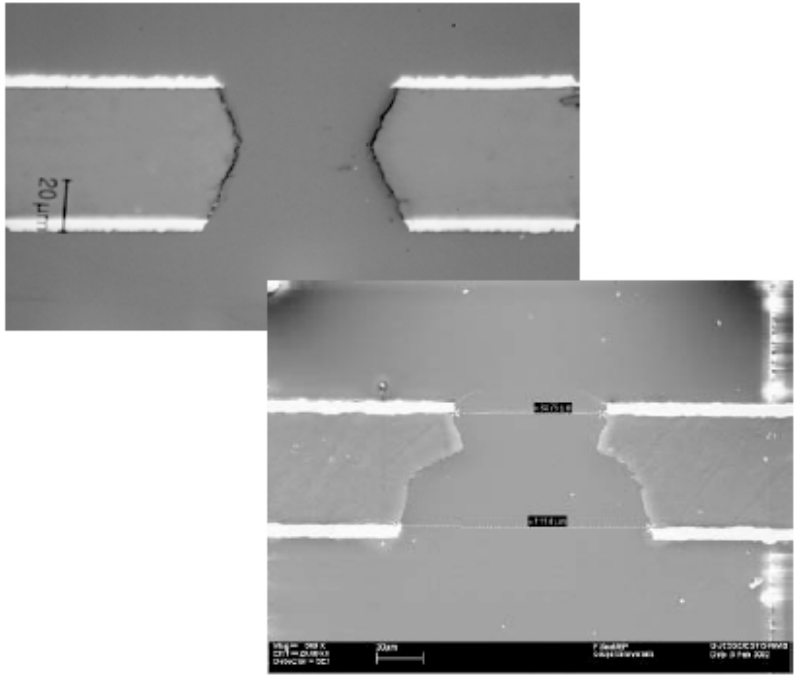

ION FEEDBACK IN MULTIGEMS

The fractional ion feedback in multi-GEM detectors results from a complex interplay of geometry, fields, diffusion:

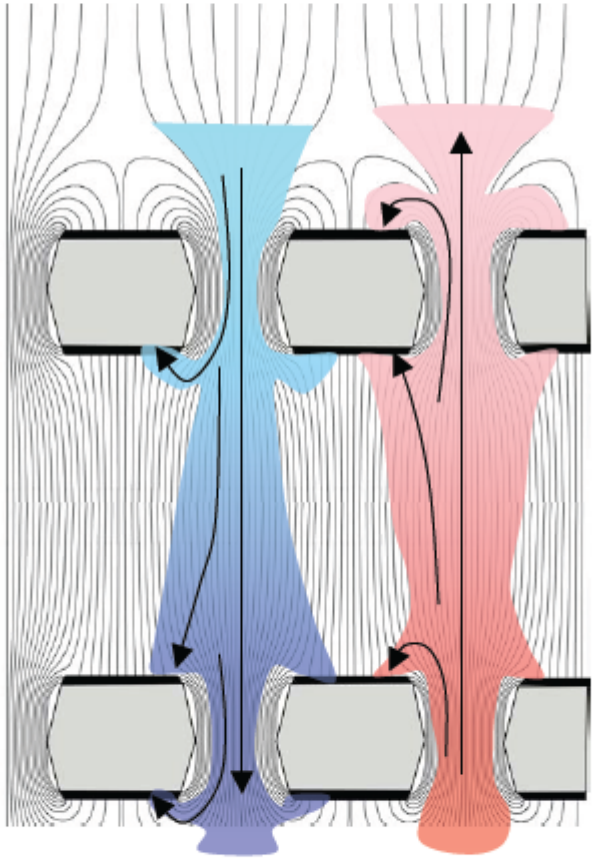

GEOMETRY:

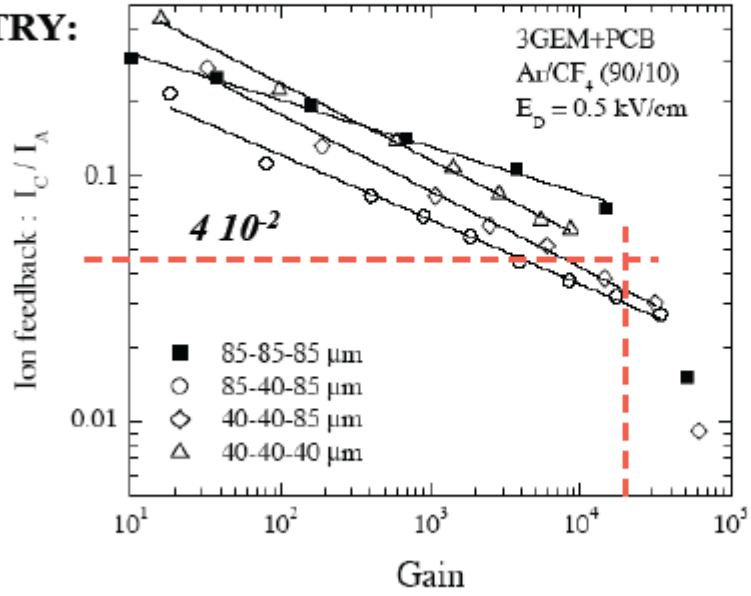

A. Bondar et al, Nucl. Instr. and Meth. A496(2003)325

MAGNETIC FIELD:

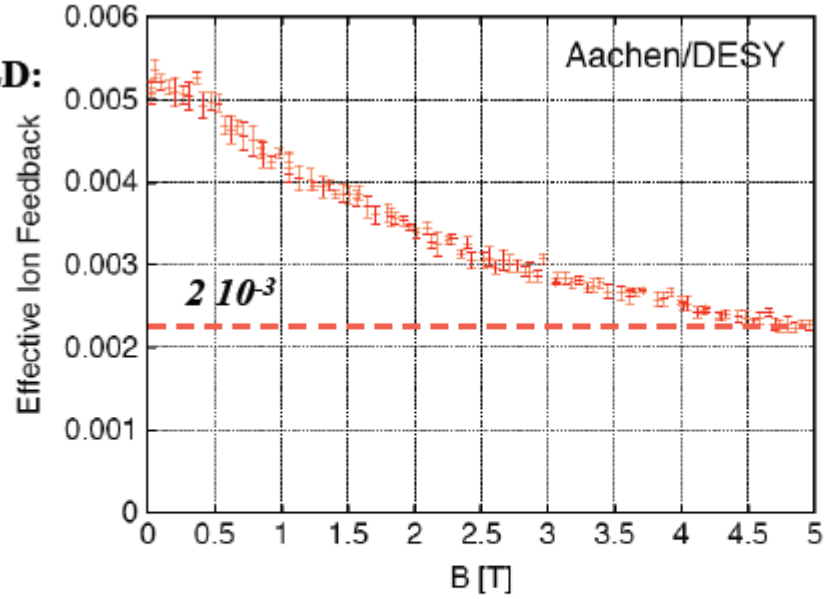

M. Killenberg et al, Nucl. Instr. and Meth. A530(2004)251

DIFFERENCE IN DIFFUSION BETWEEN IONS AND ELECTRONS:

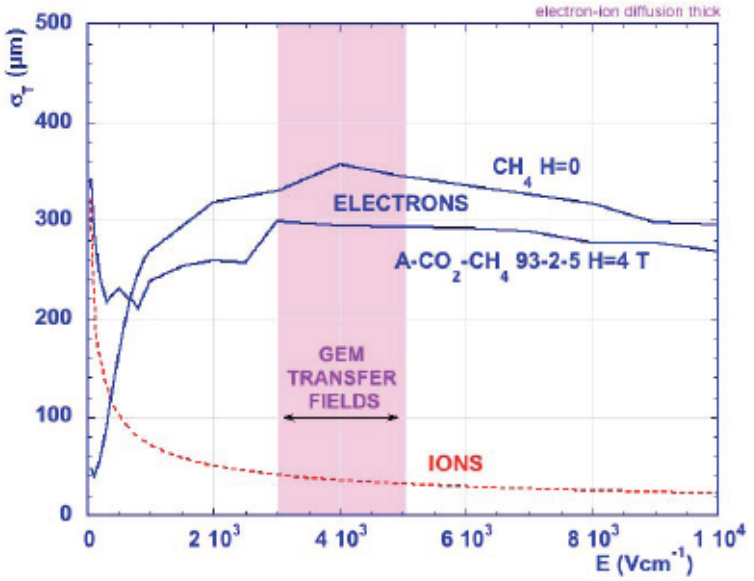

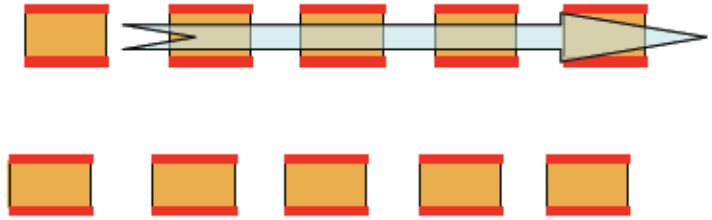

F. Sauli et al,
Nucl. Instr. and Meth. A560(2006)269

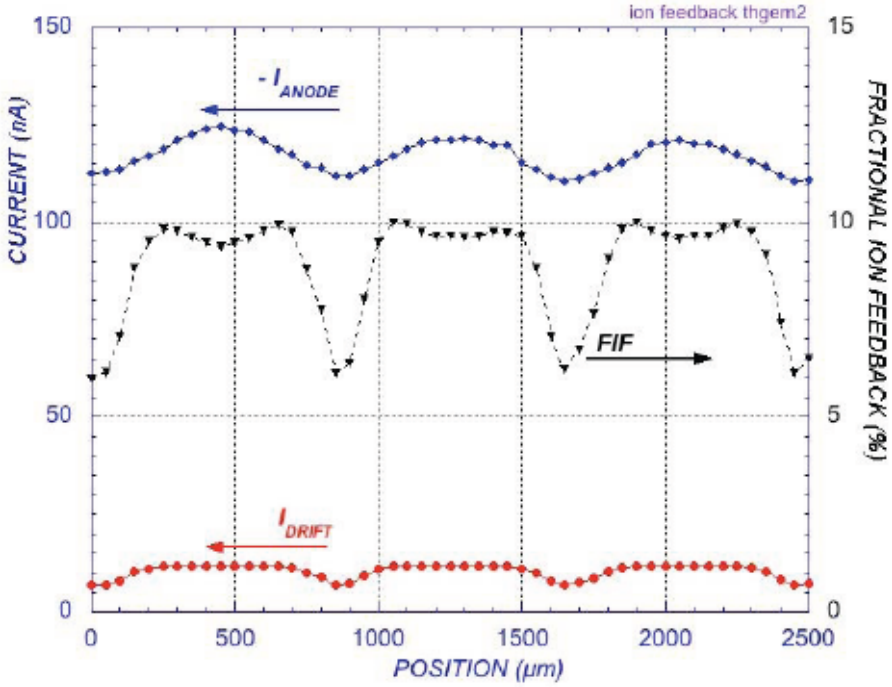

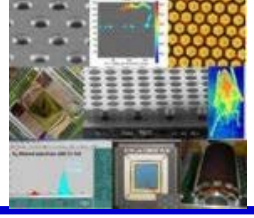

GEMs operaed in Experiments

- **Space resolution**
  - COMPASS small area trackers, ~70 μm (P. Abbon et al., NIMA 577 (2007) 455.)
- **Time resolution**
  - COMPASS small area trackers, ~12 ns (P. Abbon et al., NIMA 577 (2007) 455.)
  - LHCb, 4.5 ns - dedicated effort (M. Alfonsi NIMA 535 (2004) 319)
- **Gain**
  - At COMPASS: G ~ 8000 (B. Ketzer, private comm.)
  - At LHCb: G ~ 4000 (M.Alfonsi NIMA 581 (2007) 283)
  - At TOTEM: G ~ 8000 (G. Catanesi, private comm.)
  - Phenix HBD: G ~ 4000 (W. Anderson et al., NIMA 646 (2011) 35)
- **Material budget**
  - COMPASS small area trackers: 0.4 % X0 (P. Abbon et al., NIMA 577 (2007) 455.)
  - COMPASS pixelated GEMs: 0.2 % X0 (A. Austregesilo et al., NP B PS 197 (2009) 113

GEMs, spacers & stretching

GEM detectors w/ spacers

COMPASS

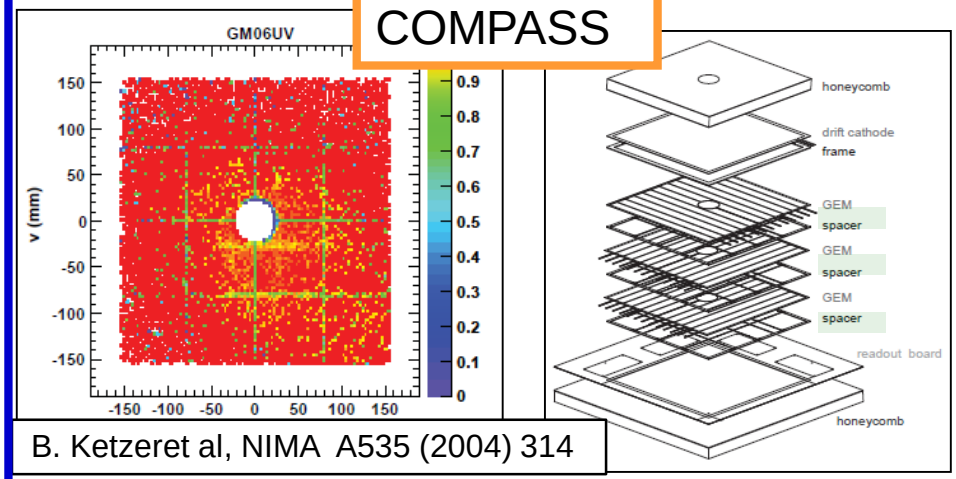

B. Ketzeret al, NIMA A535 (2004) 314

TOTEM

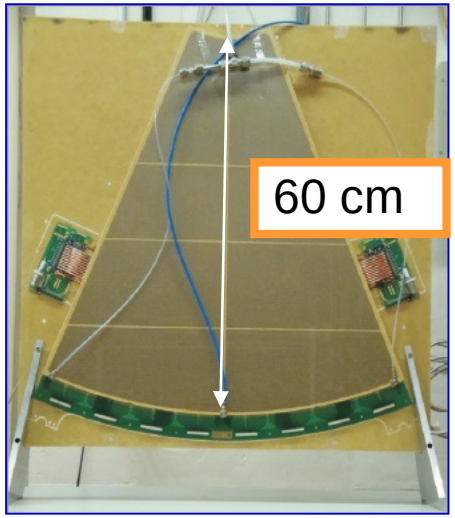

Emphasis on GEM foils stretching

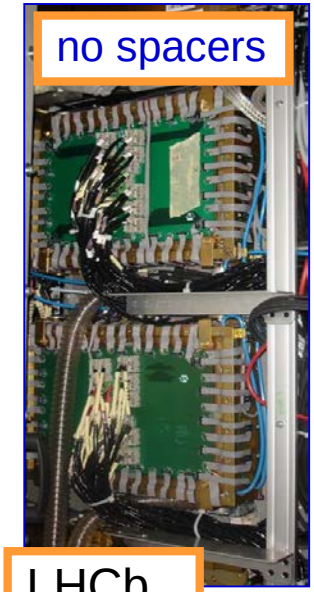

LHCb

KLOE2: Triple cylindrical GEM
assembly completed 14/3/2013

CMS upgrade: mechanical stretching for mass production

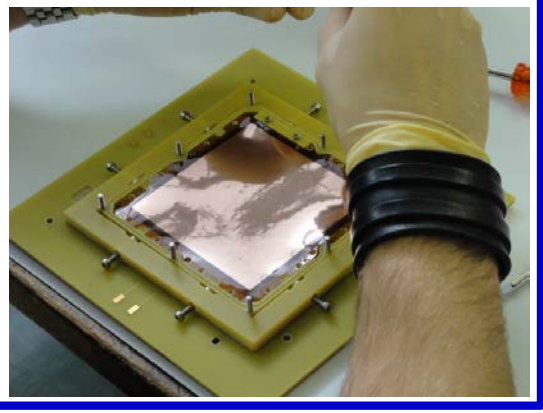

COMPASS

Fixed target tracking

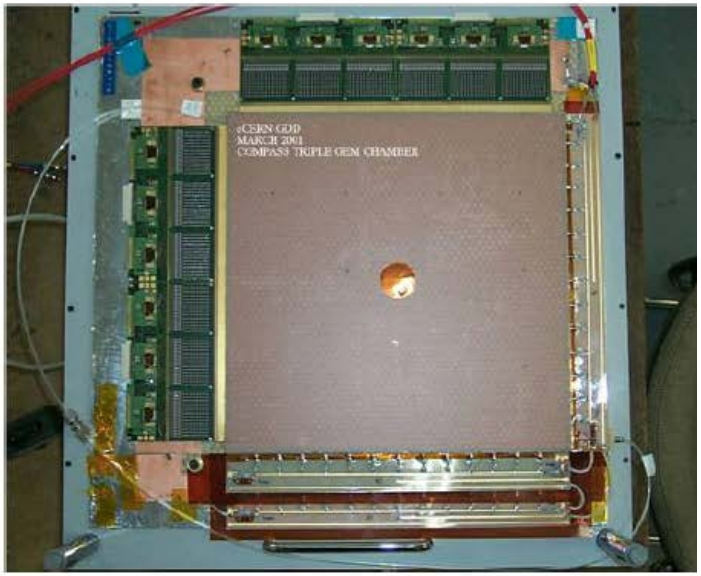

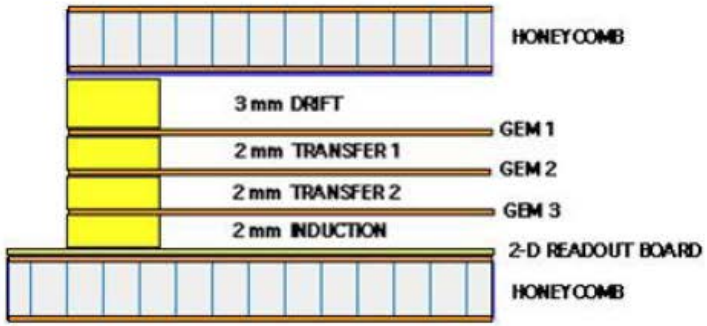

X-Y strip readout

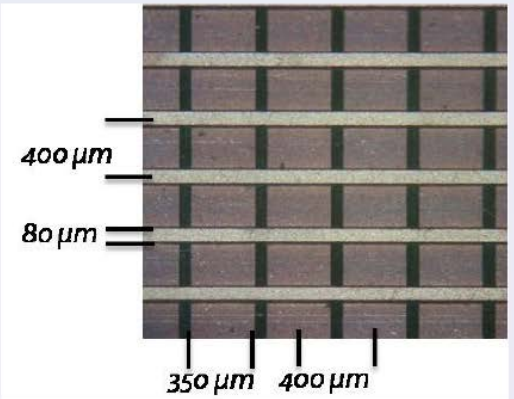

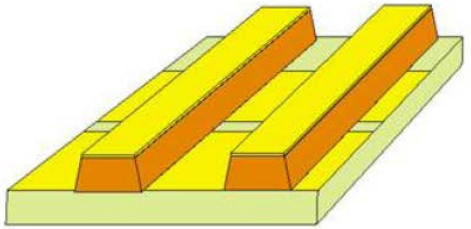

Segmented GEM electrode with beam killer

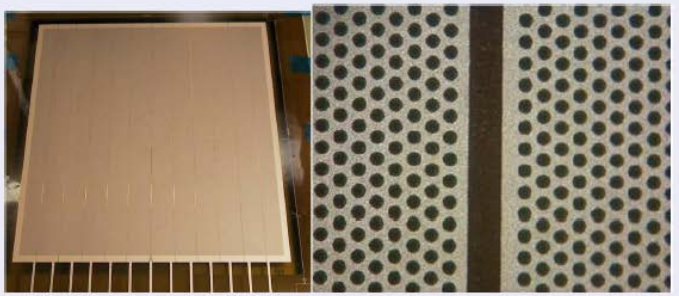

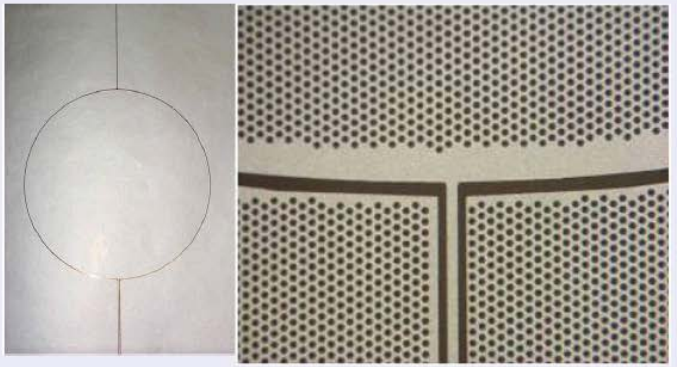

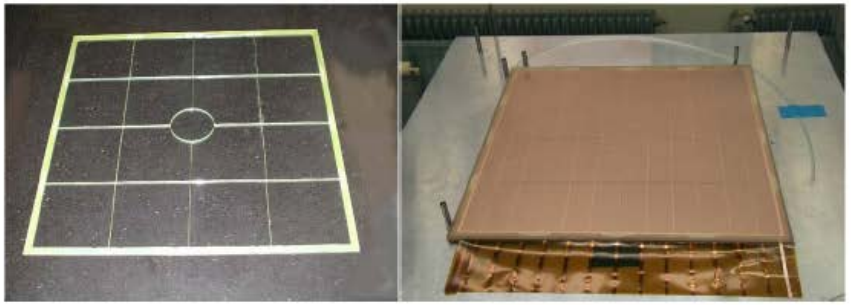

TOTEM

Forward tracking & triggering

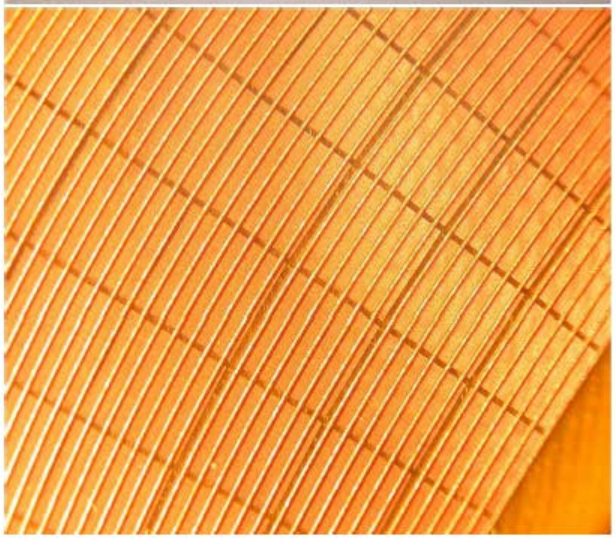

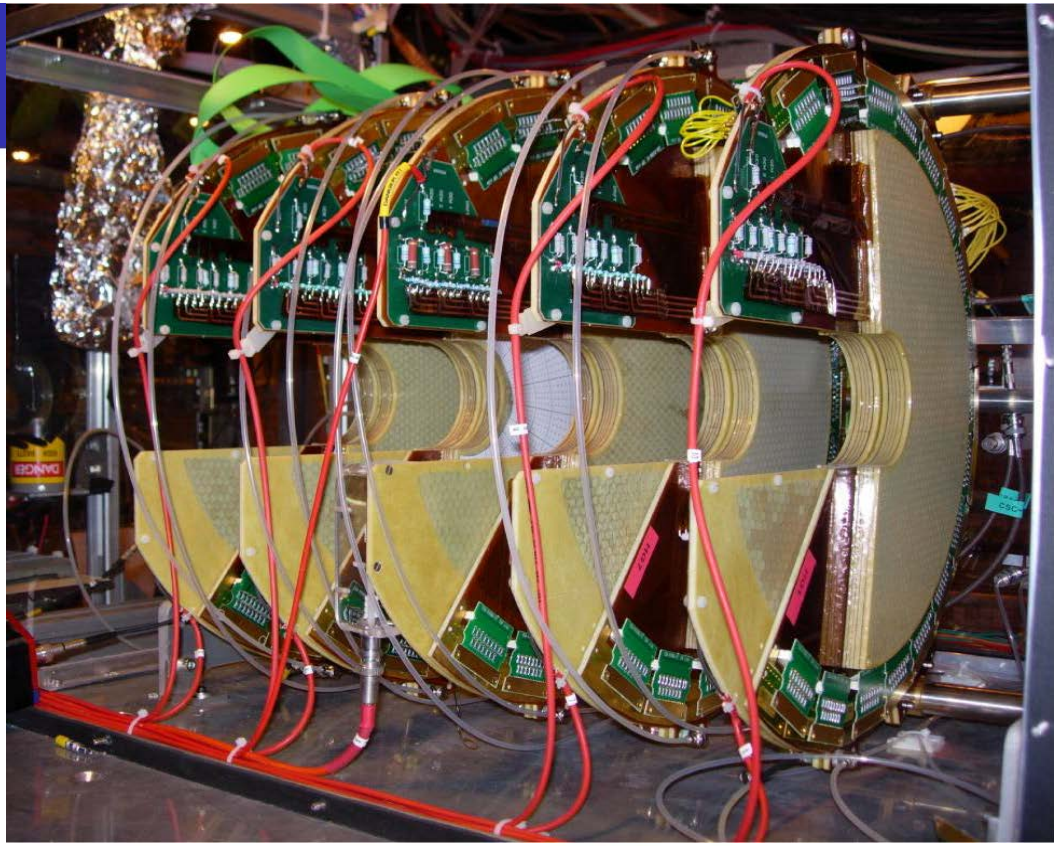

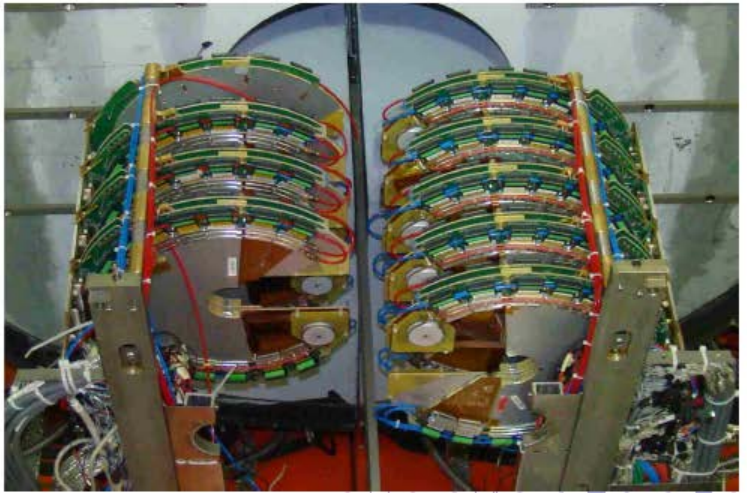

HV divider and readout boards

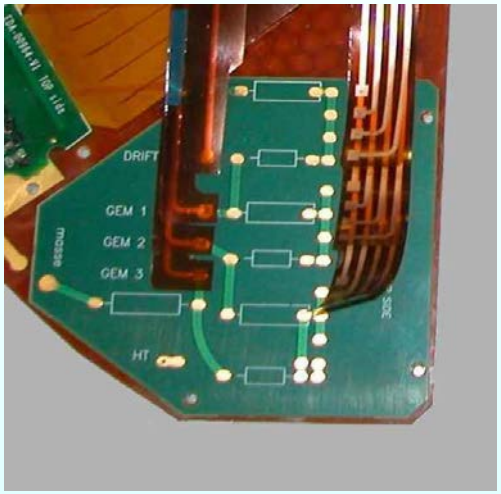

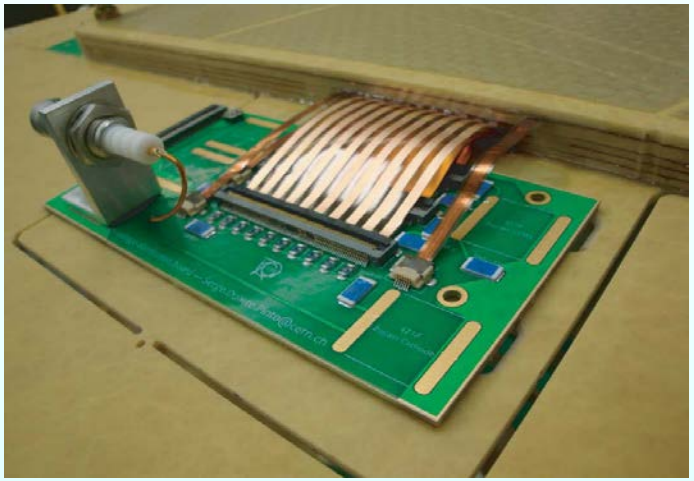

- ***Cleaning and testing after components mounting is very important !***
- ***HV components***
- ***HV values – working point***
- ***Coated Kapton soldering***
- ***Conformal coating***

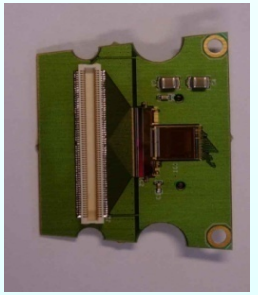

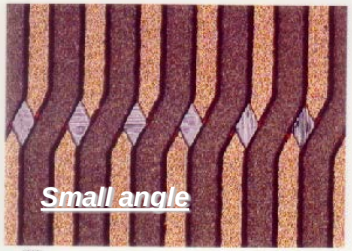

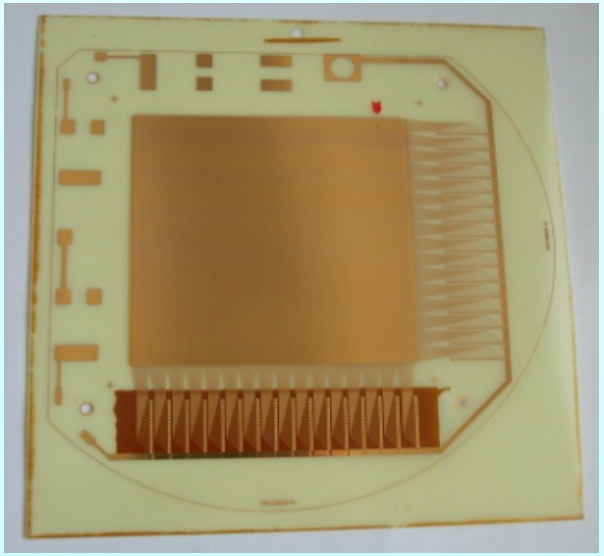

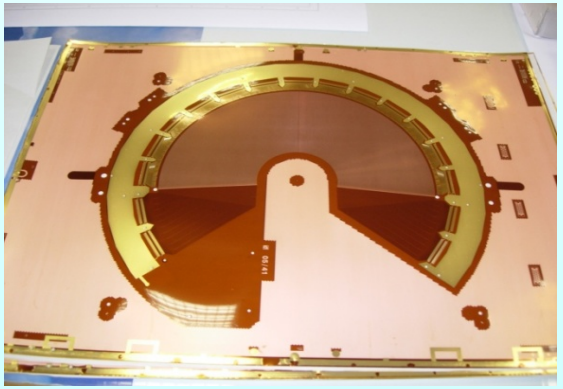

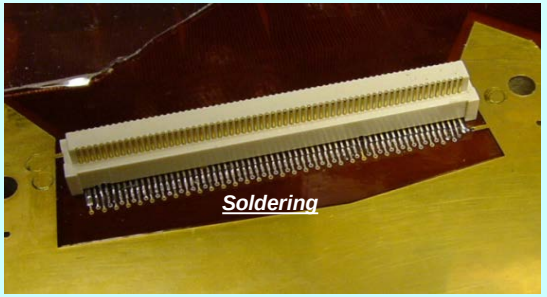

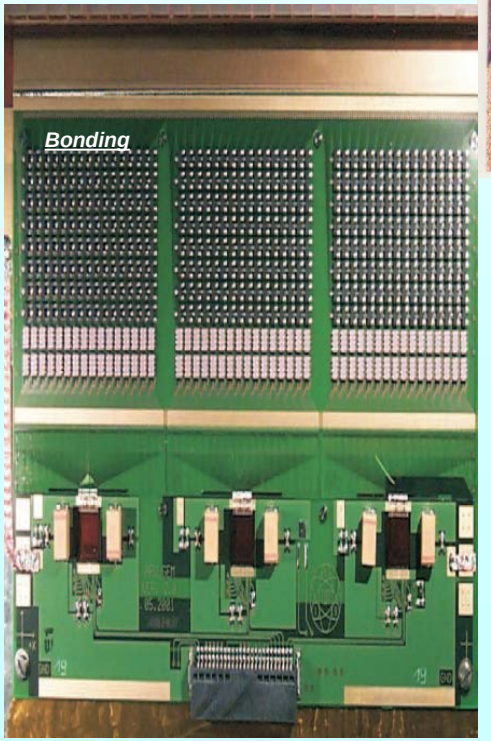

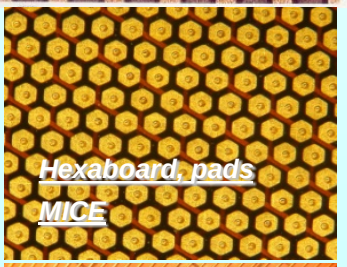

- ***Bonding is difficult***
- ***Input capacitance***
- ***Cross talk***

Tools and infrastructure

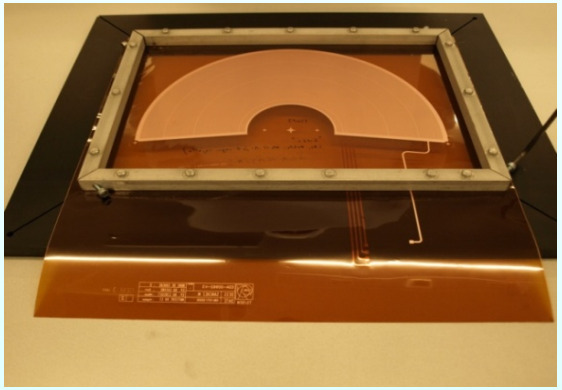

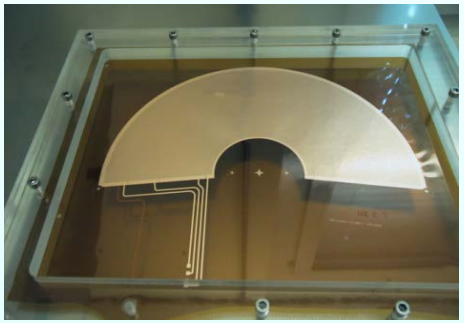

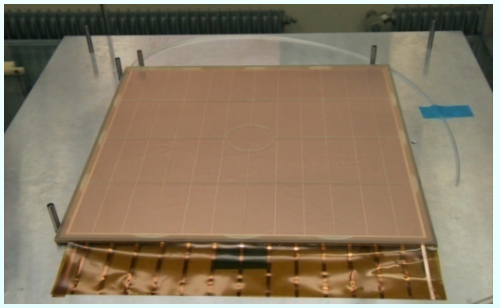

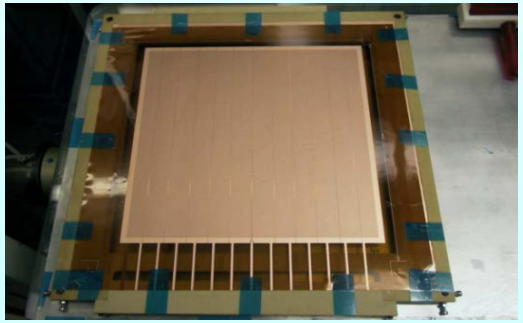

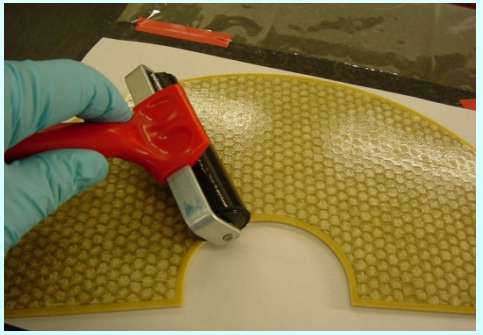

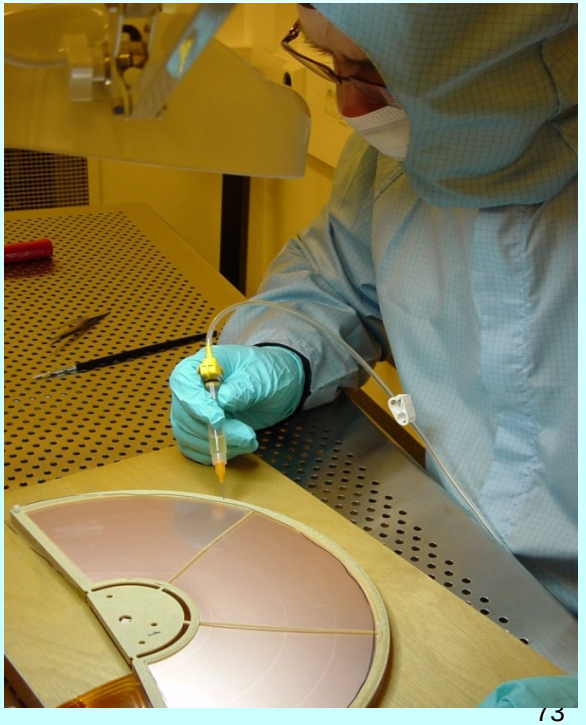

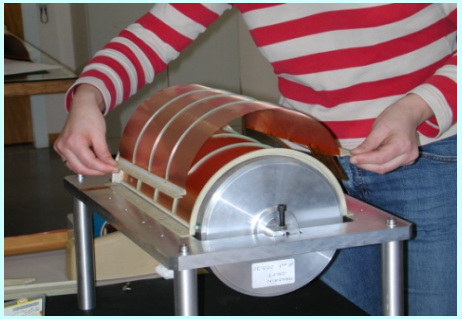

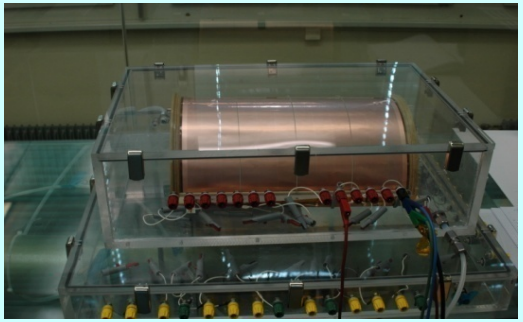

Tools and infrastructure

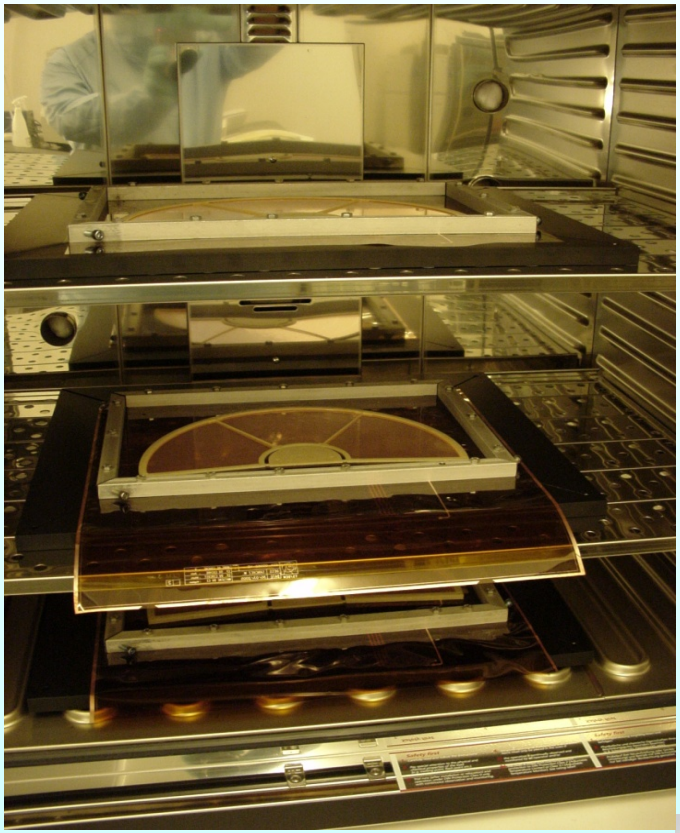

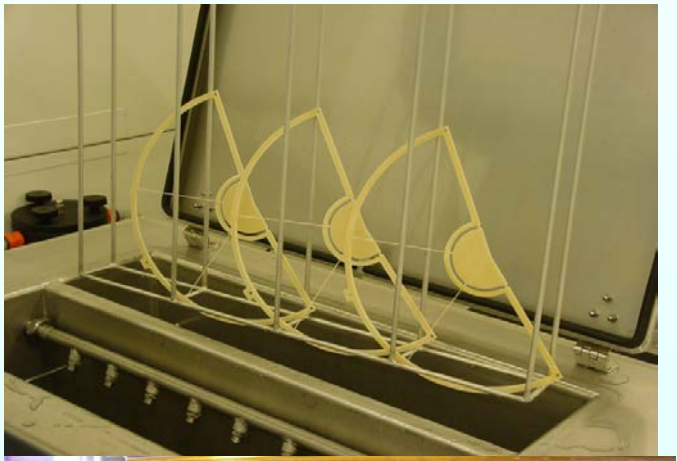

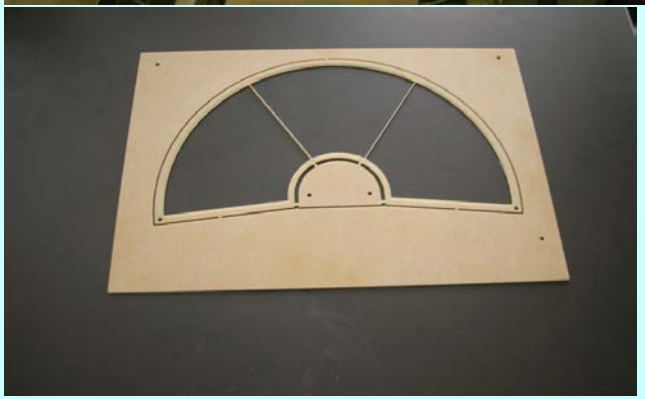

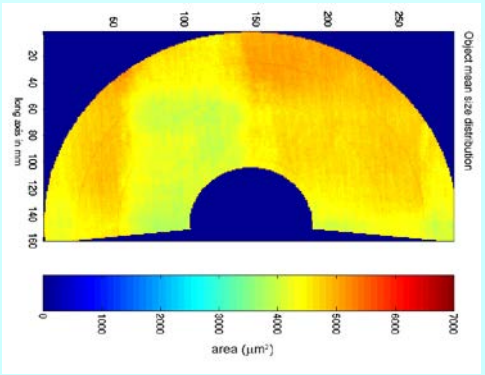

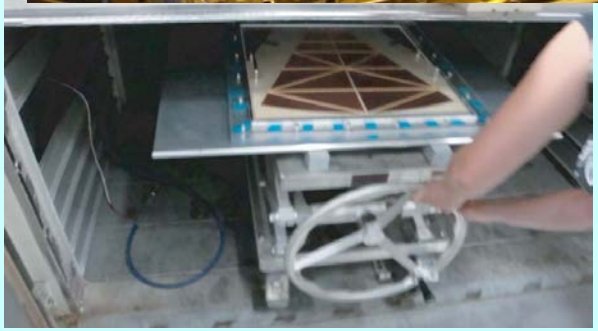

LHCb
High rapidity triggering

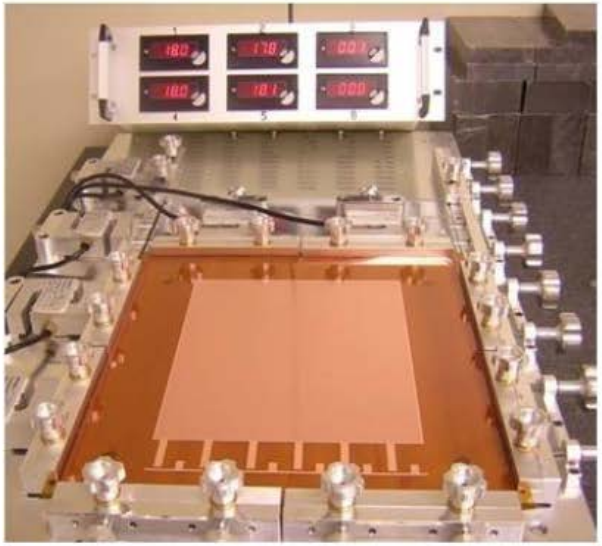

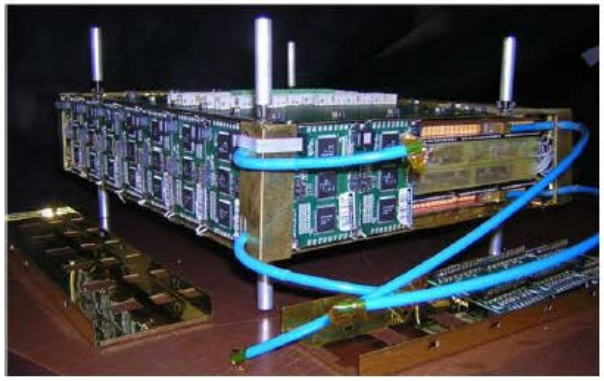

Fast, high rate triggering

- 20 × 24 cm active area
- 1 × 2.5 cm pad readout
- Gas mixture: $Ar/CO_2/CF_4$ (45/15/40)
- Time resolution: 4.5 ns (1 det.) or 3.5 ns (2)
- Required rate capability: $\sim$ 500 kHz/cm^2
- 10^{-12} discharge prob. per incoming particle (measured with intense 350 GeV π-beam)
- CARDIAC-GEM front-end electronics

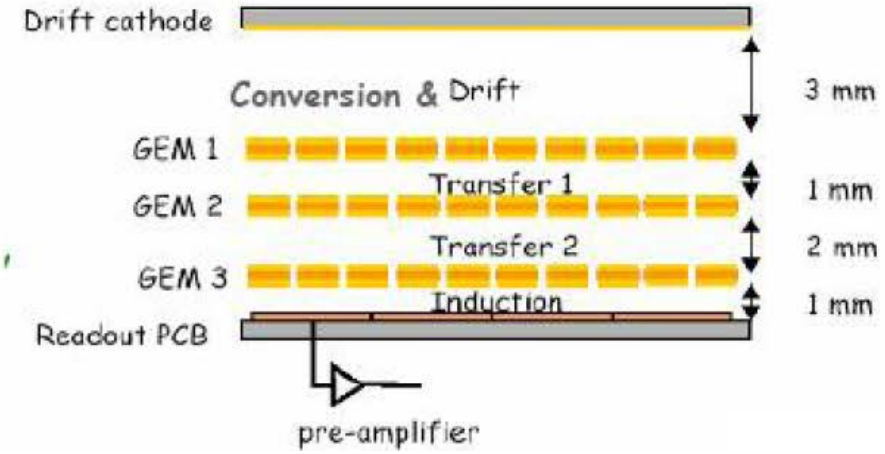

Cylindrical GEMs

Barrel tracking

π - NA49

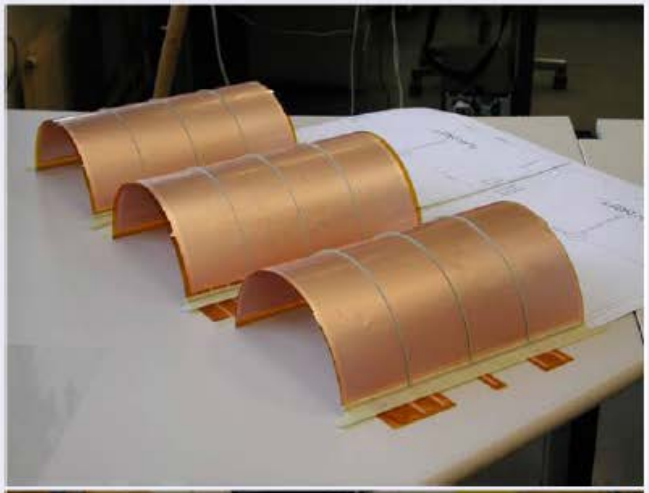

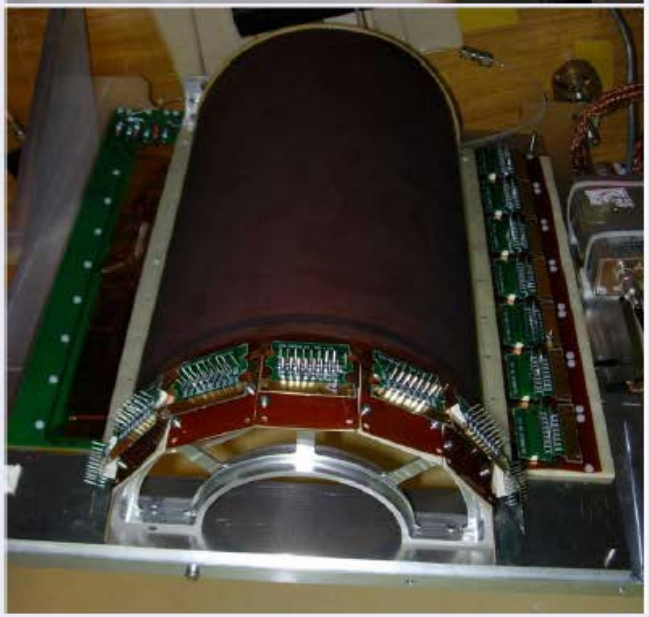

2π - KLOE-2

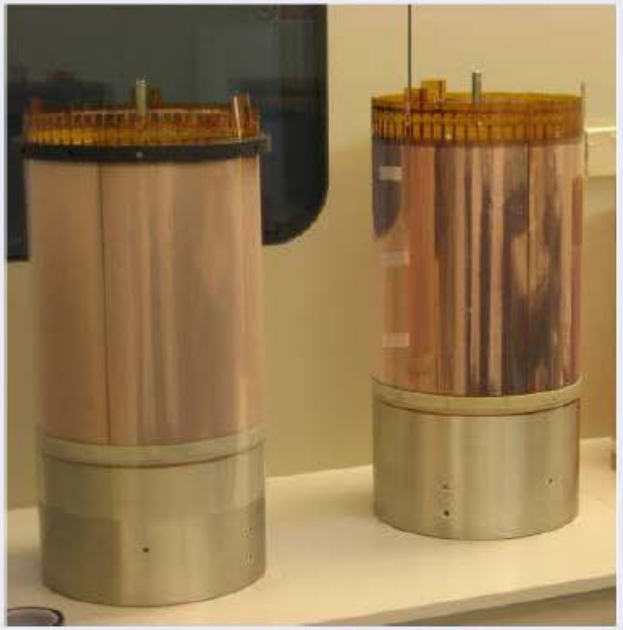

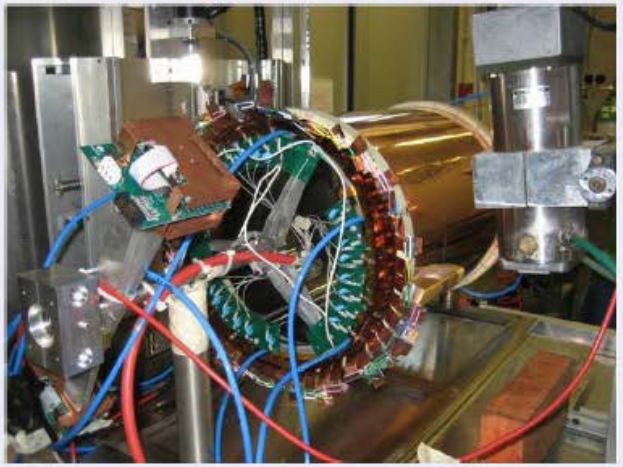

Forming spherical GEMs

In a vacuum

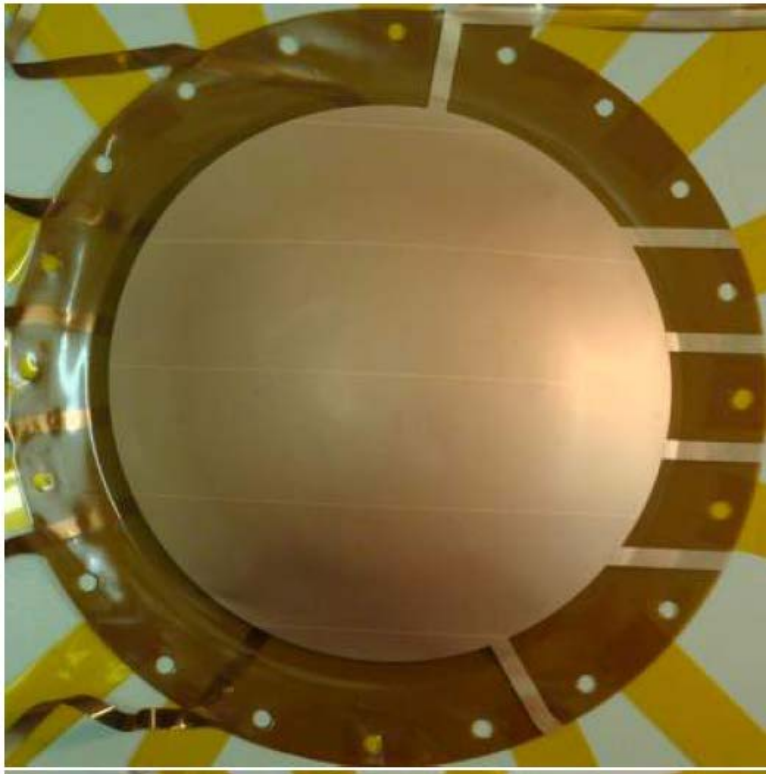

Spacers

Curved structure to keep accurate spacing

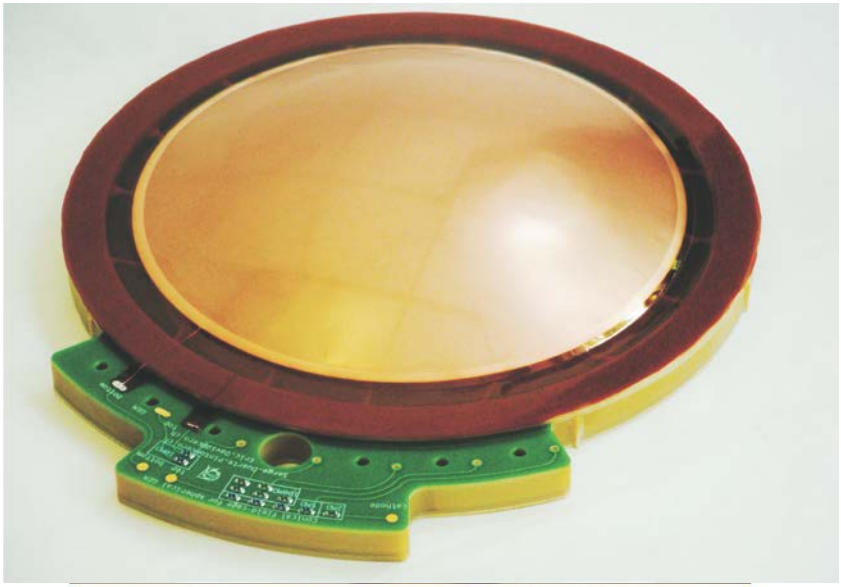

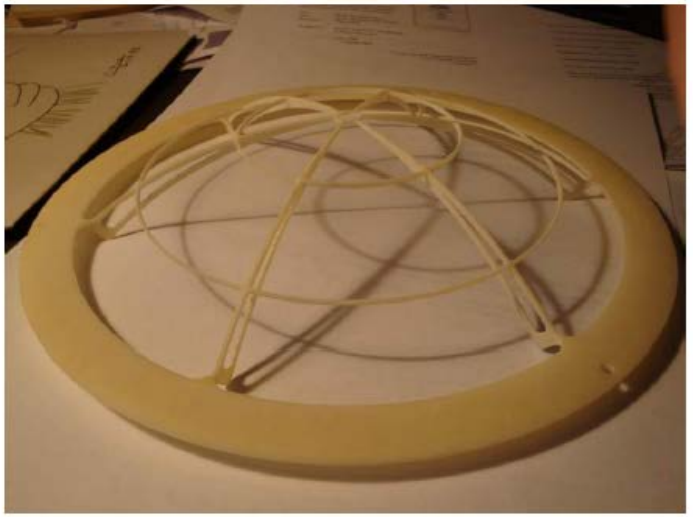

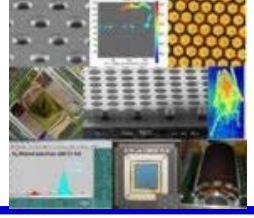

HIGH RATE applications

Pixelised GEMs (COMPASS)

Foil: 450 × 450 mm²
- 3 conducting layers 5 μm Cu
- 2 intermediate layers 50 μm Polyimide

Centre: 32 × 32 mm²
- 32 × 32 quadratic pixels

Periphery: 100 × 100 mm²
- 2 layers, 512 strips each
- equal charge sharing
- pitch: 400 μm

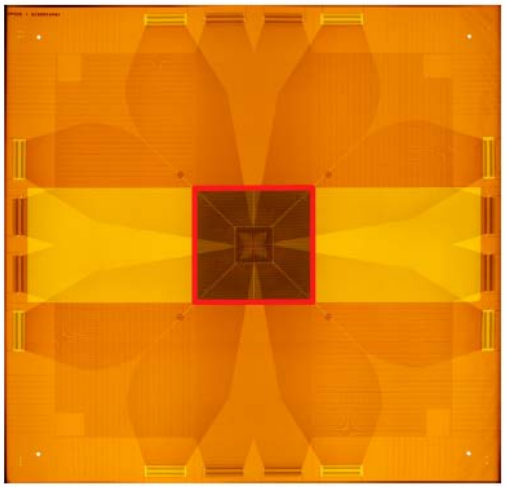

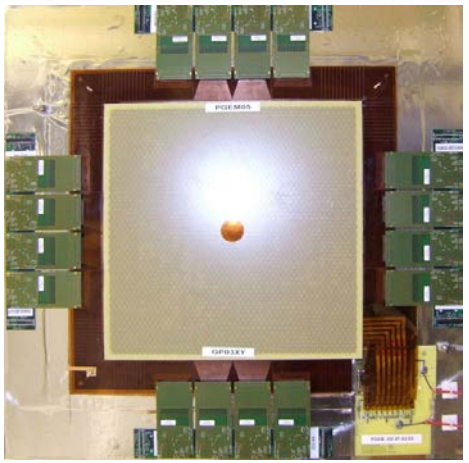

stable operation in particle flux up to $1.2 \cdot 10^5$/s/mm²
extremely thin: 0.2% X_0
spatial resolution: 90 μm

A. Austregesilo et al., NP B PS 197 (2009) 113

GEM studies for LHCb

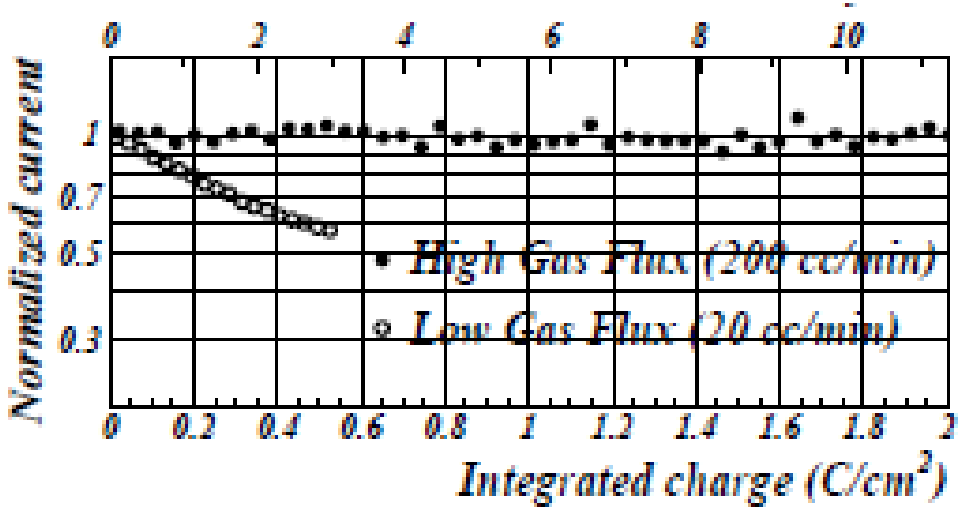

20x24 cm² GEM modules

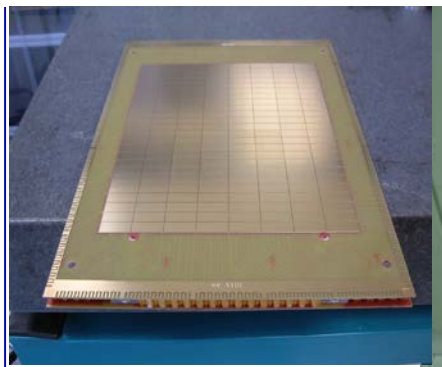

Pad readout plane

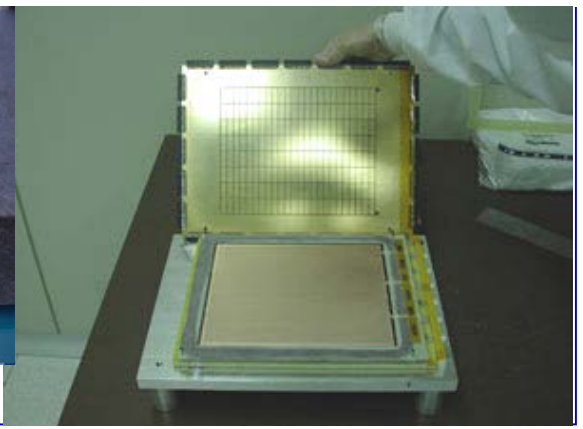

GEM development: *large* foils

Standard double mask technology
Limited to 40cm x 40cm due to
Mask precision and alignment

Single mask GEM technology:

Chemical Polyimide etching

Copper electro etching

Stripping

Second Polyimide etching

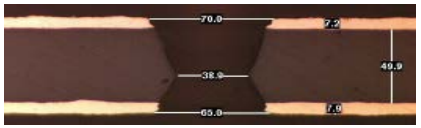

Result

- **Limited to 2m x 60cm due to**
- **Base material**
- **Equipment**

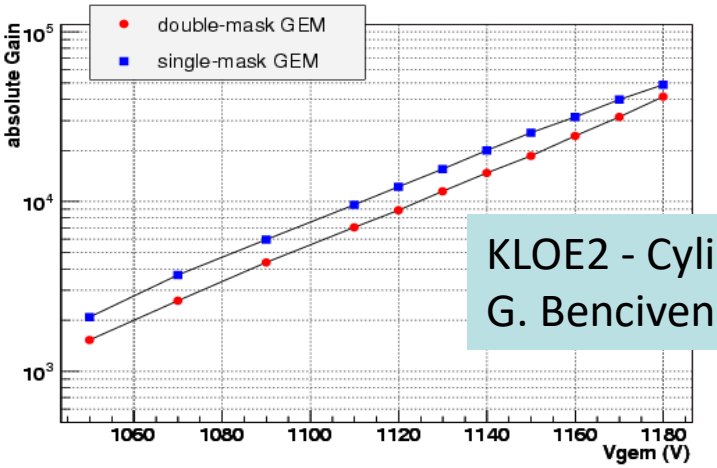

KLOE2 - Cylindrical Triple GEM
G. Bencivenni

KLOE2

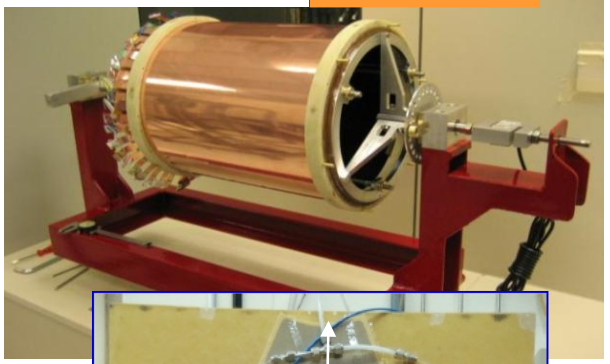

TOTEM

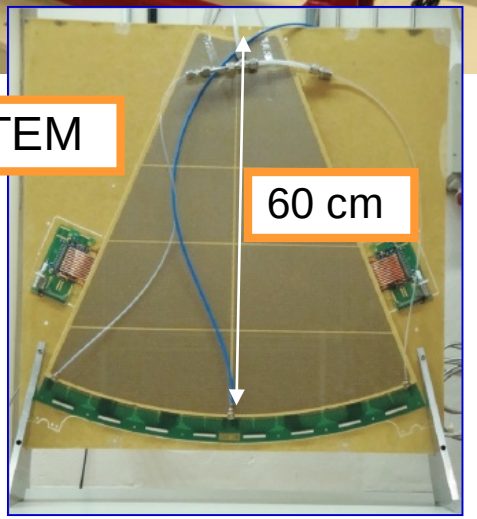

CBM @ GSI
CMD3 @ BES
……..

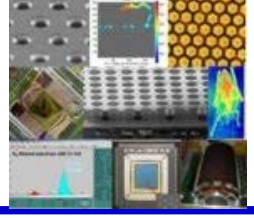

projects for the future

GEM ILC TPC,
T. Matsuda

CMD3 @ BES

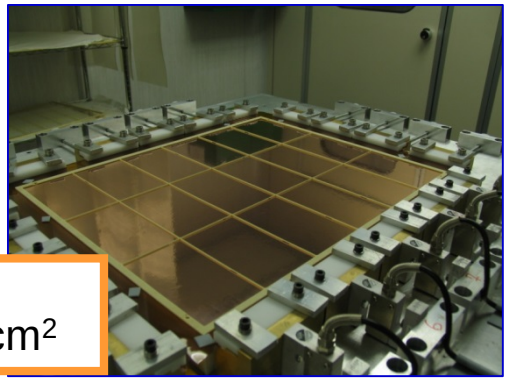

JLab Hall A
GEM 40 x 50 cm^2

STAR - Forward GEM Tracker

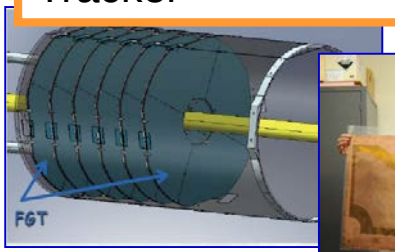

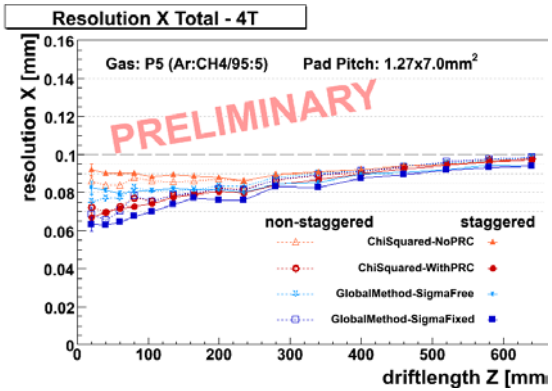

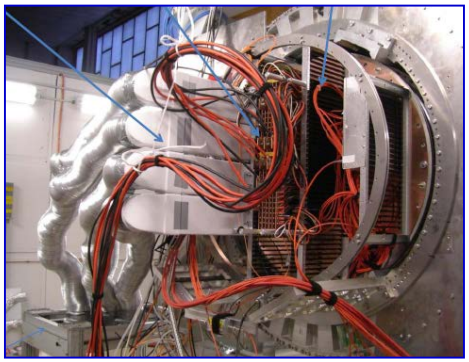

ILC TPC

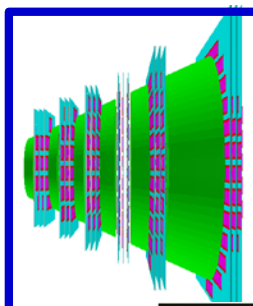

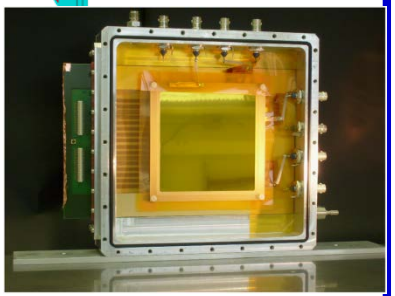

CBM: GEMs
for tracking

H calorimetry(GEM)
(ATLAS, ILC)

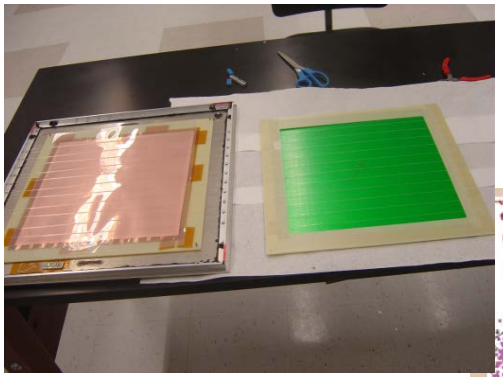

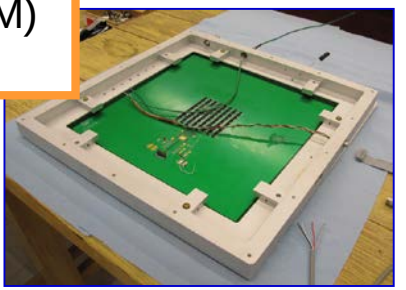

GEM ILC HCAL,
A. White

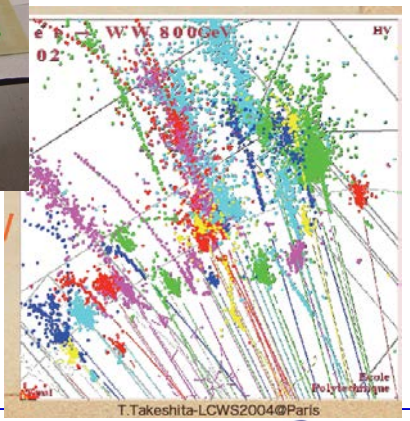

Two very large approved projects:

CMS High Eta MPGD Project (GE1/1 1.6>η>2.1)

A. Sharma

CMS High Eta MPGD - Workshop (30 September 2010)

15 institutes, 60 participants

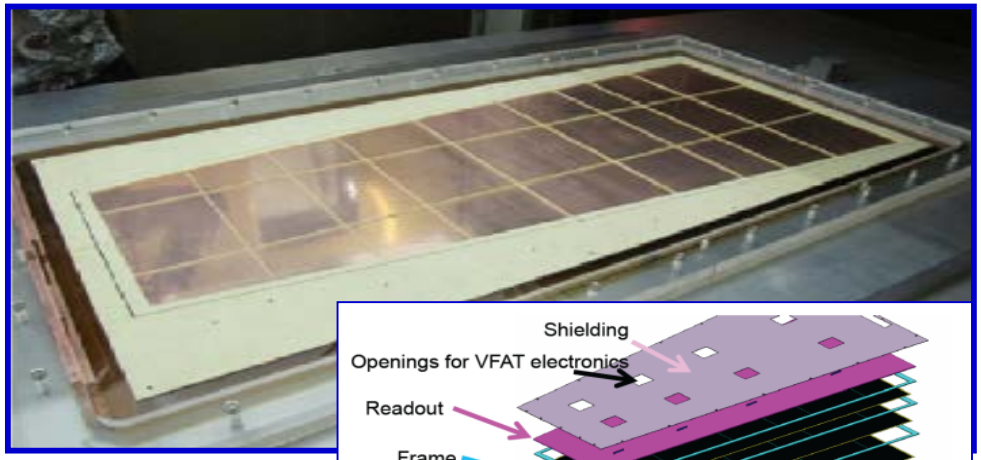

Rate capability : $10^4/mm^2$

Space/Time resolution: ~ 100 μm / ~ 4-5 ns

Efficiency > 98% ; Excellent Long Term Operation

Gas Mixture: Argon CO2 (non flammable mixture)

Large areas ~ 1m x 2m with industrial processes

CMS UPGRADE:

1000 m^2 of GEM foils, tracking & trigger

ALICE – TPC r-O, upgrade

Goal: ~.9 x 1.2 m^2

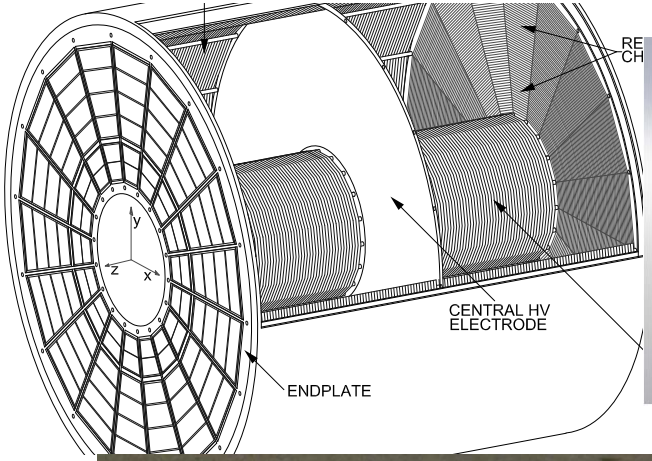

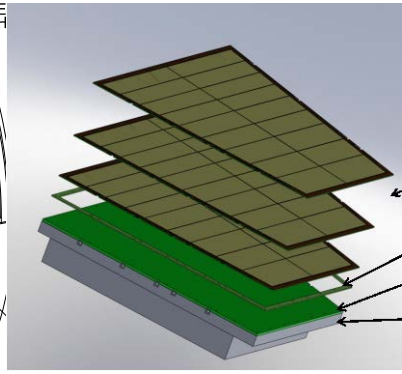

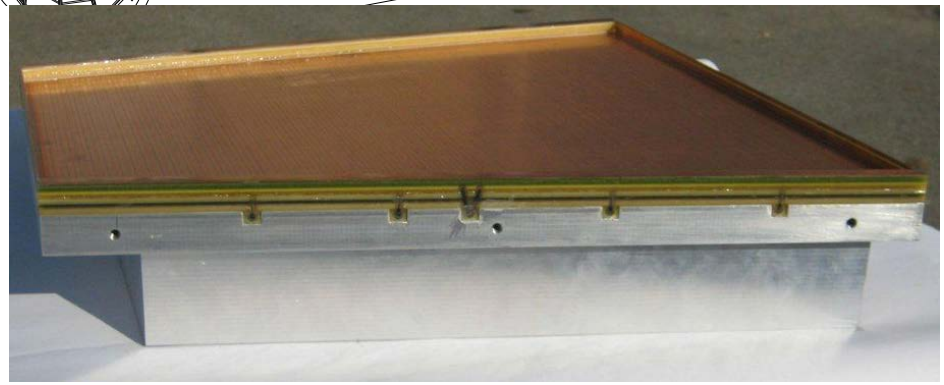

ALICE UPGRADE:

130 m^2 of GEM foils

Micromegas – Micromesh Gaseous Structure

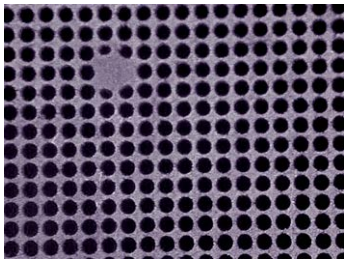

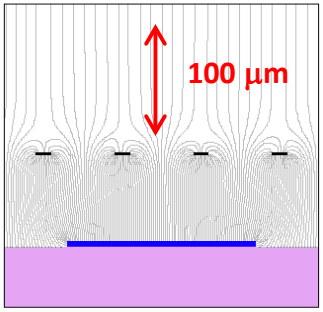

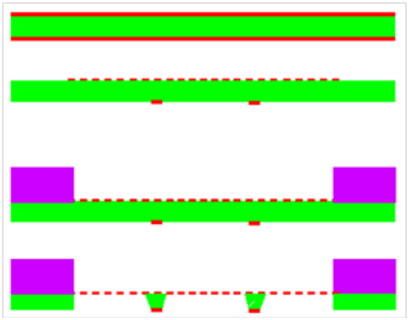

Micromesh mounted above readout structure (typically strips).
E field similar to parallel plate detector.
E_a/E_i ~ 50 to secure electron transparency and positive ion flow back suppression.

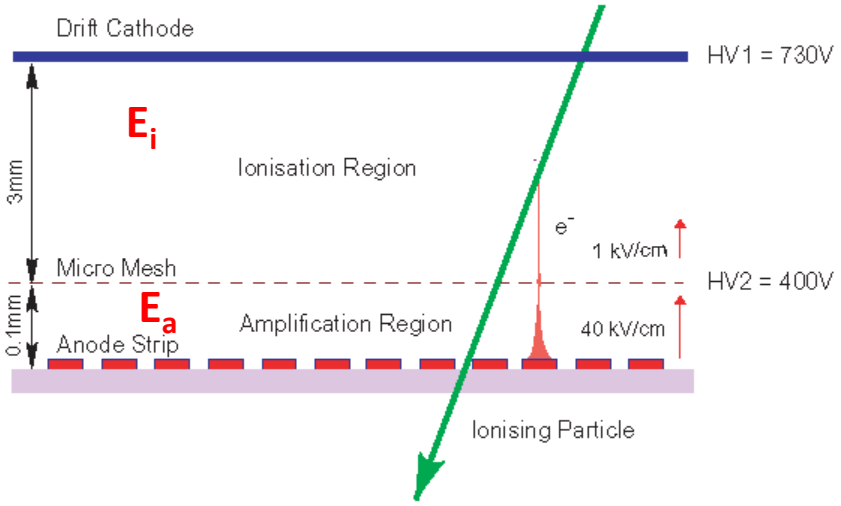

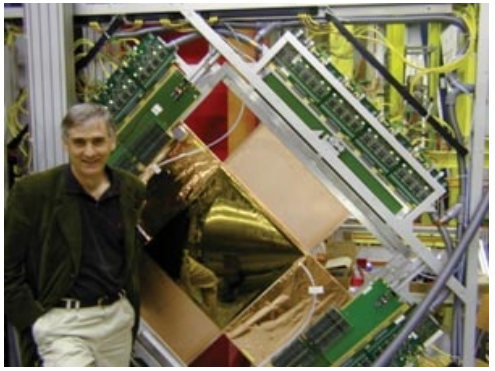

Ioannis Giomataris

Y.Giomataris et al, NIM A 376 (1996) 29

Micromegas – Micromesh Gaseous Structure

gain

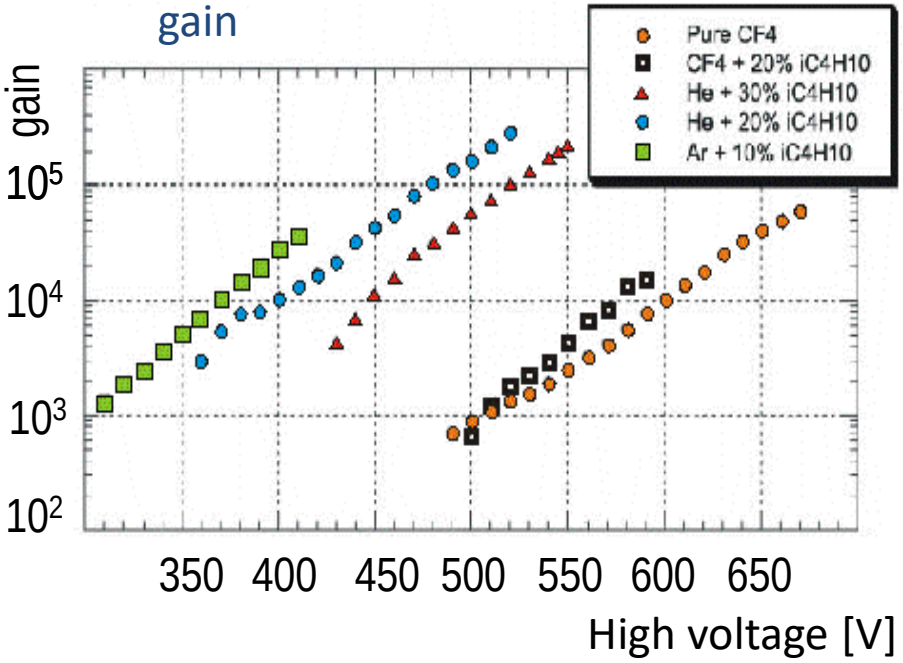

efficiency & discharge probability

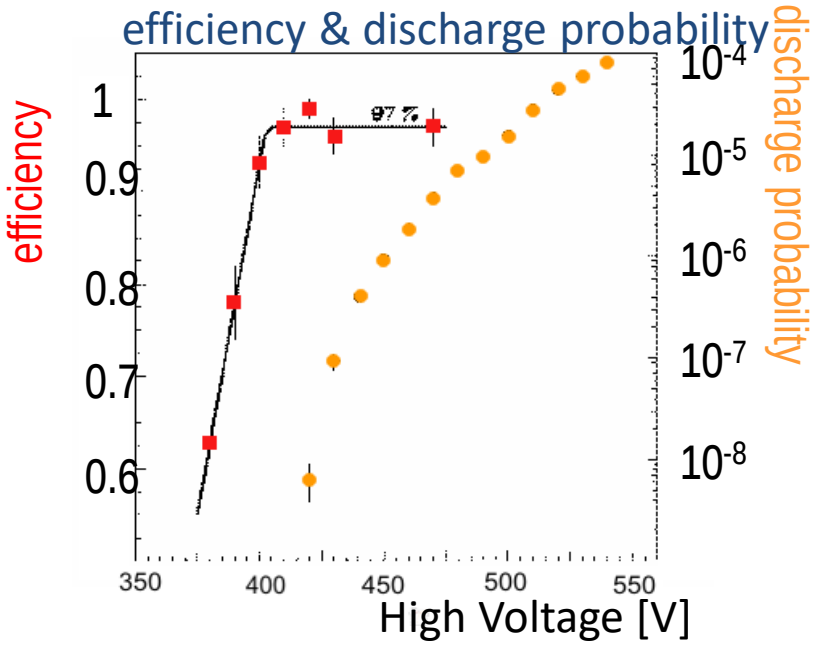

energy resolution ~ 10%

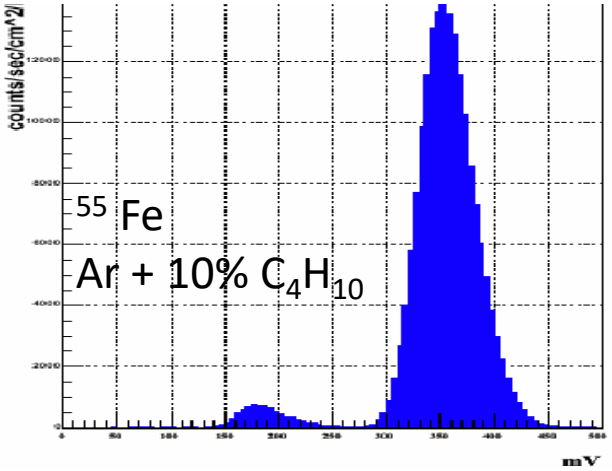

D.Thers et al NIM A 469 (2001) 133

ageing:Ar-iC_4H_{10} 94-6% up to 24.3mC/mm^2

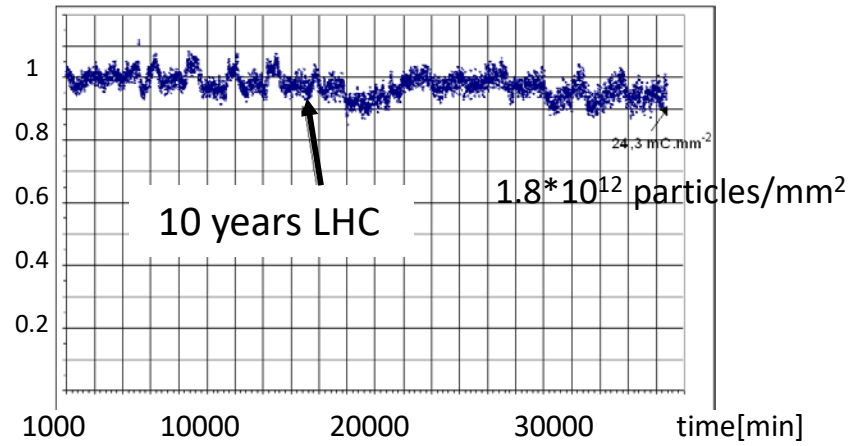

Micromegas – Micromesh Gaseous Structure

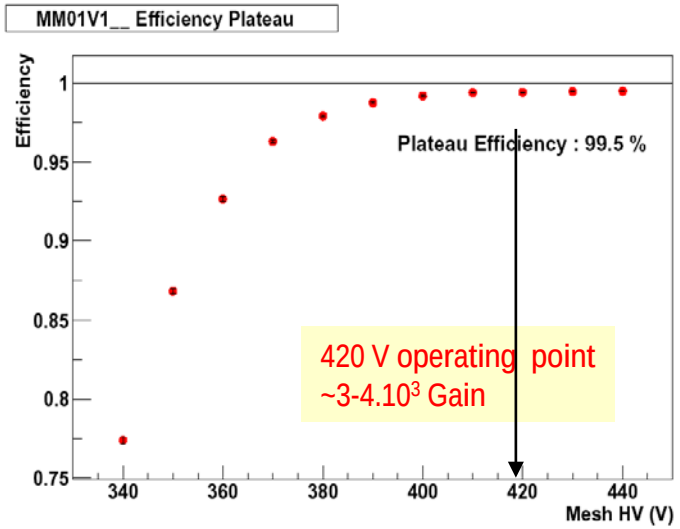

Large efficiency plateau > 40 V

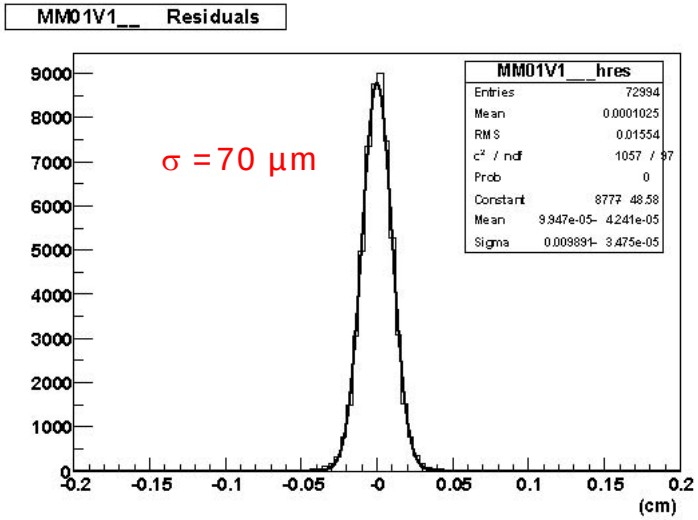

Spatial resolution < 70 µm

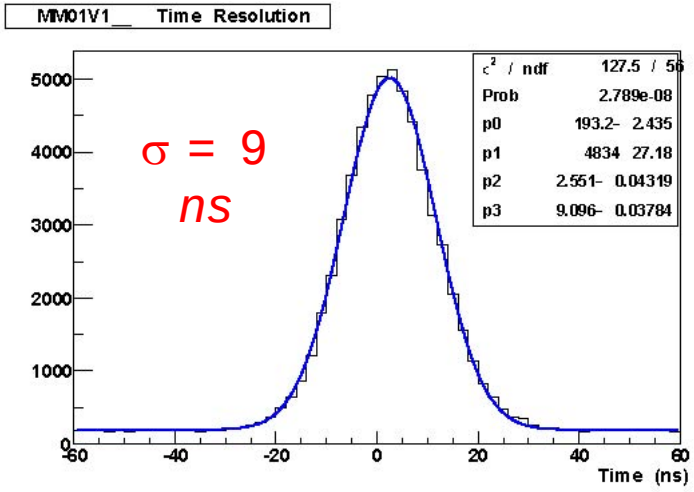

Time resolution : 9 ns

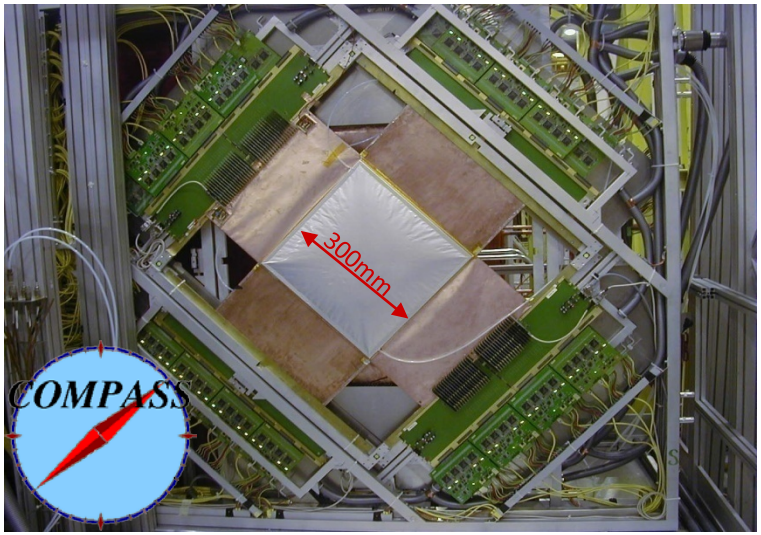

D.Thers et al NIM A 469 (2001) 133

Micromegas – Micromesh Gaseous Structure

T2K TPC, J. Beucher

24 bulk-Micromegas + FEE + mechanicals
3 m^2 of bulk Micromegas
41472 FEE channels

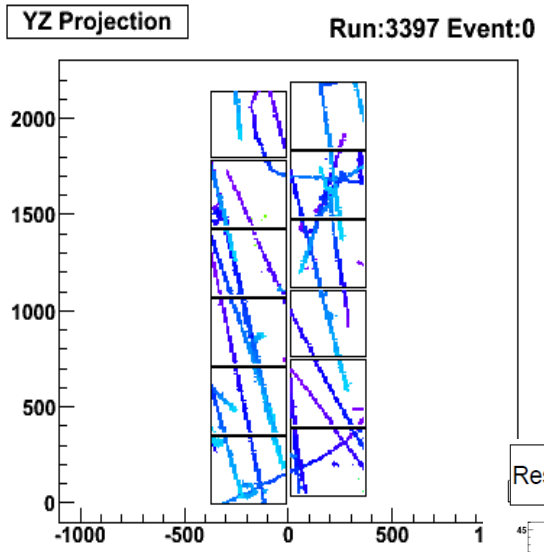

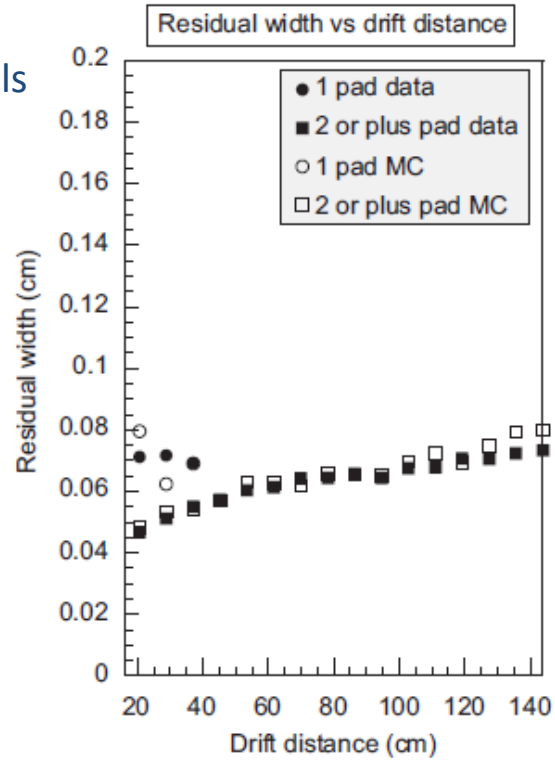

Reconstructed cosmics
by a readout plane
(beam tests @ TRIUMF on-going

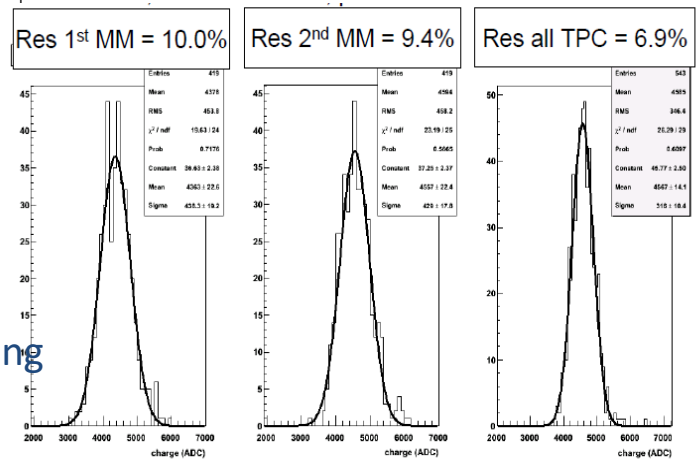

Micromegas ILC-TPC,
D. Attie, P. Colas

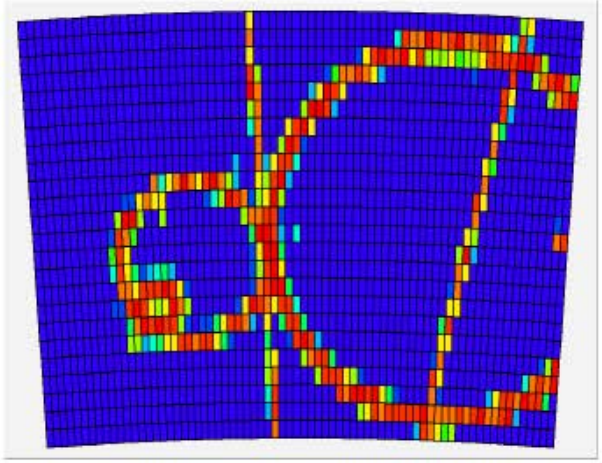

Curved Micromegas CLAS12,
S. Aune

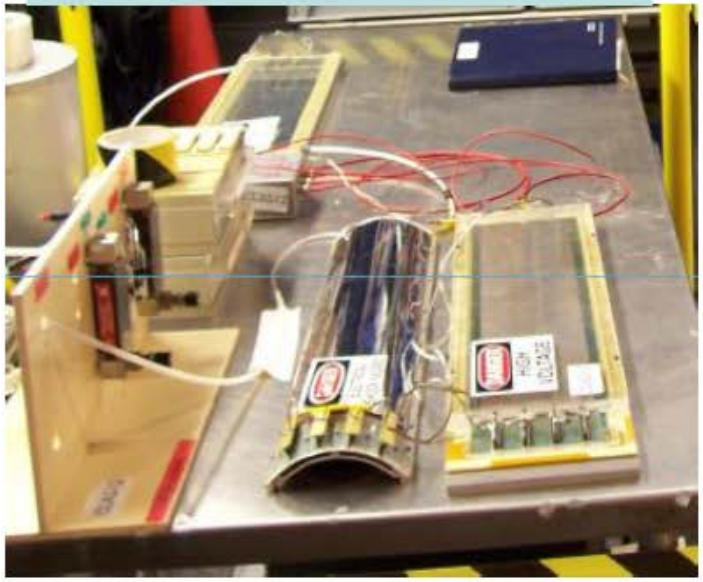

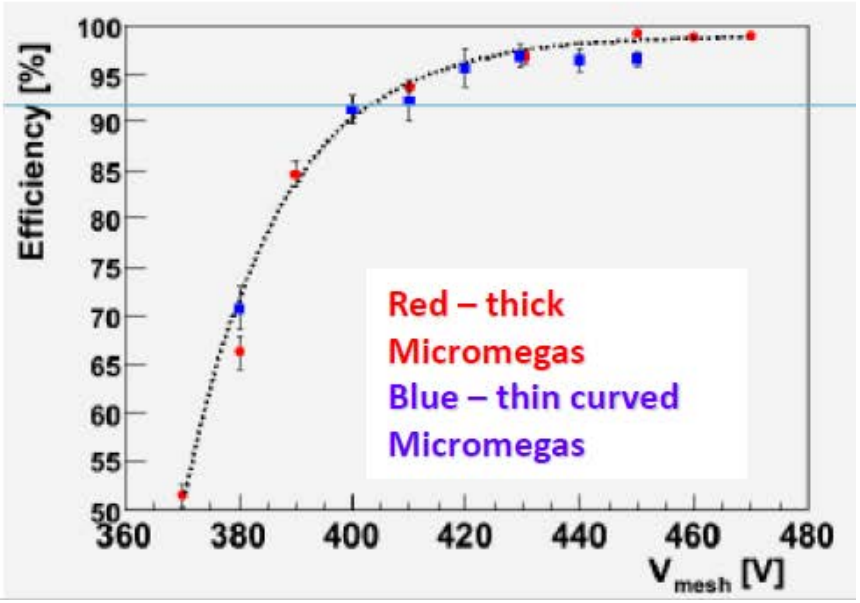

Micro-Bulk Micromegas

Low background Micromegas,
J. Galan, E. Ferrer, A. Tomas

Micro-Bulk Micromegas
Th. Papaevangelou

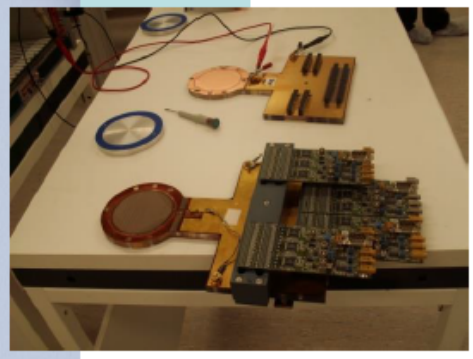

Readout plane + mesh all in one

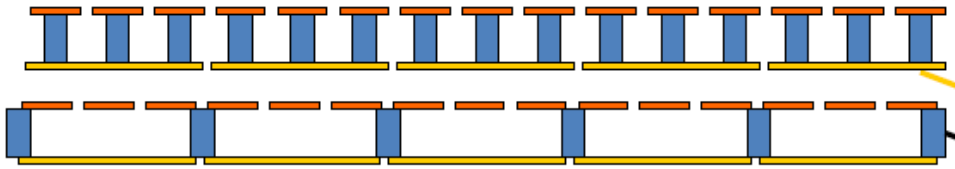

Micromesh
5μm copper

Kapton 50 μm

Readout pads

Lower capacitance
Under development

An I. Giomataris and R. De Oliveira idea

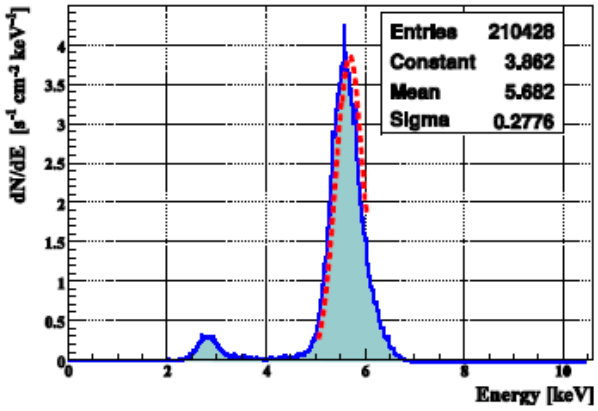

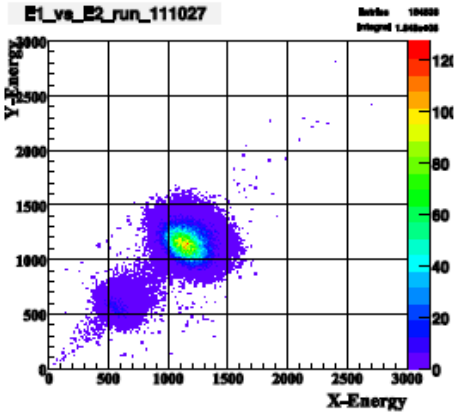

^{55}Fe Calibration with Ar – 5% isobutane @ 1 bar
Collimated source to avoid border effects
FWHM @ 6 keV = 11.5 %

INGRID

Integrated Micromegas and Pixel Sensor

Postprocessing of the TIMEPIX chip to build a metal mesh on insulating pillars

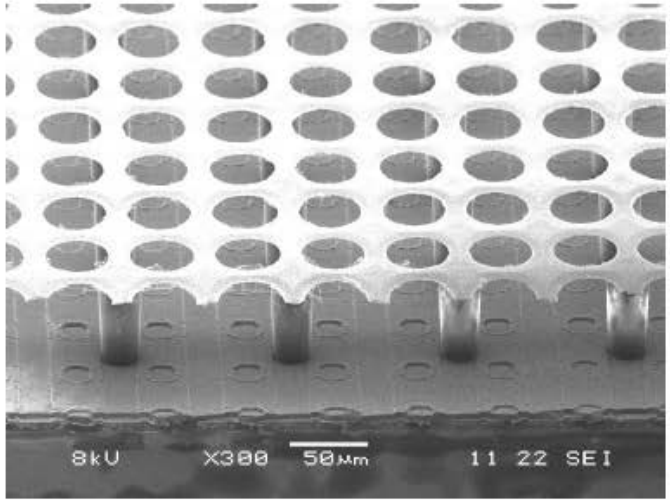

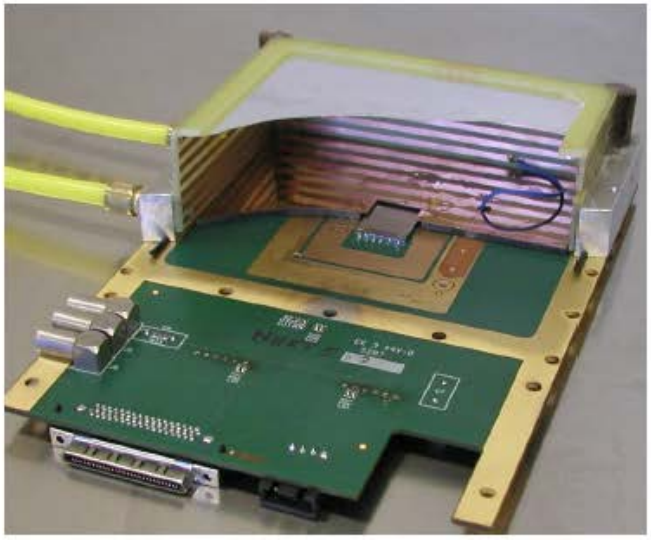

Electron tracks from ^{90}Sr in magnetic field (0.2 T):

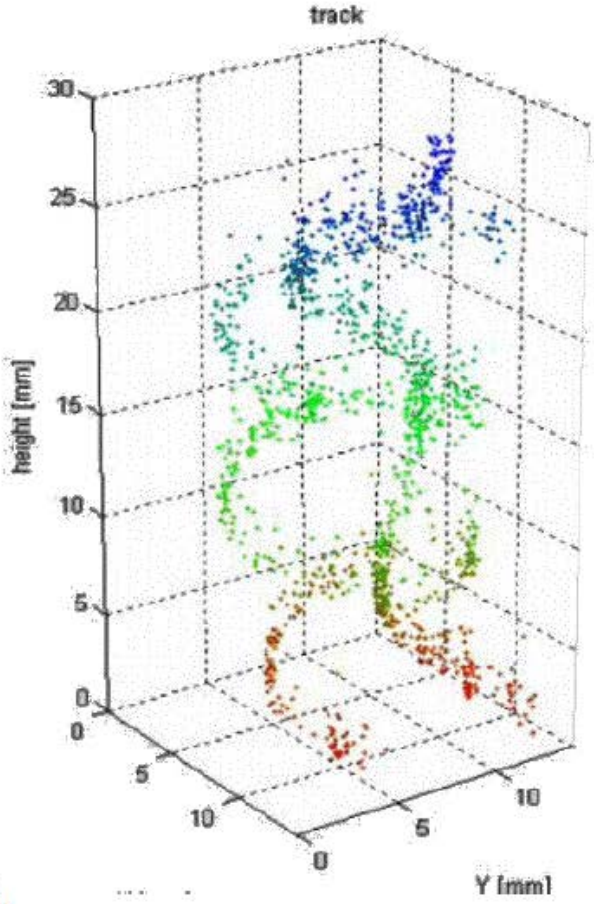

H. Van der Graaf ,
IEEE Nucl. Sci. Symp. Conf. Rec. (Dresden, October 2008)

Technology Development Highlights

Resistive MicroMegas

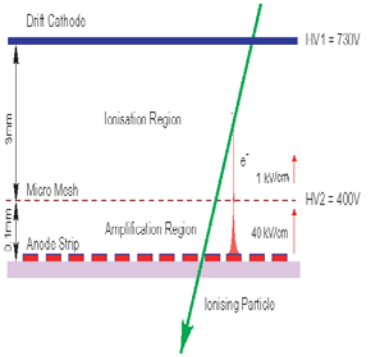

Bulk MicroMegas Process

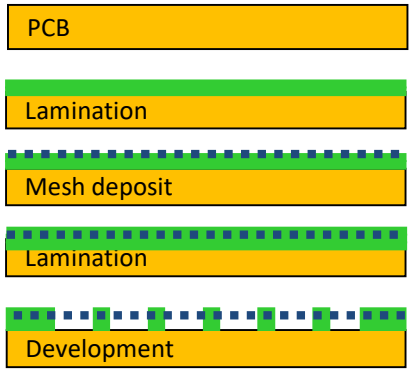

Standard Bulk MicroMegas suffers from limited efficiency at high rates due to discharges induced dead time

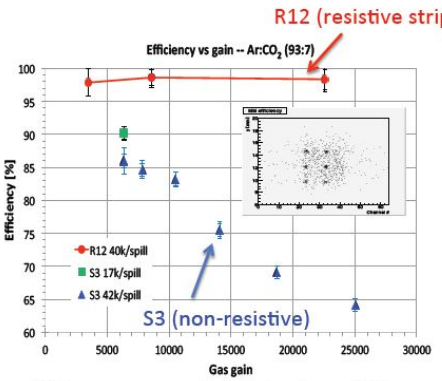

Efficiency measured in H6 pion beam (120 GeV/c); S3 is a non-resistive MM, R12 has resistive-strip protection

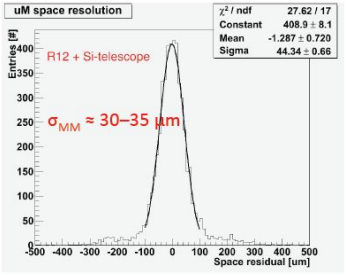

Spatial resolution measured with an external Si telescope, shown is convoluted resolutions of Si telescope + extrapol. (≈30 μm) and MM with 250 μm strip pitch

The resistive-strip protection concept

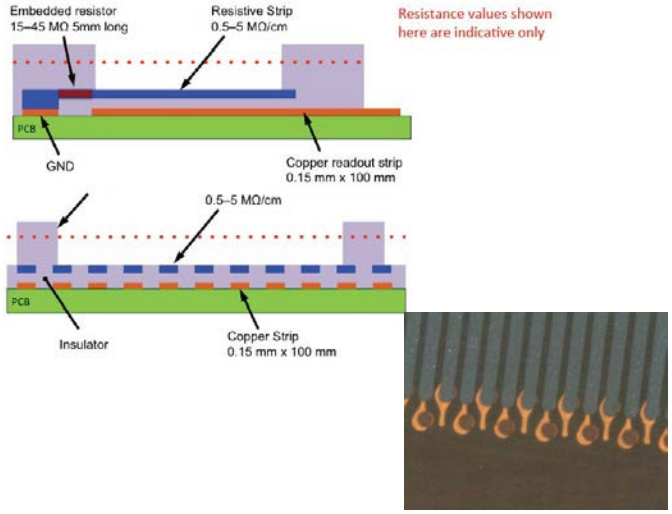

ATLAS small wheels upgrade project resistive MicroMegas prototype

89

Simulations:

- Elastic mean free path of electrons in Ar: 2-5 μm,
- diffusion: ~250 μm for 1 cm.

Compare with:

- Micromegas mesh pitch: 63.5 μm
- GEM polyimide thickness: 50 μm
- Micromegas wire thickness: 18 μm
- GEM conductor thickmess: 5 μm

Hence:

- mean free path approaches small structural elements;
- diffusion is not likely to be Gaussian;
- such devices should be treated at a molecular level.

Simulations:

Micromegas in detail

- Avalanche shape:
  - The avalanche develops in the high field region between the mesh and the pad plane
  - Electrons move to the pad plane, ions to the mesh
  - Most electrons and ions are produced in the immediate vicinity of the pad plane;
    - electrons are almost immediately absorbed,
    - ions have the complete gap to traverse.
    - Micromegas has ion-dominated signals.

$^{55}Fe \rightarrow {}^{55}Mn$ (EC), relaxing via
Auger (70 %, 5 keV and lower) or
γ (25 %, 5.9 keV and lower) ...

E = 41.4 kV/cm
gain ~ 3000

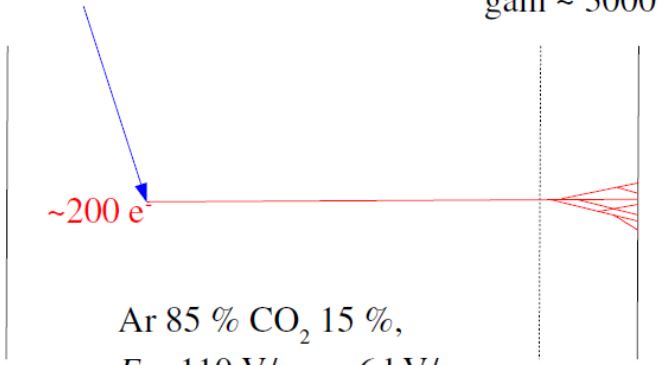

Mesh transparency

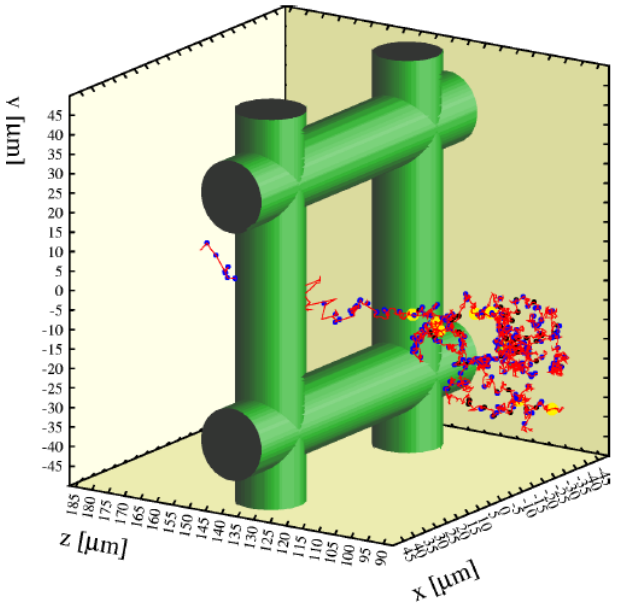

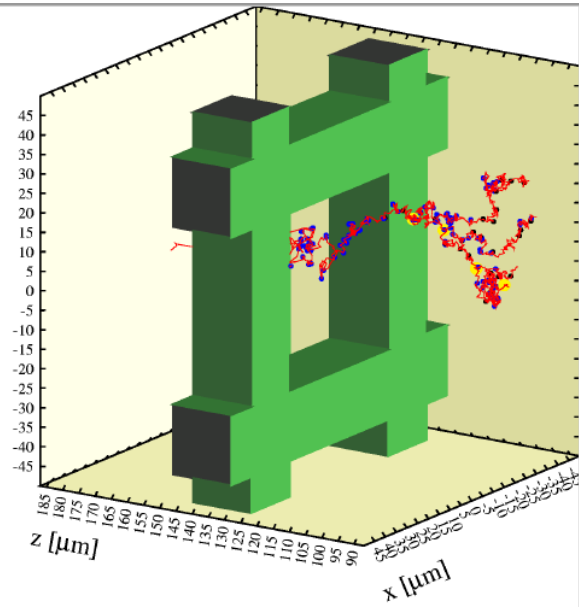

Legend:
- – electron
- O inelastic
- O excitation
- O ionisation

Simulations:

GEM in detail

- Avalanche shape:
  - electrons are produced in the GEM foil, near the exit;
  - the electron cloud traverses the gap between the GEM and the pad plane;
  - ions try and return to the drift plane; there are hardly any ions between the lower electrode and the pad plane;
  - GEMs have an electron-dominated current.

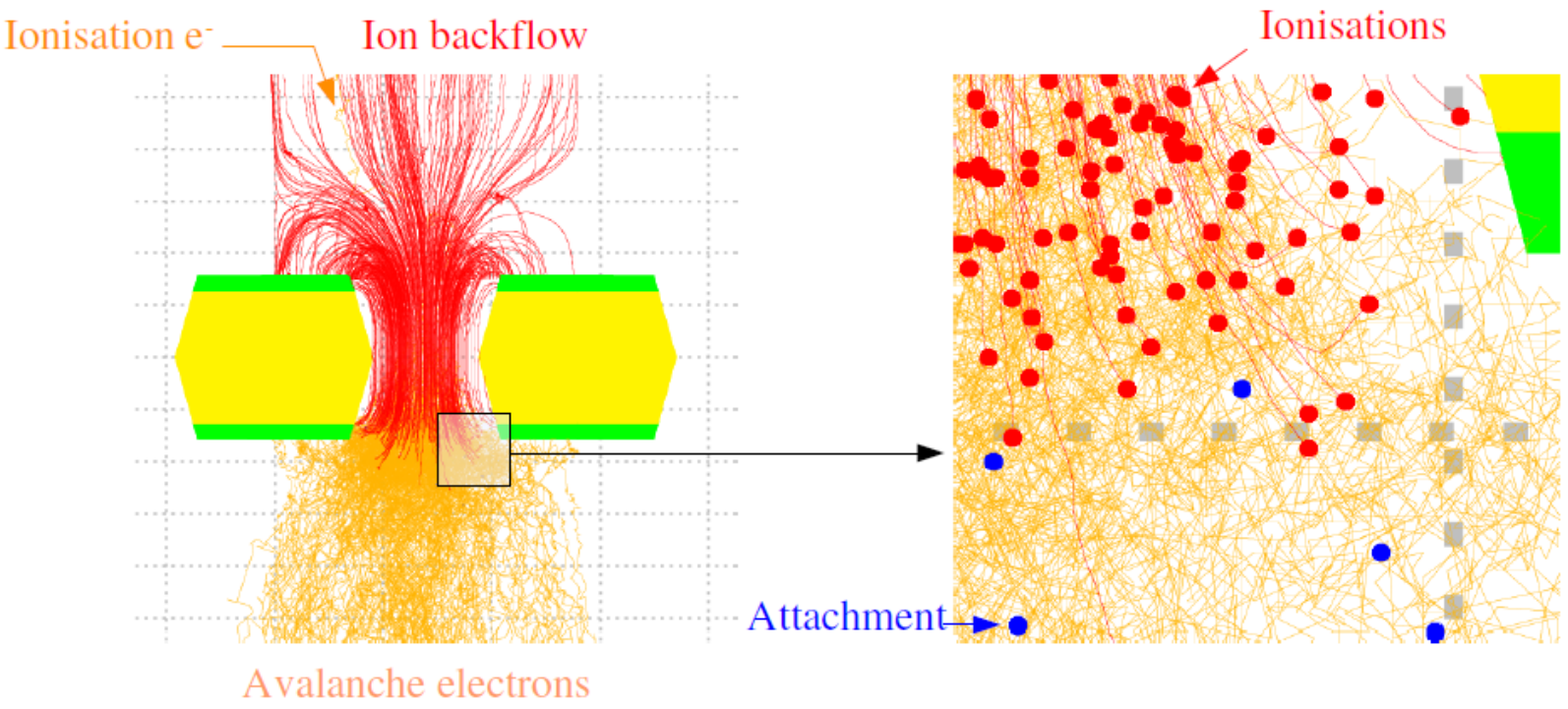

[Plot by Gabriele Croci and Matteo Alfonsi]

Cross-talk in GEM signals

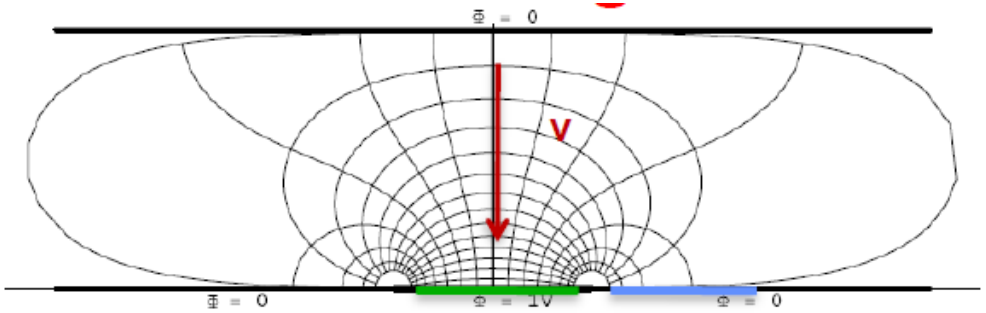

D = 1mm

Central Strip First Neighbour

w

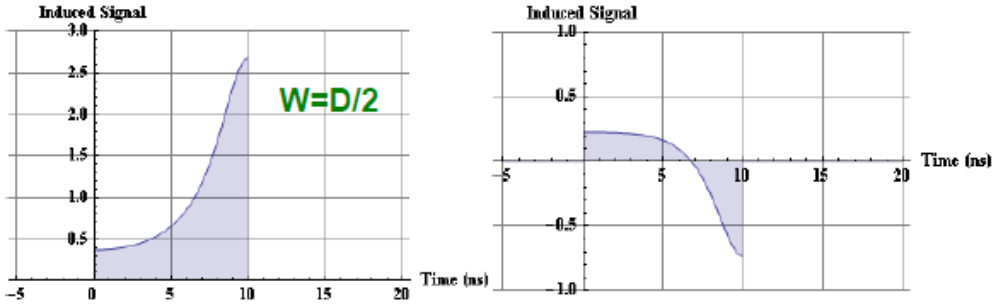

W=D/2 (D=1mm, w=0.5mm)

Connecting an amplifier with Peaking Time = 10ns

→ 10% crosstalk !

In case the electronics peaking time is smaller or of similar size as the time the electron takes to pass the induction gap, there is a sizable signal on the neighboring strips that do not even receive charges.

Central Strip First Neighbor

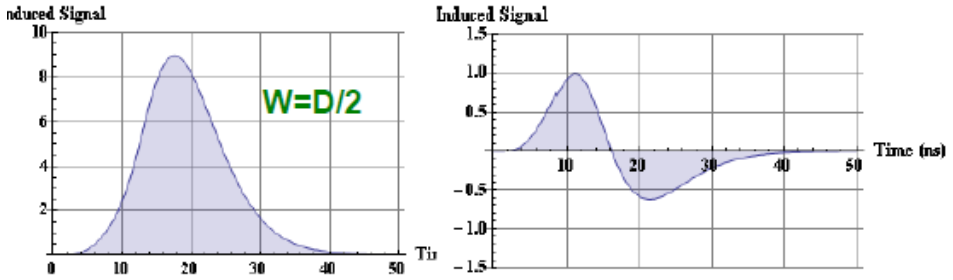

Ballistic deficit in Micromegas signals

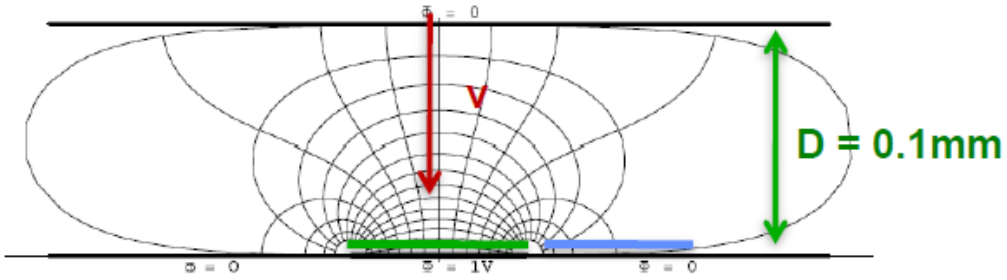

$I(t,x) = -e_0 * Exp[\alpha\, v\, t] * Ez[x, D - v*t] * v \rightarrow$ Electrons

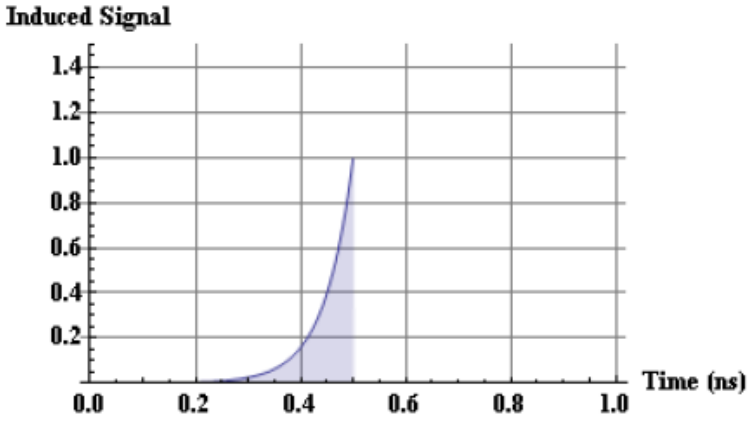

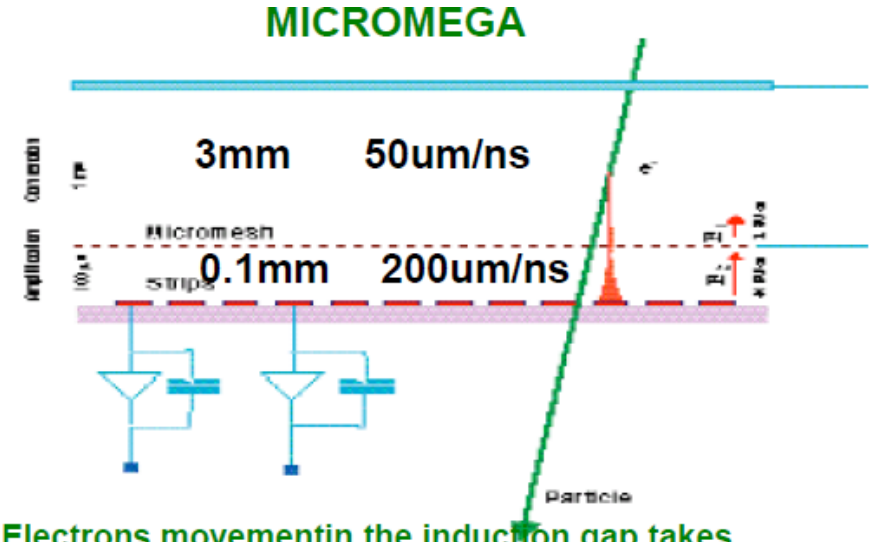

Electrons movementin the induction gap takes about $0.1mm/v_1=0.5ns$.

Collecting all electrons from the drift gap takes a maximum of $3mm/v_1=60ns$.

The MICROMEGA electron signal has a length of about 50 ns.

Typically w>>D – cluster size from electron component is dominated by diffusion and not by direct induction.

However, ion component has a length of about 100ns → Ballistic Deficit for fast electronis (e.g. 10ns peaking time).

Detection of photons

PHOTON ABSORPTION

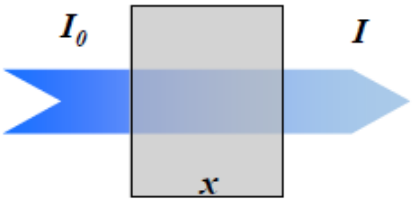

$$I = I_0 e^{-\frac{x}{\lambda}} \qquad \lambda = \frac{1}{N\sigma}$$

x : material thickness (cm)
λ : linear absorption length (cm)
σ : cross section (cm²)
N : molecules/cm³

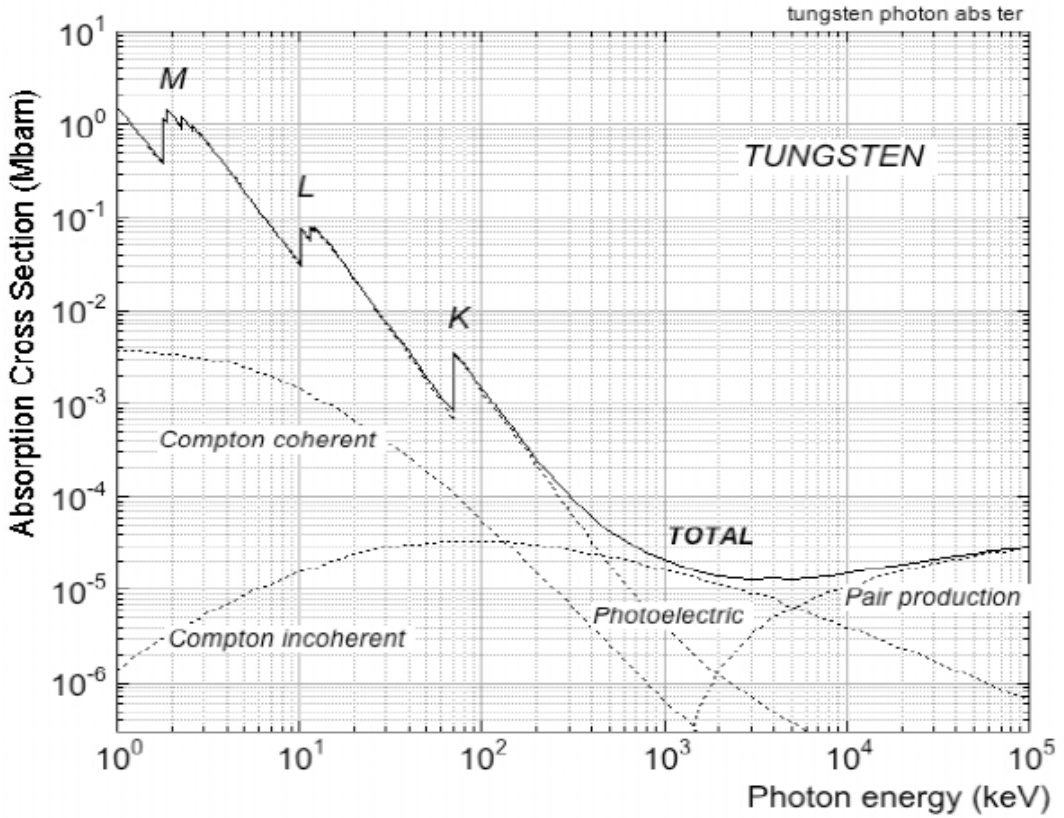

A. Thompson et al, X-RAY DATA BOOKLET (2001)

Potoelectric:

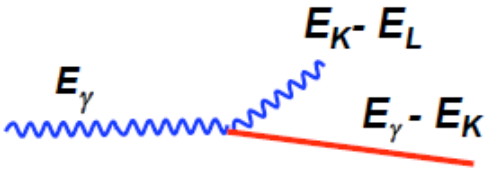

Compton:

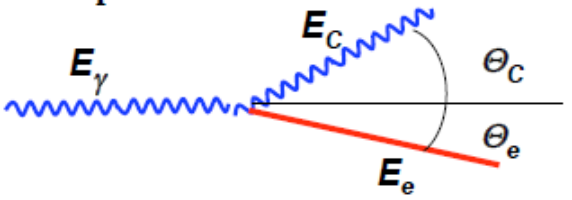

Pair Production:

Photoionization

PHOTOIONIZATION CROSS SECTION FOR XENON:

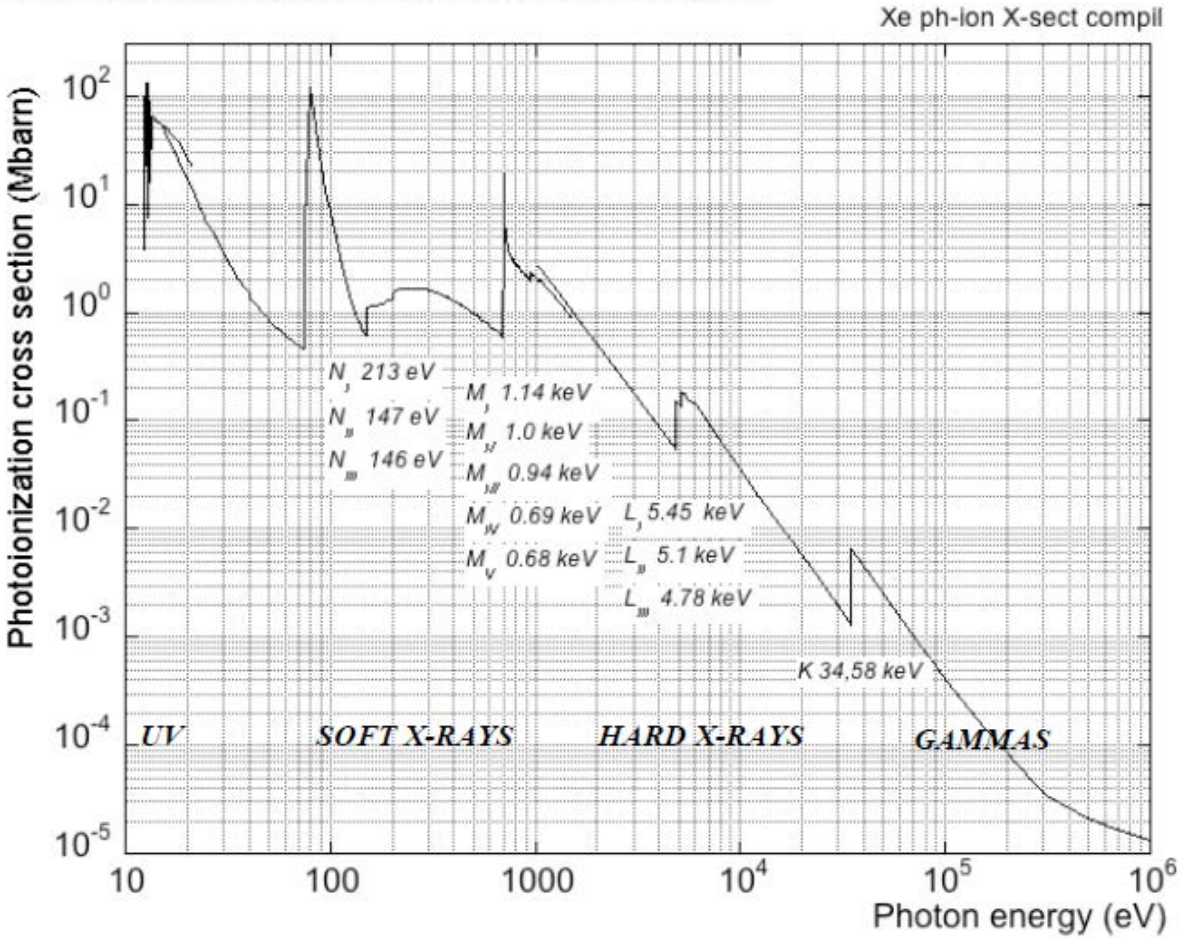

http://xdb.lbl.gov/

http://henke.lbl.gov/optical_constants/

http://physics.nist.gov/PhysRefData/FFast/html/form.html

Soft X-rays

ABSORPTION LENGTH IN GASES AT NTP

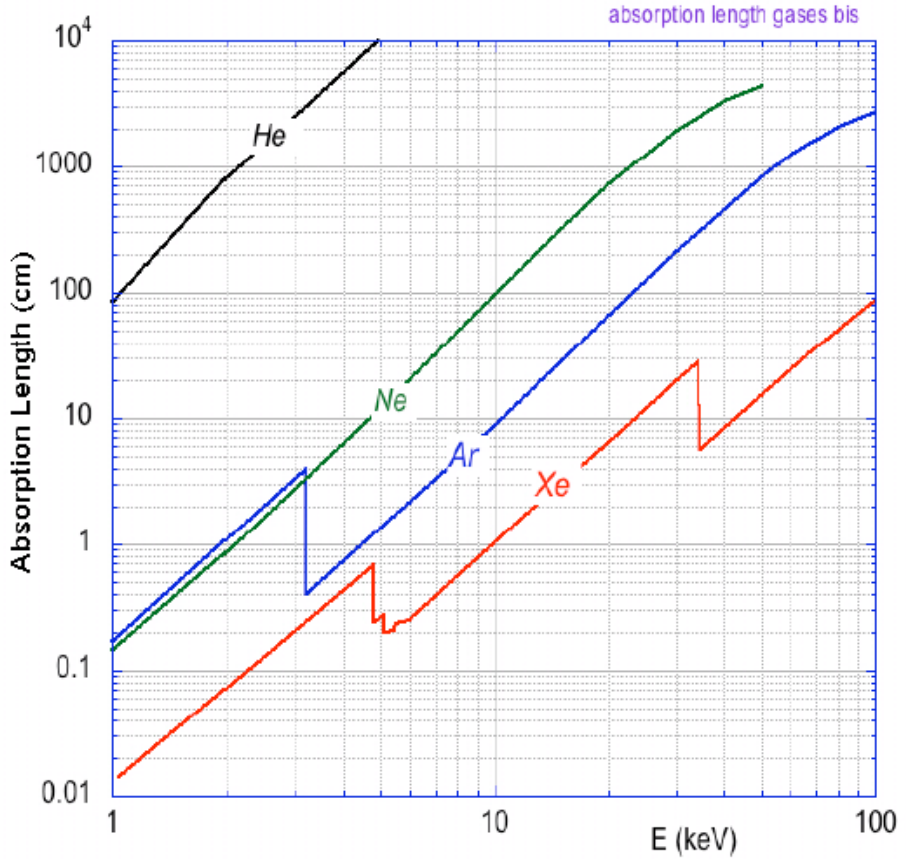

For gases at STP (0°C, 1 Atm): N=2.687 10^{19} cm^{-3}

$$\lambda(cm) = \frac{1}{26.87\,\sigma(MBarns)}$$

FLUORESCENCE:

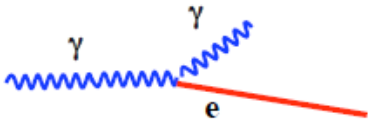

NON-RADIATIVE (AUGER):

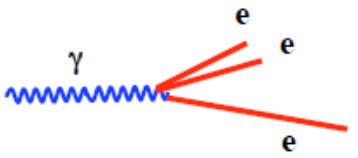

FLUORESCENCE YIELD $= \dfrac{N_{FL}}{N_{FL} + N_{NR}}$

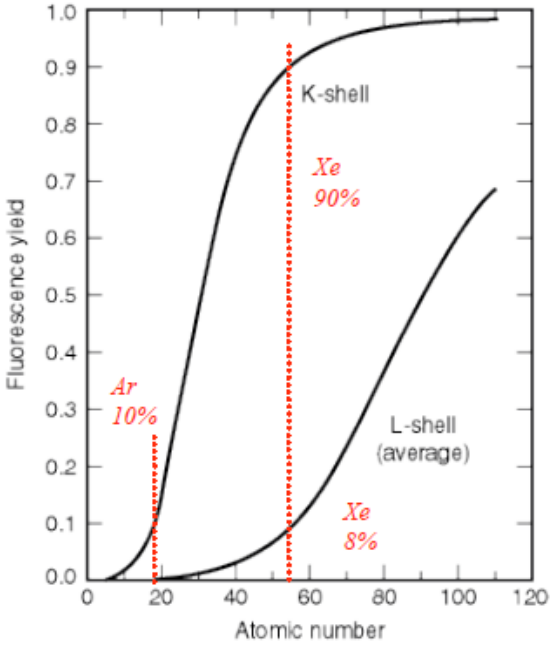

M. O. Krause, J. Phys. Chem. Ref. Data 8 (1979) 307

^{55}Fe X-ray

X-RAY ABSORPTION SPECTRUM

^{55}Fe X-Rays (5.9 keV) in Argon:

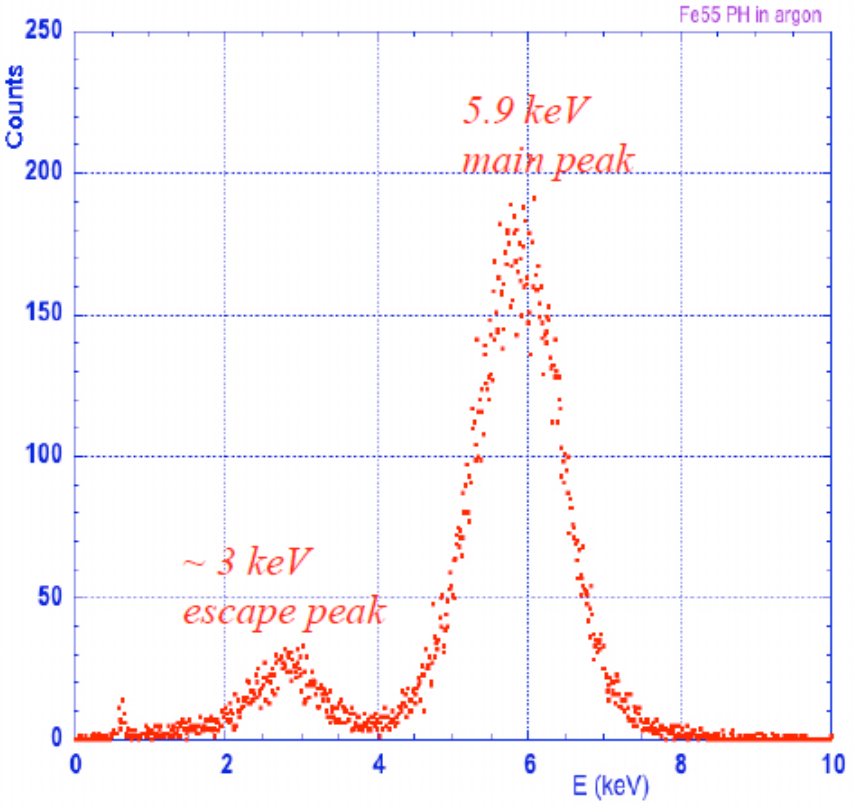

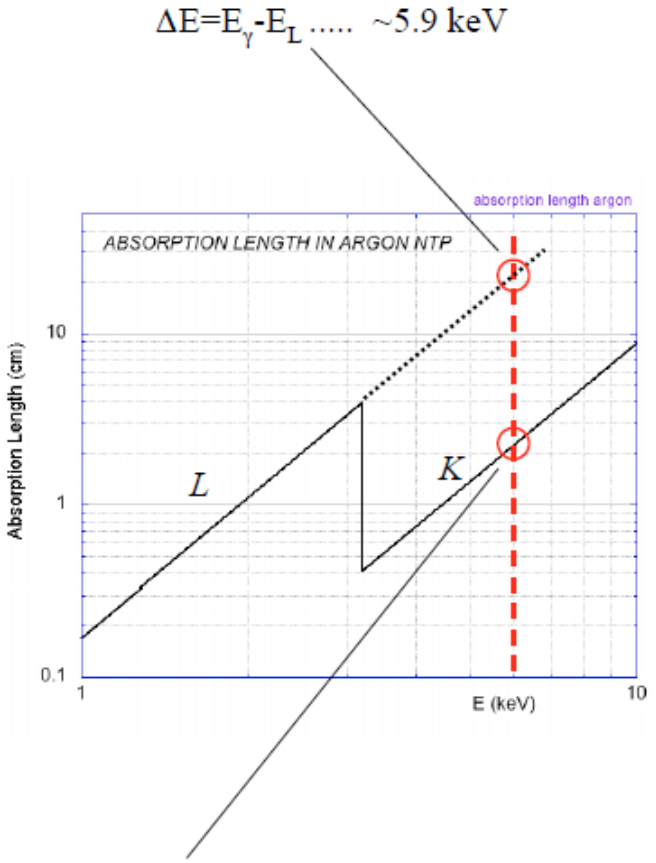

Auger: E~5.9 keV

Fluorescence: reconverted E~5.9 keV

escaped E~3.2 KeV

X-ray polarimeter

GEM X-RAY POLARIMETER

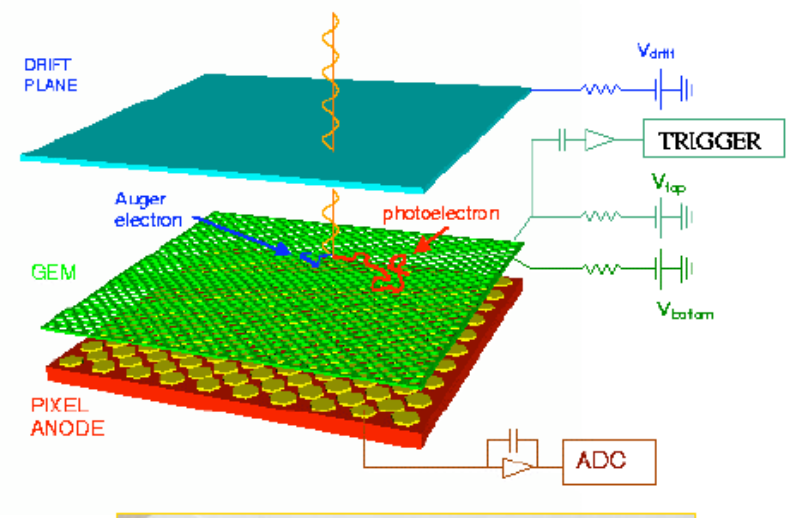

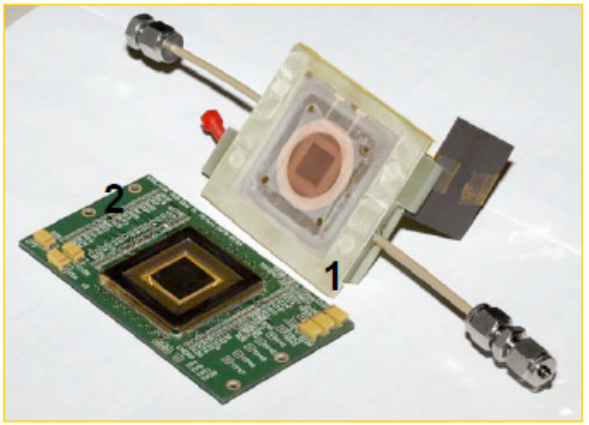

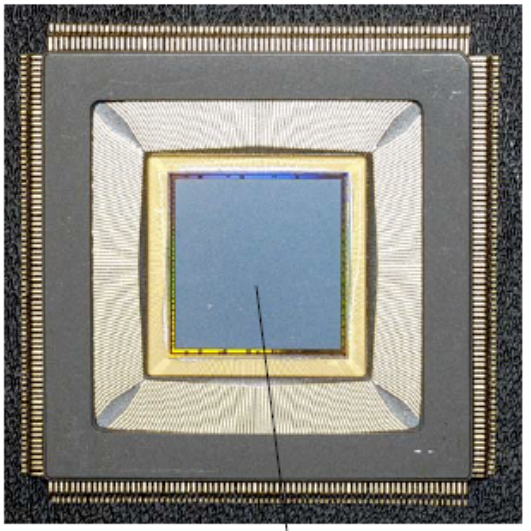

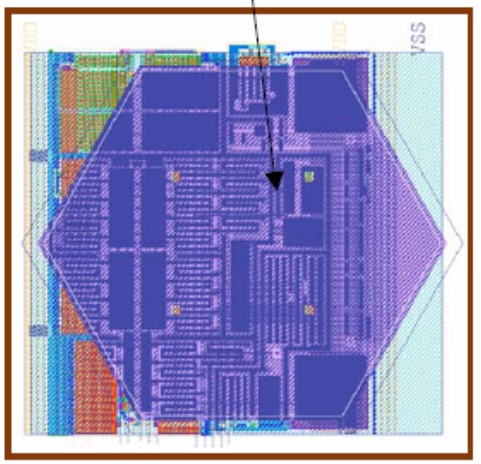

E. Costa et al, Nature 411(2001)662
R. Bellazzini et al, Nucl. Instr. and Meth. A478(2002)13
R. Bellazzini et al, Nucl. Instr. and Methods A435(2004)477

X-ray polarimeter

PHOTOELECTRON ANGULAR DISTRIBUTION FOR POLARIZED SOFT X-RAYS:

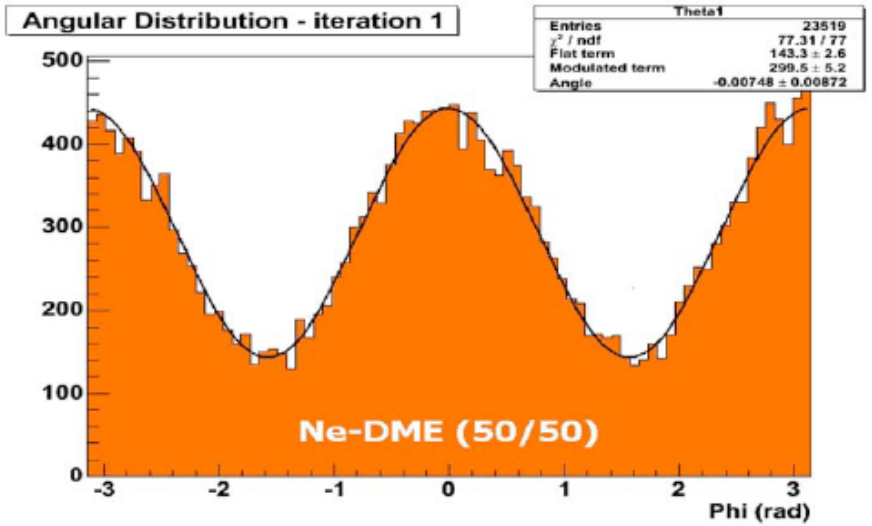

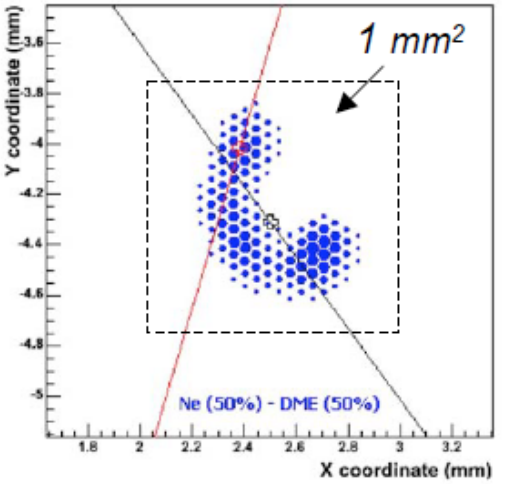

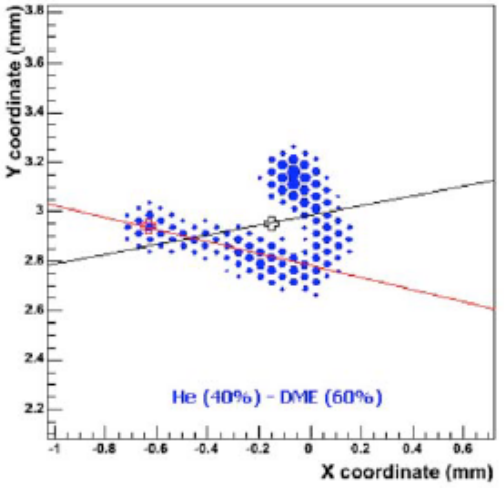

R.Bellazzini et al, Nucl. Instr. And Meth. A572(2007)160

UV photons

TOTAL AND PHOTOIONIZATION CROSS SECTIONS:

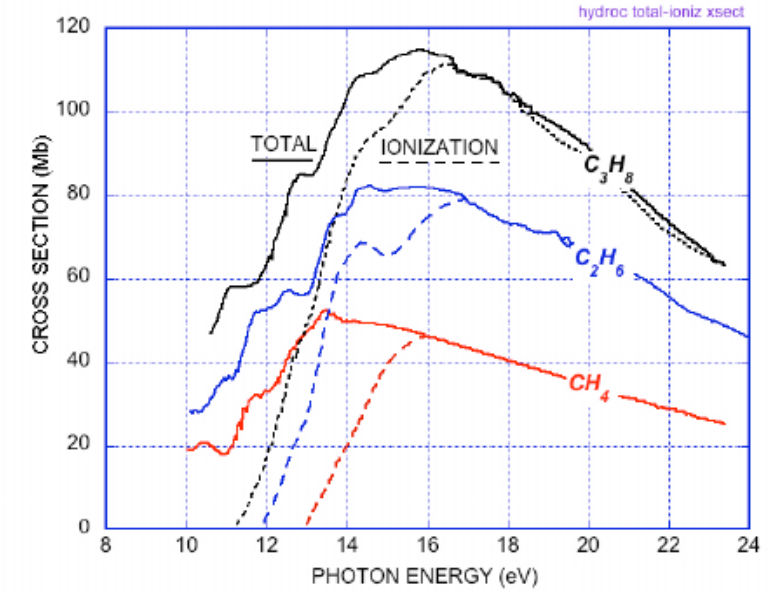

	E_I (eV)
C_6H_6	9.3
TEA	7.45
TMAE	5.6

TEA: Triethylamine $(C_2H_5)_3N$

TMAE: Tetrakis-dimethylamino ethylene $[(CH_3)_2N]_2C$

PHOTOELECTRIC EFFECT:

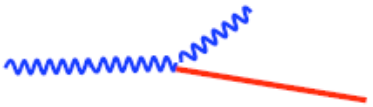

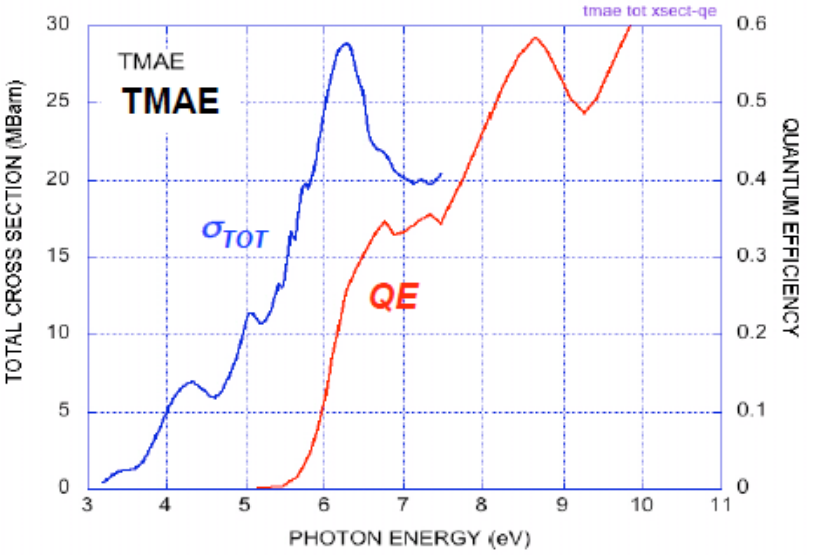

X-ray polarimeter

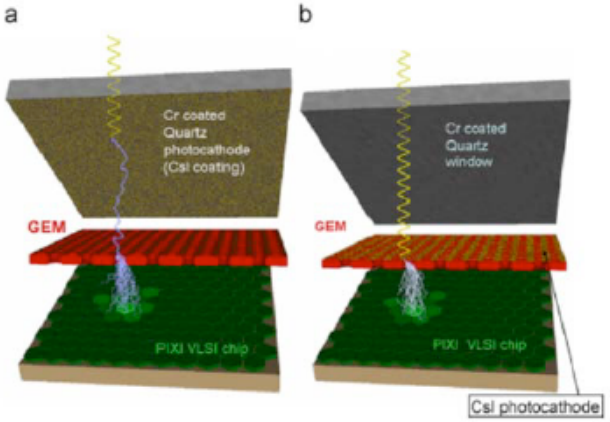

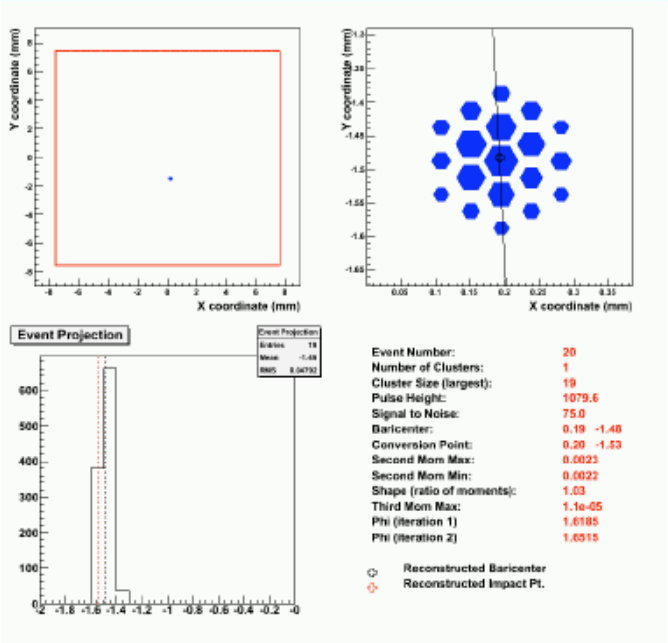

IMAGE OF THE GEM FOIL (30 µm HOLES AT 50 µm PITCH):

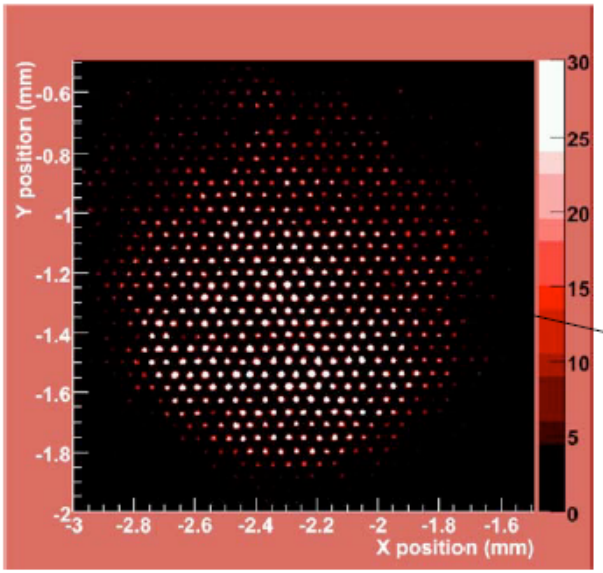

4 µm rms

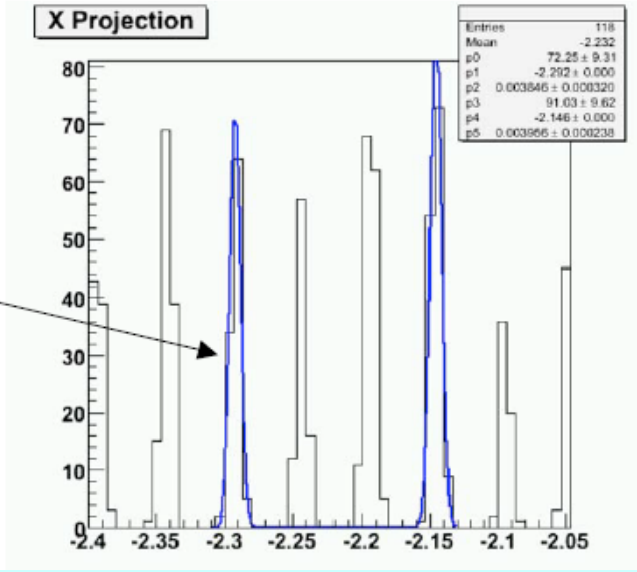

R. Bellazzini et al, Nucl. Instr. And Meth. A581 (2007) 246

Introduction to μ-PIC

- μ-PIC：micro pixel gas chamber
- Large area with PCB tech.
- pitch :400μm
- high gas gain
- small discharge damage

	MSGC	μ-PIC
Maximum gain	1700(with capillary)	15000
Stable Gain	1000	7000
Long time		>30 days
Area	$10 \times 10 cm^2$	$30 \times 30 cm^2$
Pitch	200μm	400μm (300μm possible)
uniformity(σ)	~35%	4%

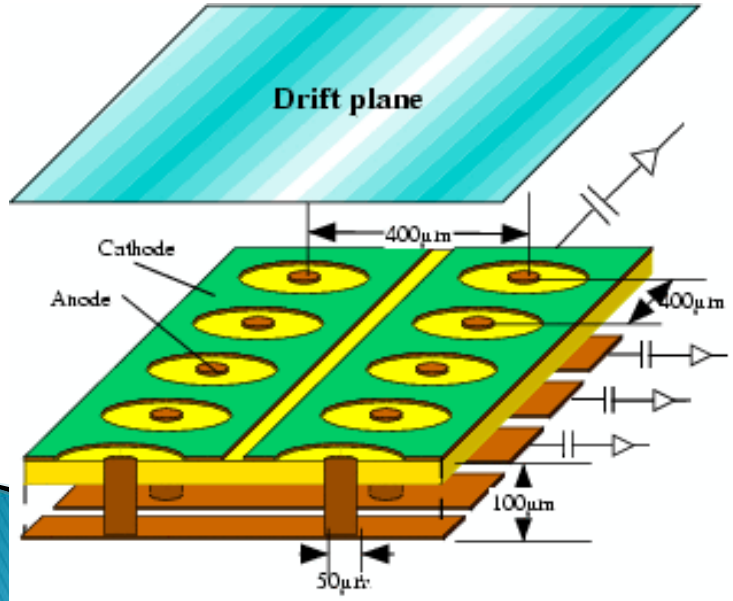

- Invented by A.Ochi and T.Tanimori (NIMA 471 (2001) 264)
- Application: X-ray imaging, Gamma camera, Medical RI tracing, etc.

μ-PIC Principle of operation

- Why this shape?
  - μ-PIC shape is cross section of proportional counter.
  - The electric field is decreased along radial direction from anode.
    - The streamer from anode will be self-quenched
    - Proberbility of electron emission is smaller

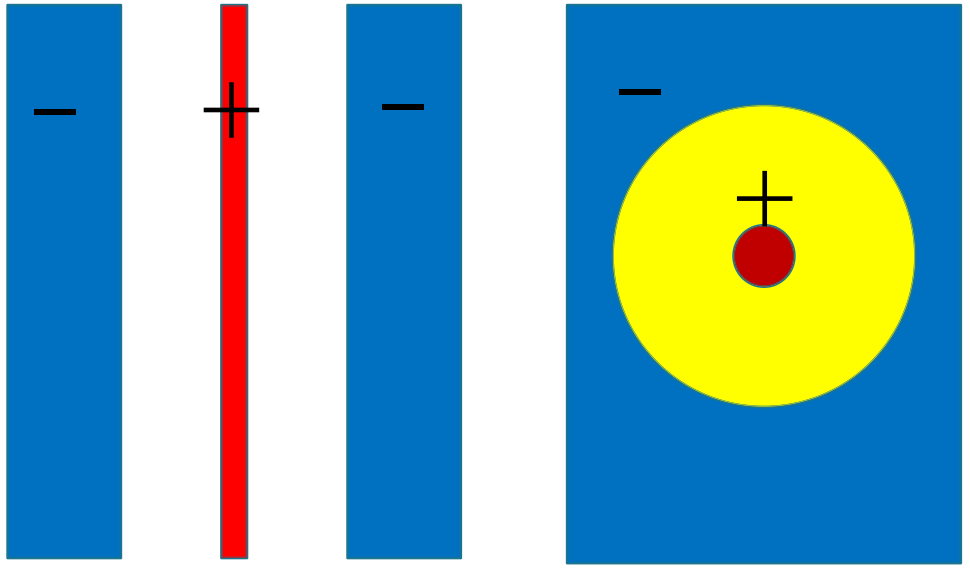

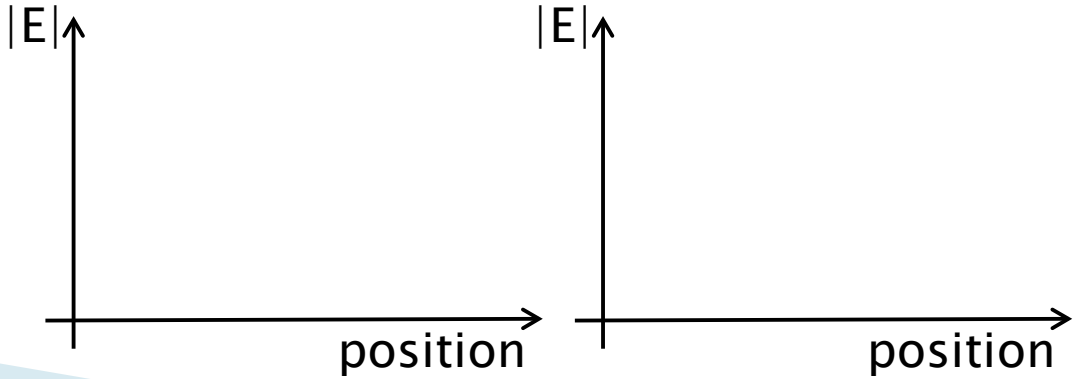

Feature of μ-PIC

- Direct collection of charge
  → Equal signal from anode and cathode

- Upward electric field
  → No charge-up

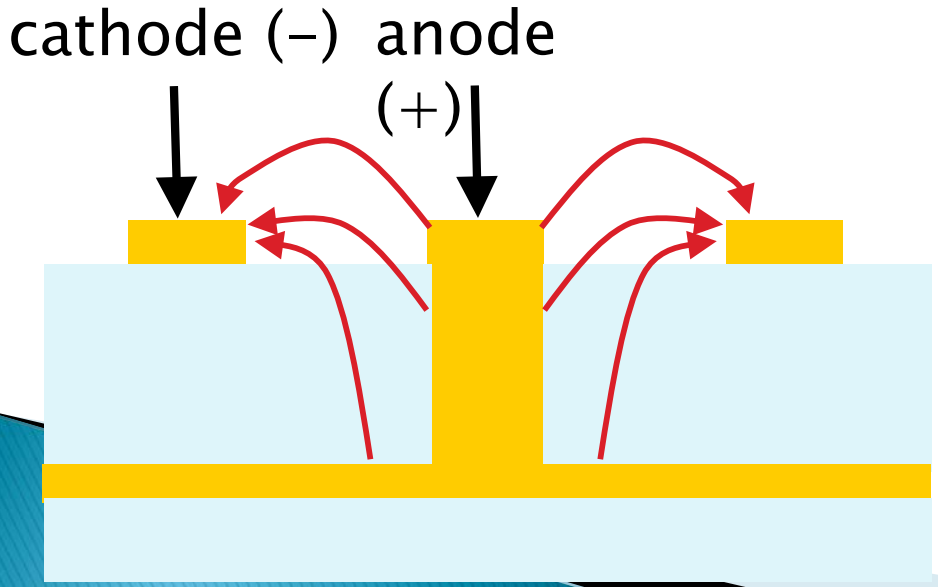

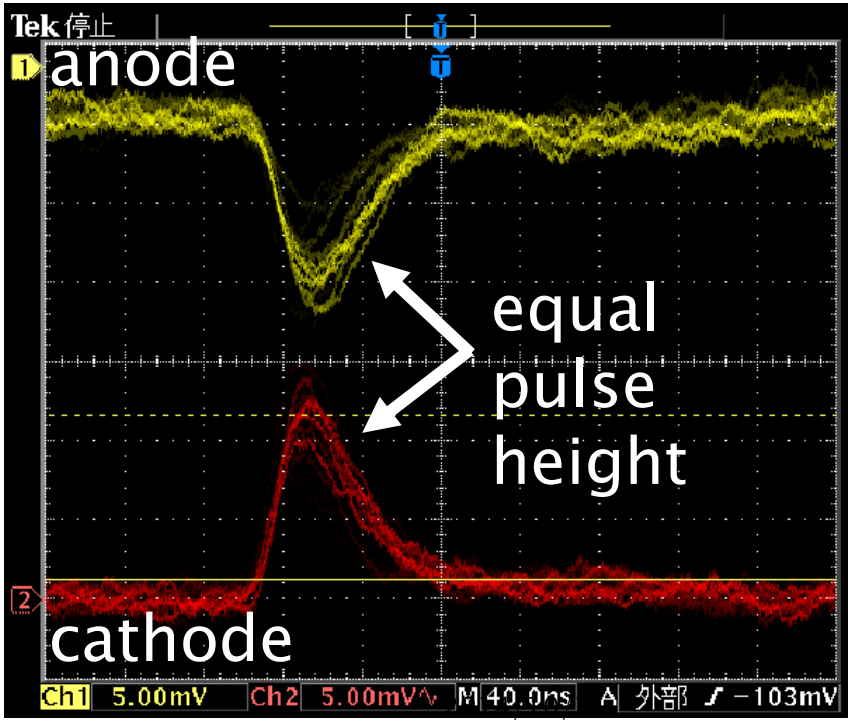

Design of M³-PIC

- Micro pixel chamber (μ-PIC)

+

- With micro mesh
  - Higher gain in stable operation (~5x10⁴)
  - Low ion backflow (<1%)

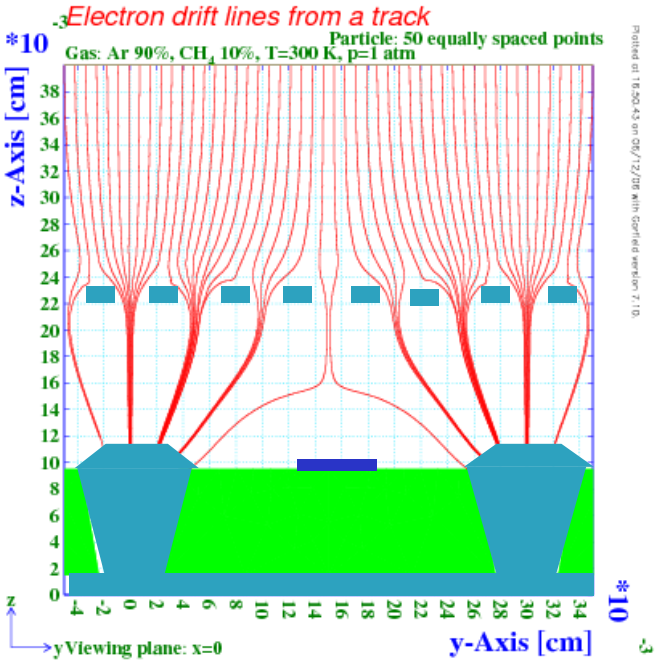

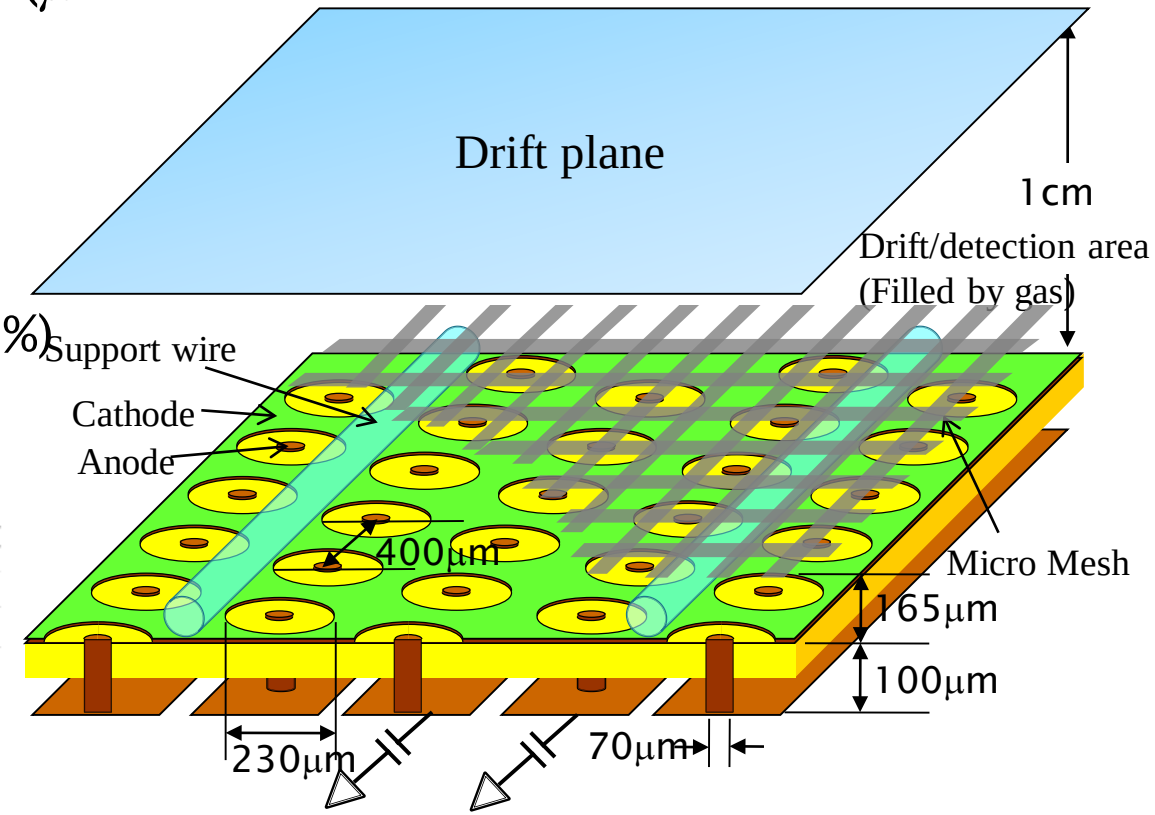

μ-PIC with resistive cathode and capacitive readout

- Detector design
  - All cathodes are made from carbon-polyimide
  - Pickup electrodes are lied under cathodes and insulator
  - We have two dimensional signals

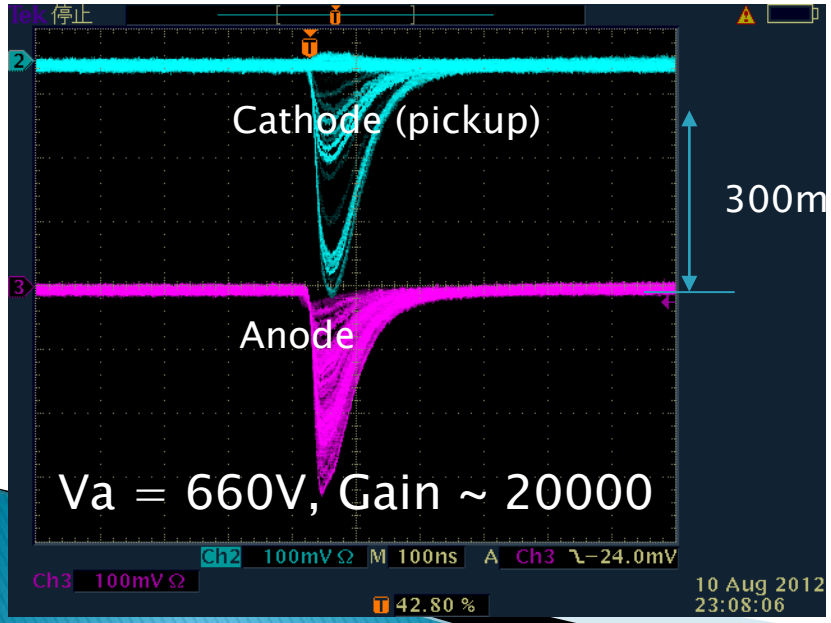

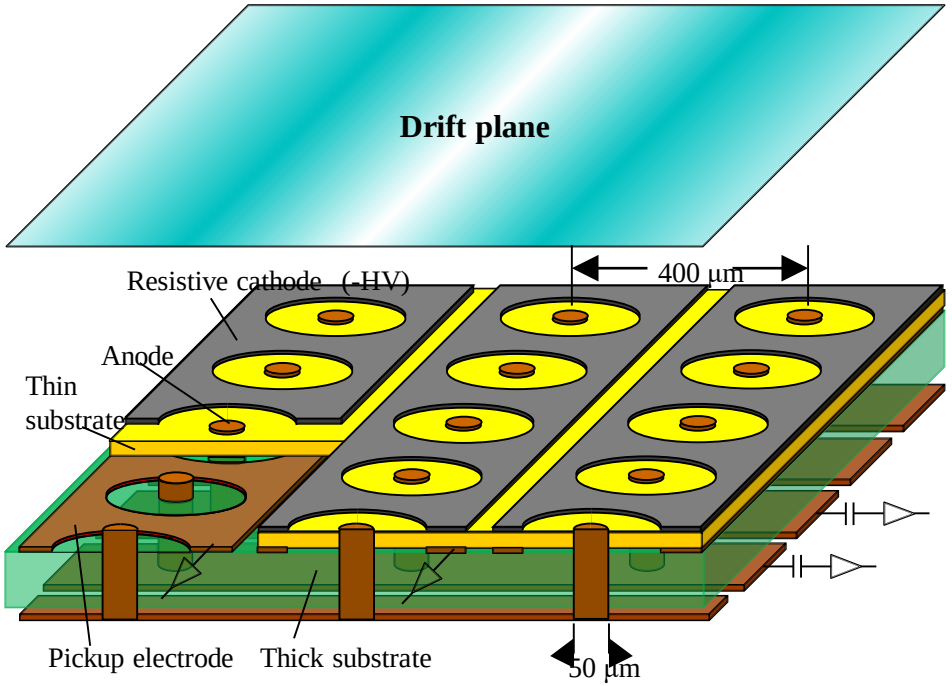

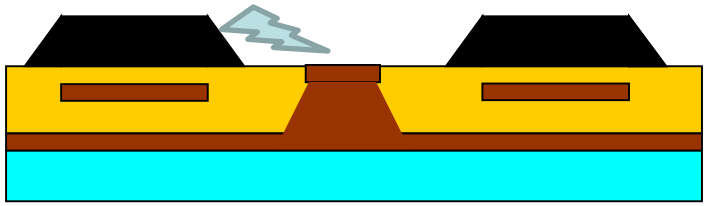

- Cathode signal on oscilloscope is inverted on opposite sign.
- Two dimensional signal is induced
- Not charge shareing.

THGEM- based neutron detector

Proposal for a fast neutron detector for fan-beam

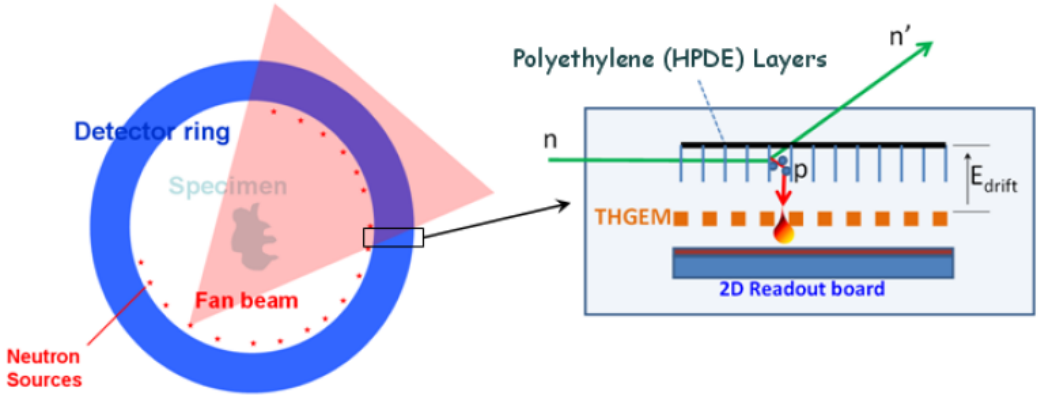

2.5 MeV neutrons; 8% efficiency; 1 mm resolution

Figure 1. Part a: conceptual design of the high-frame-rate fast neutron tomographic system. Part b: schematic drawing of a vertical section of the imaging detector based on a THGEM-based imaging detector.

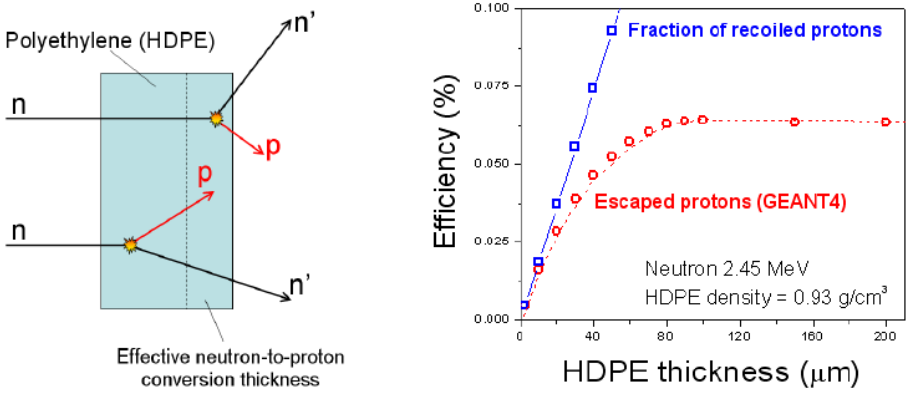

Figure 2. Red symbols: detection efficiency as a function of the converter thickness. Blue symbols: neutron-to-proton conversion efficiency as a function of the converter thickness. The converter foils are made of polyethylene (mass density of 0.93 g/cm3).

study phenomena opaque to X-

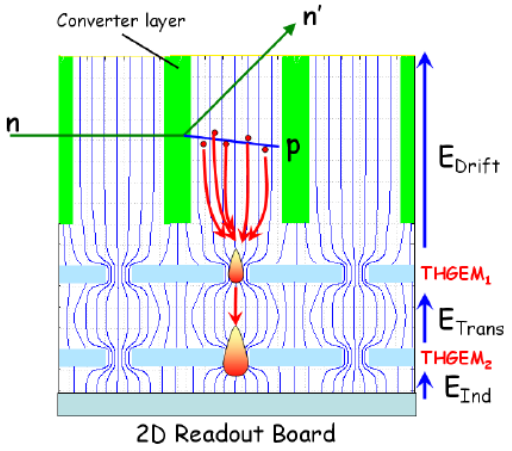

Figure 5. Concept of the fast neutron detector based on THGEM readout.

Concept of a novel fast neutron imaging detector based on THGEM for fan-beam tomography applications

M. Cortesi,[a,1] R. Zboray,[a] R. Adams,[a,b] V. Dangendorf[c] and H.-M. Prasser[a,b]

An event in the Big European Bubble Chamber

1965

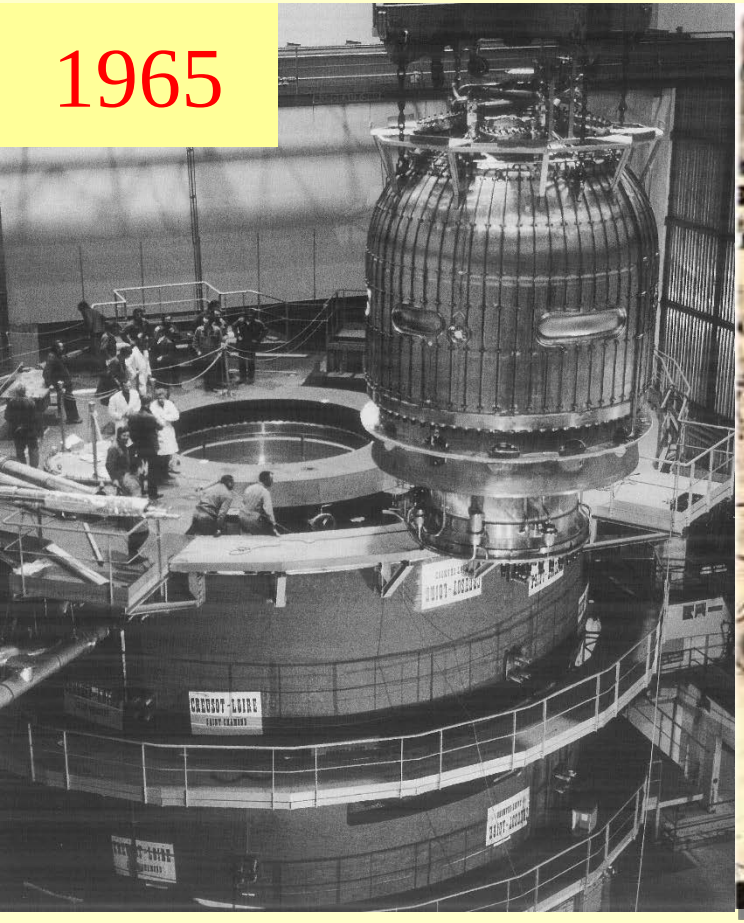

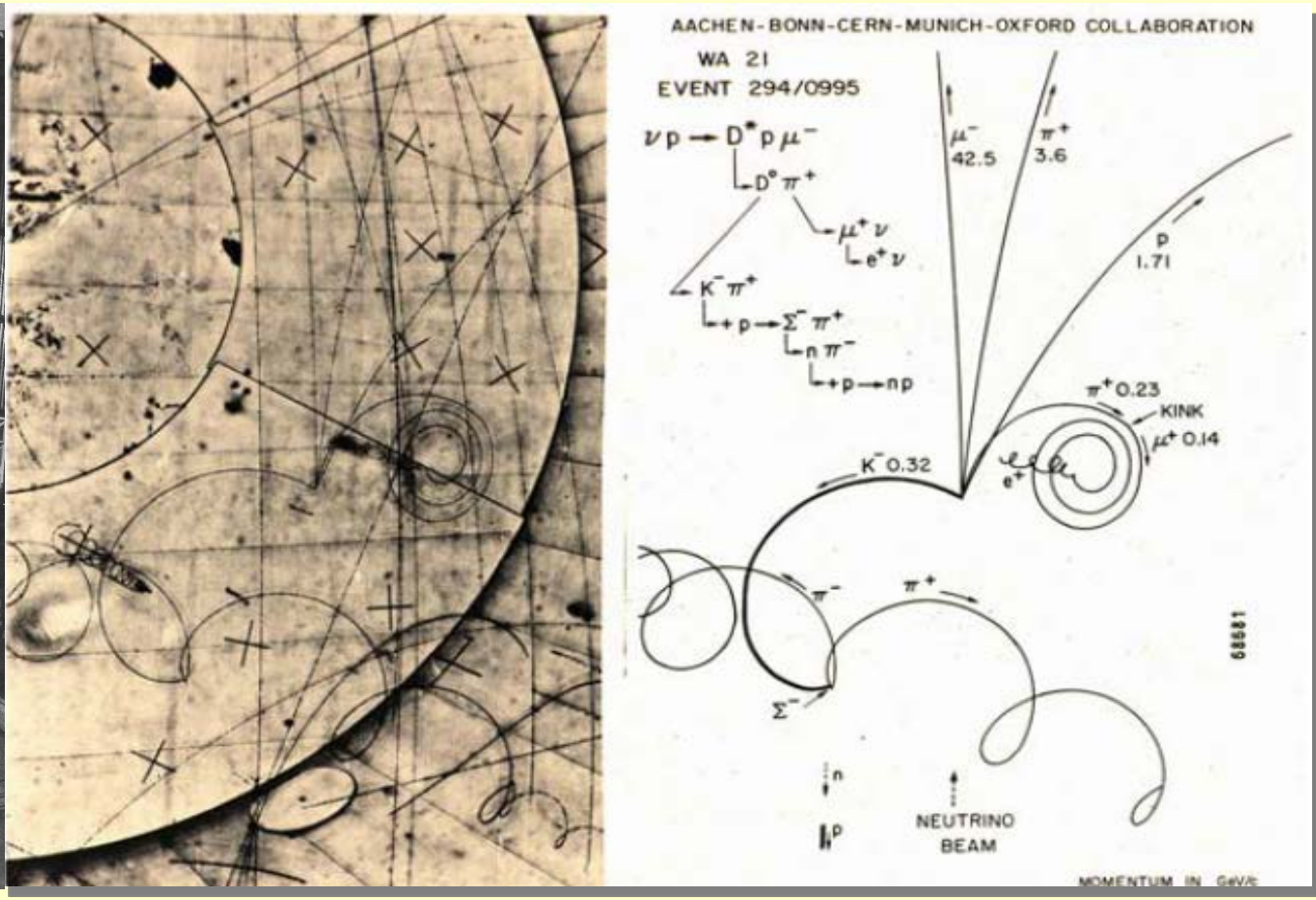

Complete reconstruction of an event from BEBC picture, neutrino beam, WA21 Experiment, CERN, 1978.

$\nu p \to D^* p \mu^-$

Tracking and Calorimetry

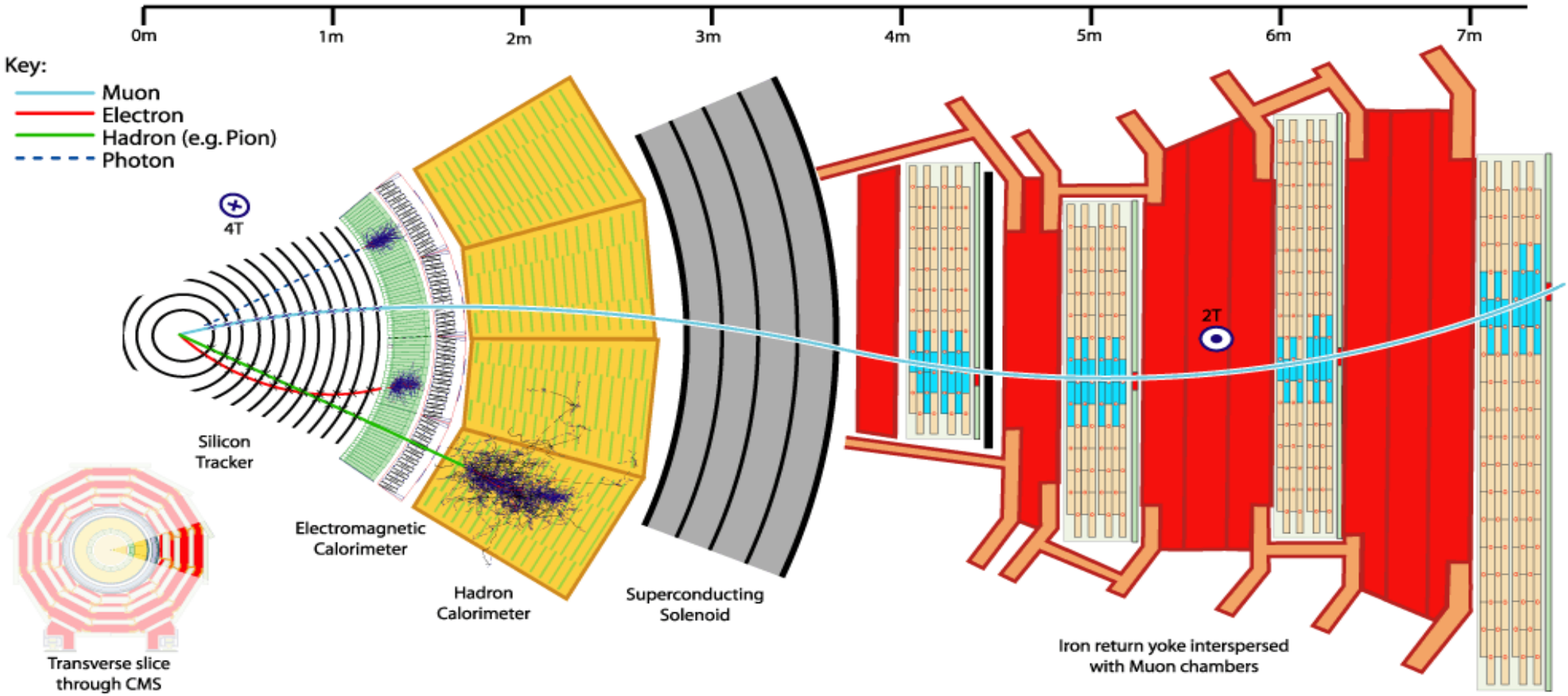

Good identification of photons, electrons and muons:

photons and electrons produce electromagnetic showers.

muons travel through the entire detector

Showers Properties

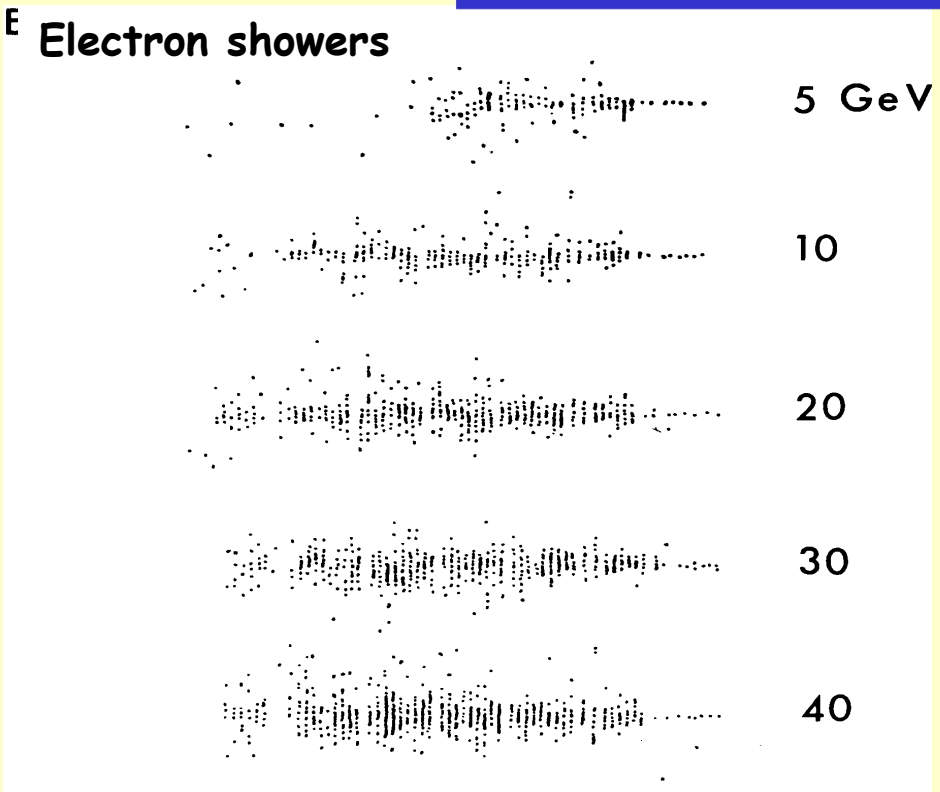

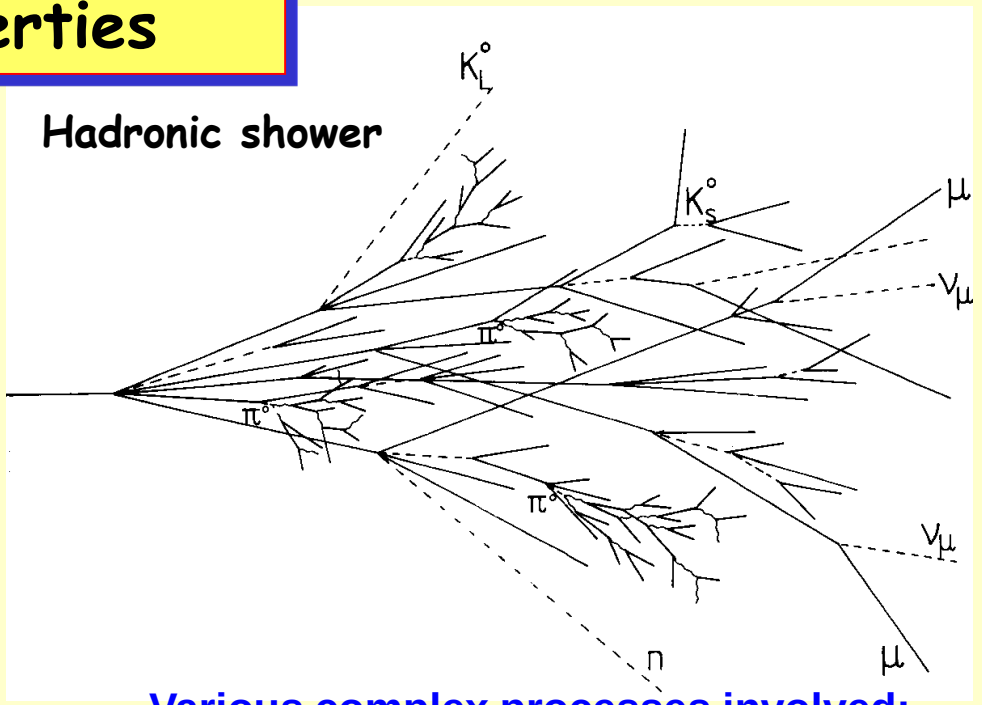

Various complex processes involved:
hadronic and electromagnetic components

charged pions, protons, kaons ….
breaking up of nuclei,
neutrons, neutrinos, soft γ's
muons …. → invisible energy

neutral pions → 2γ →
electromagnetic cascade

$$n(\pi^0) \approx \ln E(GeV) - 4.6$$

The lateral spread of the shower is mainly governed by the multiple scattering of the electrons.
95 % of the shower is contained inside a cone of size $2R_M$ (Moliere radius)

good position resolution allows
good π° identification

hadronic showers are much longer and broader than electromagnetic ones

Large energy fluctuations → limited energy resolution

useful for neutron (antinutron) identification

hadronic calorimeters do not identify charged hadrons

hadronic showers from π, K, p all look alike
calorimeter energy resolution is not enough to allow measuring mass from $m^2=E^2-p^2$

Exemple du calorimètre hadronique de CMS

Absorbeur en cuivre (1500 t) + scintillateurs

Résolution en énergie : $\frac{\sigma_E}{E} = \frac{65\%}{\sqrt{E_{(GeV)}}} \oplus 5\%$

for 16 Gev/c charged hadron, **σ(E) ≈ 2.7 GeV**, while **E(K) – E(π) ≈ 7 MeV**

2 orders of magnitude missing

The alternative: to measure the particle velocity

$$E = \sqrt{m^2c^4 + \left|\vec{p}\right|^2 c^2}$$

$$p = mc\gamma\beta;\ \gamma = \frac{E}{mc^2}\ \text{(Lorentz factor)}$$

$$\left(\frac{\mathrm{dm}}{\mathrm{m}}\right)^2 = \left(\gamma^2 \frac{d\beta}{\beta}\right)^2 + \left(\frac{dp}{p}\right)^2$$

$$\left.\begin{aligned} &\frac{dp}{p} \cong 0 \\ &m_1^2 - m_2^2 = p^2 \frac{\Delta\beta(\beta_1 + \beta_2)}{c^2(\beta_1 * \beta_2)^2} \end{aligned}\right\} \frac{\Delta\beta}{\beta} \cong \frac{(m_1^2 - m_2^2)c^2}{2p^2}$$

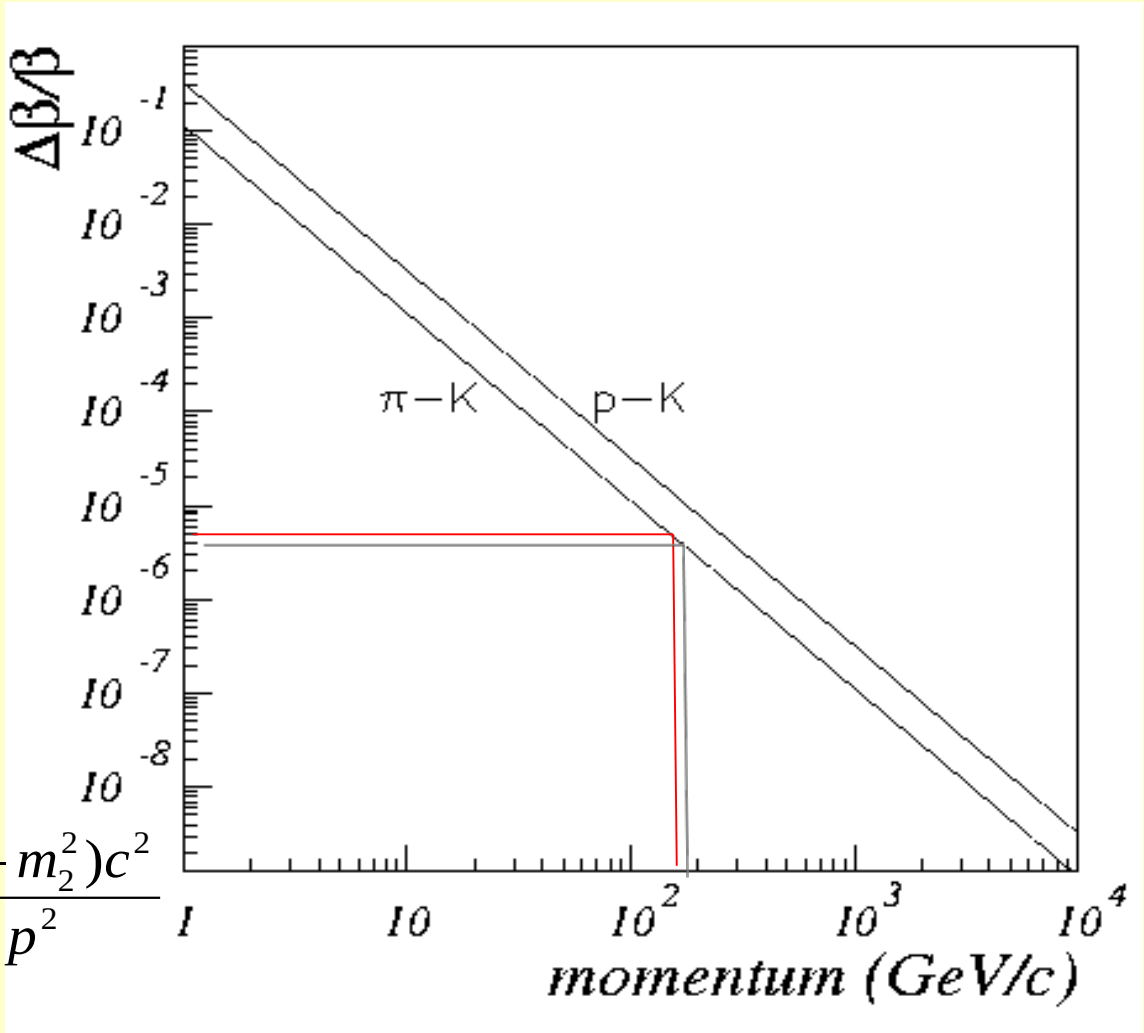

Particle Identification Techniques

PID techniques are based on the measurement of charged particle velocity via velocity dependence of their interaction with matter: (ionization and excitation)

The applicable methods depend strongly on the particle momentum (velocity) domain of interest

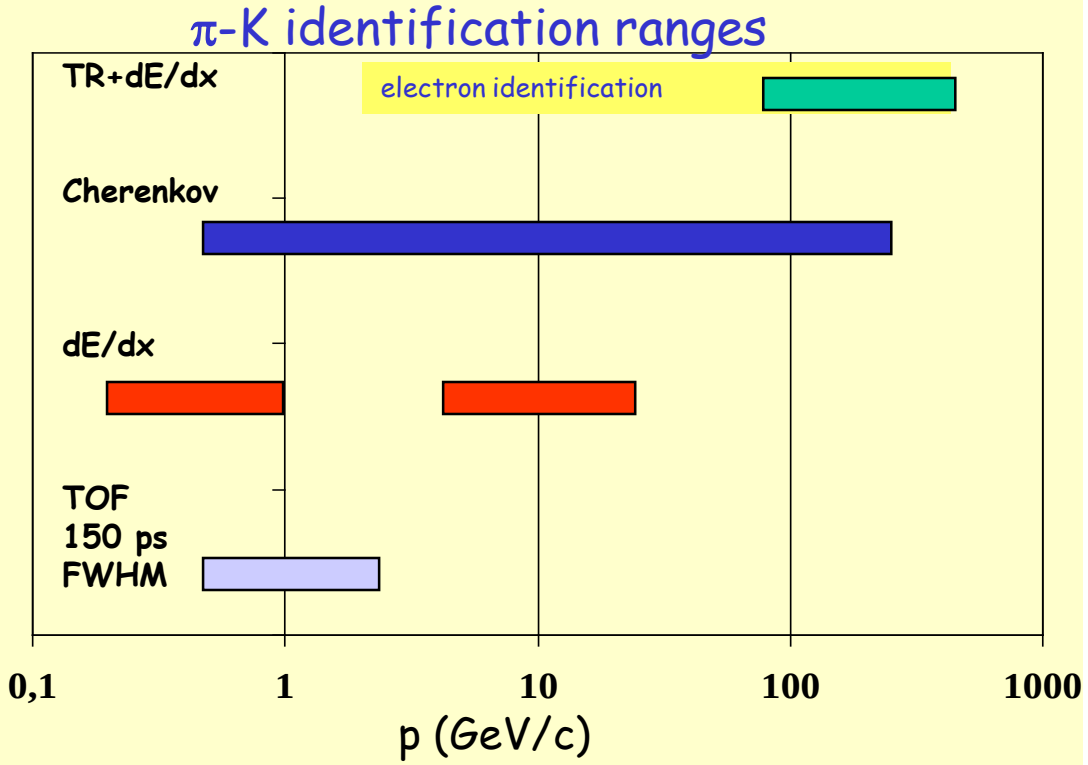

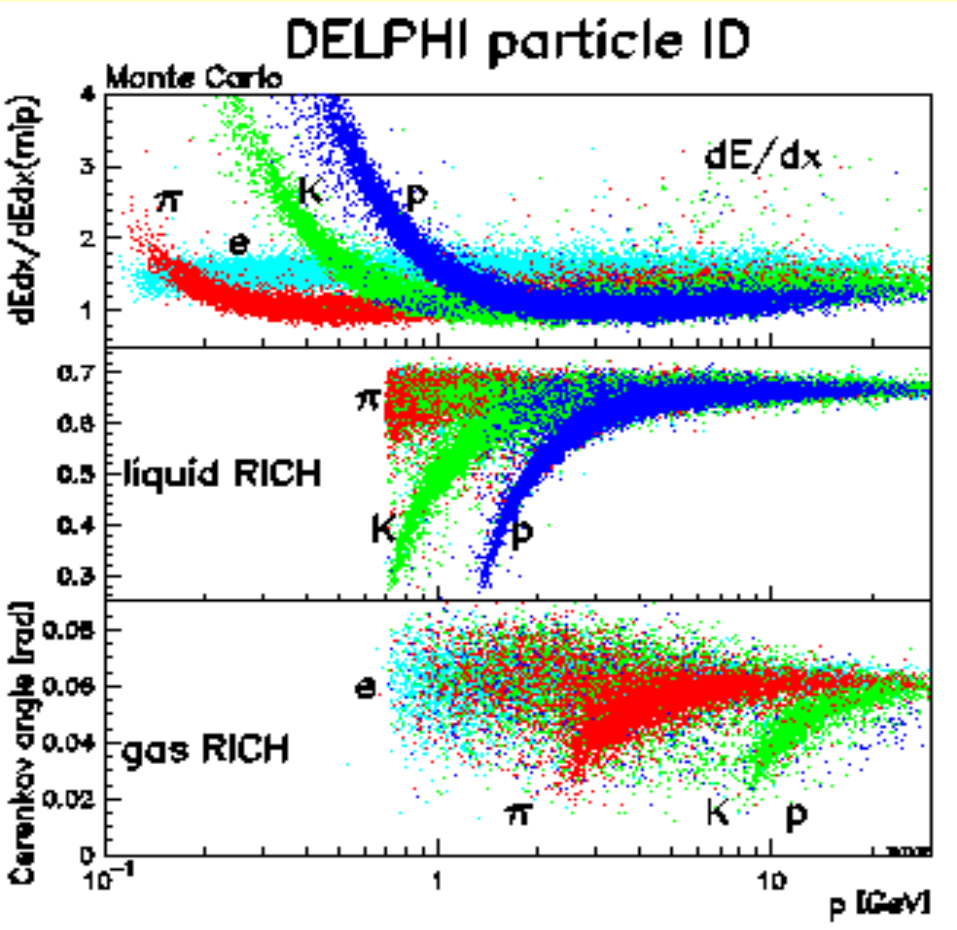

The main properties of Cherenkov emission

are directly derived from the fundamental equation:

$$\cos\theta_c = \frac{1}{n\beta}$$

1) no emission for $\beta < 1/n$

2) the emission angle depends on β

3) chromaticity: $n(\lambda_1) \neq n(\lambda_2) \rightarrow \theta_1 \neq \theta_2$

1) particle velocity threshold for Cerenkov emission

2) a measurement of the Cherenkov angle corresponds to a measurement of β

3) the measurement resolution is intrinsically limited by chromaticity

Threshold and saturation

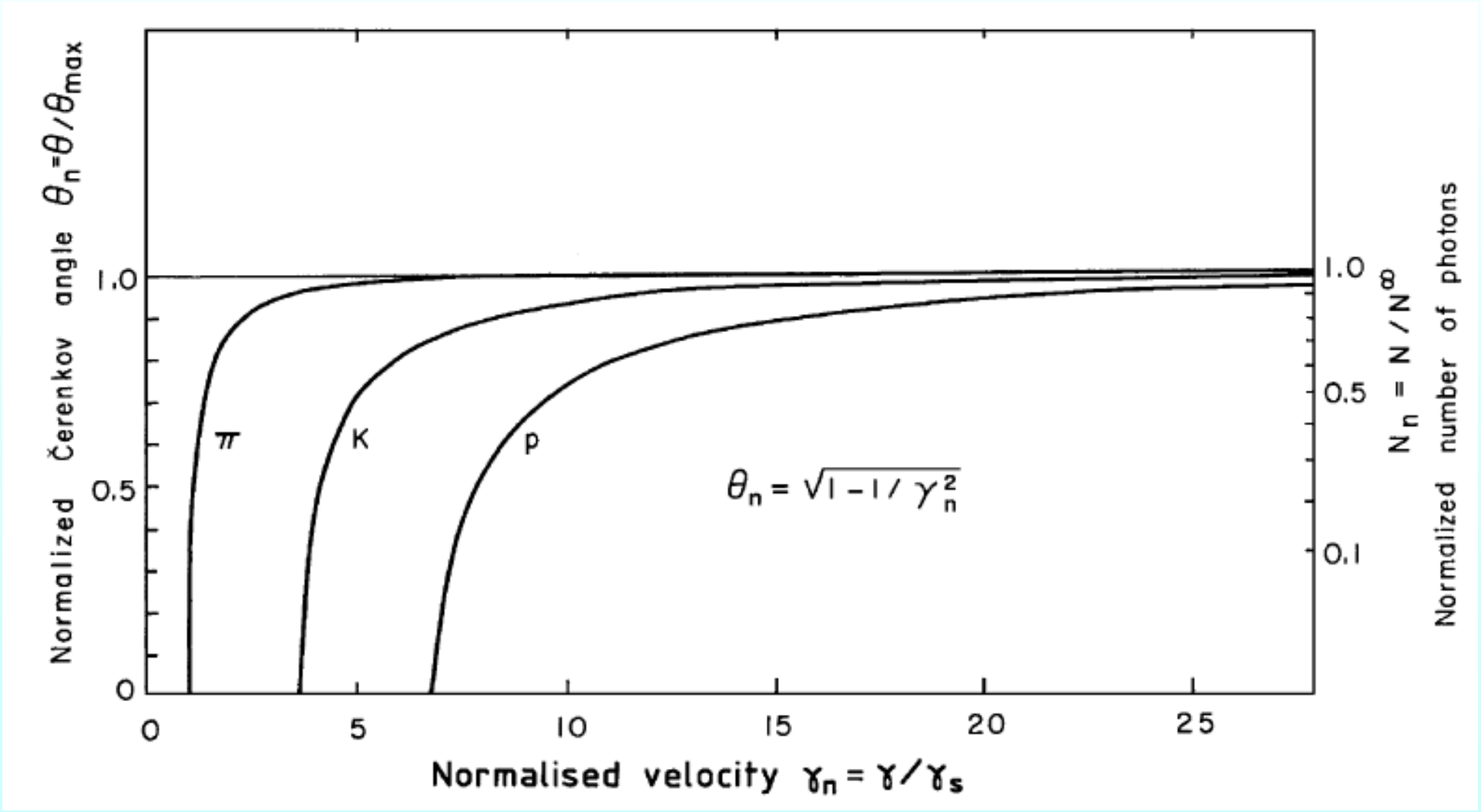

using an angle to measure velocity

Determine the velocity of this bullet:

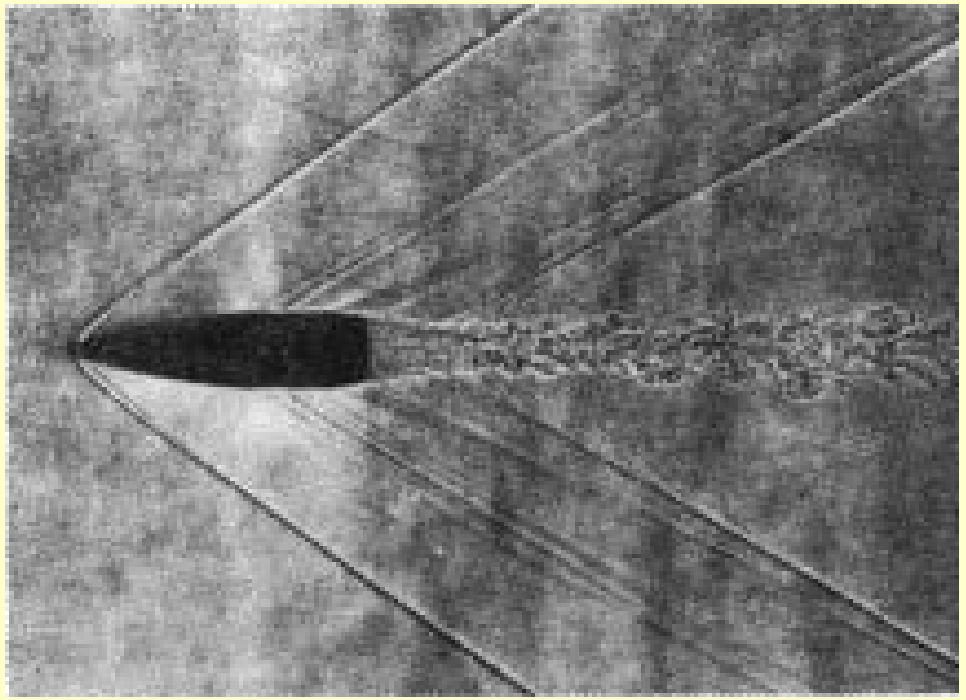

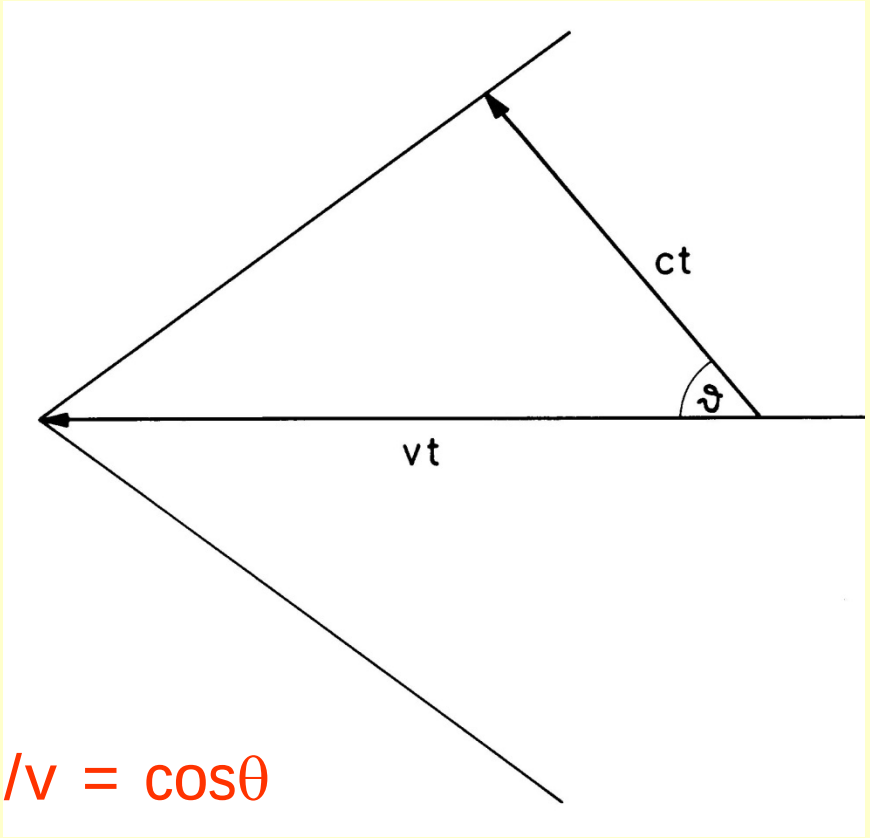

$c/v = \cos\theta$

from the photo:

angle: 52^o; $v = c/\cos\theta = 340$ m/s / $\cos 52^o = 552$ m/s

Cherenkov Light Imaging

Ring Imaging CHerenkov counters

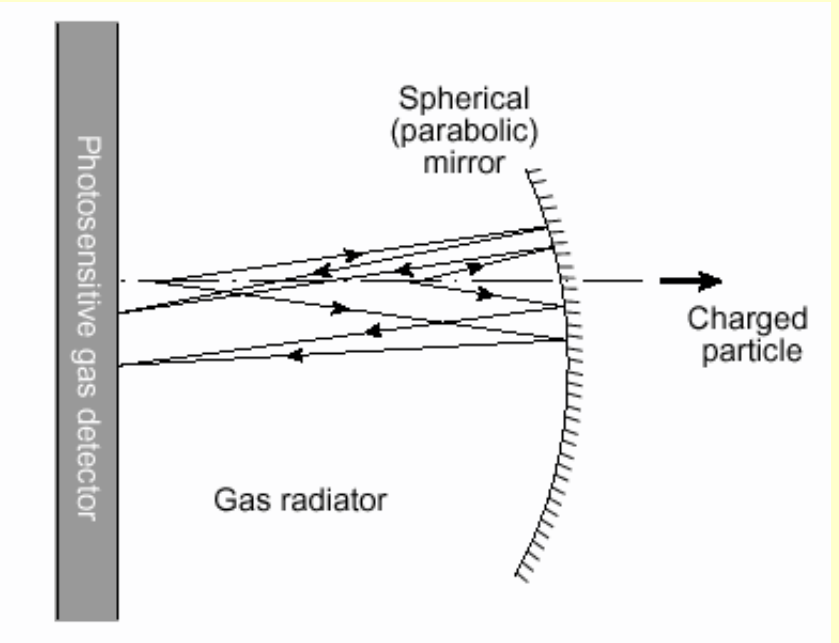

How many detected photoelectrons?

$$N_{pe} = 370L\int \varepsilon \sin^2\theta_c dE = L\,N_0 \sin^2\theta_c$$

E.g., for No = 50, β = 1;

		n	N_{pe}/cm
Solid	SiO_2	1.47	27
Liquid	H_2O	1.34	22
Gas	C_5F_{12}	1.0017	0.17
Gas	He	0.00004	0.004

The number of photo-electrons N_{pe} is always "too small".

Historical steps

- 1888 - O. Heaviside : a superluminal charged particle in vacuum (!) emits an e.m. radiation
- 1919 - M. Curie: **faint blue light from concentrated solutions of radium in water**
- 1934 - P. A. Cherenkov: **exhaustive series of experiments on visible light emitted by Compton electrons produced by bombarding pure liquids with γ rays**
- 1937 - I. M. Frank and I. J. Tamm: **classical theory of Cherenkov radiation**
- 1940 - V. L. Ginzburg: quantum theory of Cherenkov radiation
- 1951 - J. V. Jelley: first Cherenkov detector finalized to PID in a physics experiment
- 1955 - E. Segre', O. Chamberlain, C. Wiegand and T. Ypsilantis: discovery of the antiproton
- 1958 - P. A. Cherenkov, I. M. Frank and I. J. Tamm: **Nobel prize for Physics**
- 1960 - A. Roberts: **first conception of Ring Imaging CHerenkov technique**
- 1977 - J. Seguinot and T. Ypsilantis: **"imaging" of Cherenkov patterns in a gas detector**
- 1981 - First use of a RICH for high energy PID: E605 Experiment at FNAL
- 1982 - Proposal for large RICH systems: Ω and DELPHI at CERN; 1984: SLD CRID at SLAC

from 1993 Workshops on RICH detectors (Bari, Uppsala, Ein Gedi, Pylos, Playa del Carmen, Trieste)

Large Surface Sensitive to Single Photons

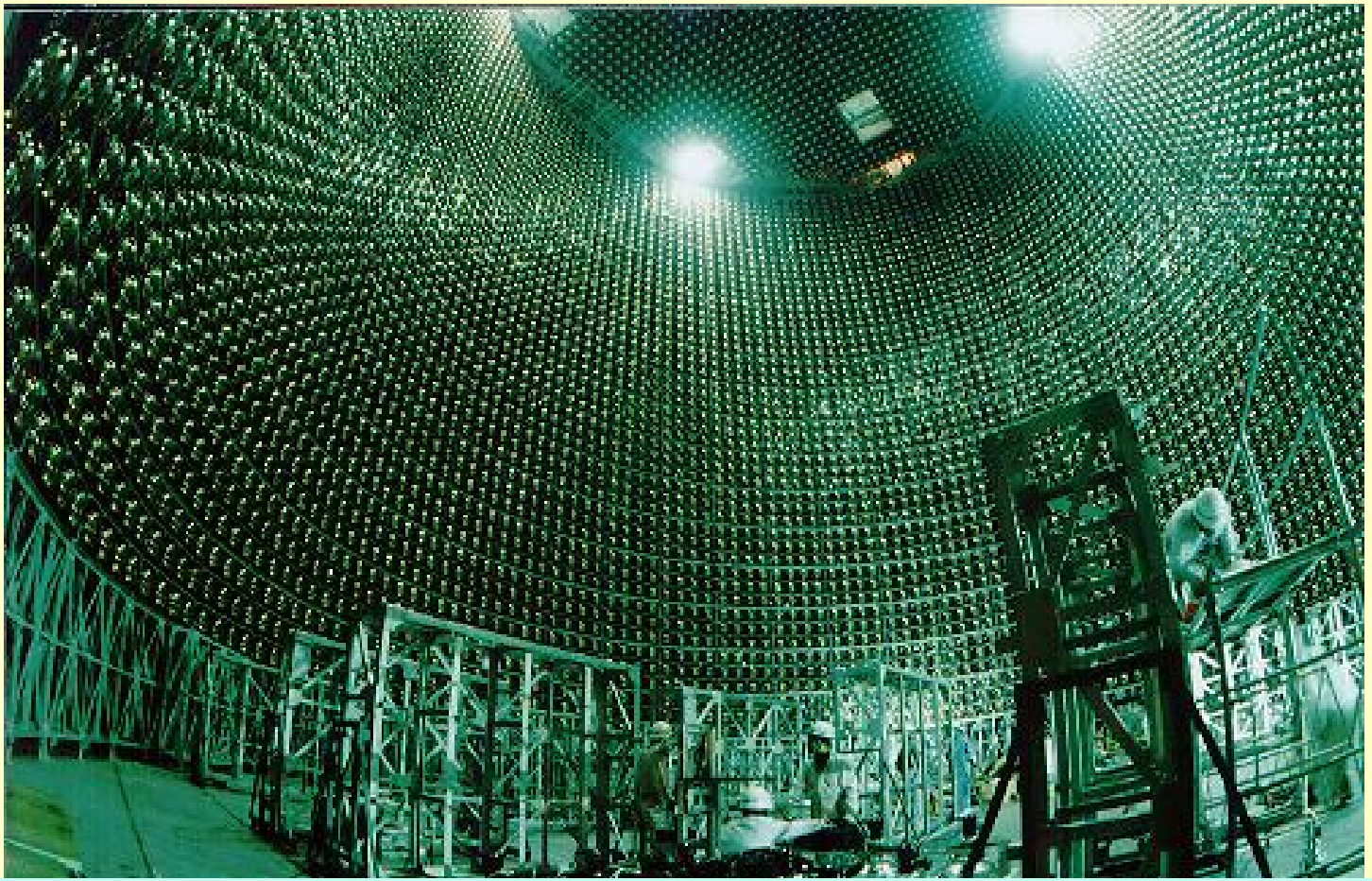

Super-Kamiokande: 50 000 ton water ~11000 PMTs, 50cm ∅

Photon Detectors used for RICHs belong to three categories:

Vacuum based PDs, Si PDs, Gaseous PDs